THESIS

INVESTIGATING BEST MANAGEMENT PRACTICES TO REDUCE SELENIUM AND NITRATE CONTAMINATION IN A REGIONAL SCALE IRRIGATED AGRICULTURAL GROUNDWATER SYSTEM: LOWER ARKANSAS RIVER VALLEY, SOUTHEASTERN COLORADO

Submitted by

Ravi Kumar Tummalapenta

Department of Civil & Environmental Engineering

In partial fulfillment of the requirements

For the Degree of Master of Science

Colorado State University

Fort Collins, Colorado

Summer 2015

Master's Committee:

Advisor: Ryan T Bailey

Timothy K. Gates
Subhas K. Venayagamoorthy
Troy A. Bauder

ABSTRACT

INVESTIGATING BEST MANAGEMENT PRACTICES TO REDUCE SELENIUM AND NITRATE CONTAMINATION IN A REGIONAL SCALE IRRIGATED AGRICULTURAL GROUNDWATER SYSTEM: LOWER ARKANSAS RIVER VALLEY, SOUTHEASTERN COLORADO

The Lower Arkansas River Valley (LARV) is well known for its rich agricultural production, with 109,000 ha of irrigated area. Due to agricultural production extending for more than 100 years, the LARV now faces challenges of soil salinity, water logging from shallow groundwater tables, and a high concentration of selenium (Se, both within the alluvial aquifer system and within the Arkansas River and its tributaries). Se originates primarily from bedrock and outcropped marine shale, released due to chemical oxidation in the presence of dissolved oxygen and nitrate. Se is a dynamic element that is biologically essential for plants, animals and humans. However, it is known that Se can be harmful at elevated concentrations. Therefore, elevated concentration levels in the surface water and groundwater in the LARV are considered problematic, and methods must be found to decrease groundwater concentrations and Se loadings from the aquifer to the Arkansas River.

This thesis assesses plausible methods that will decrease Selenium (Se) contamination in groundwater and surface water in the LARV. Best management practices (BMPs) to reduce selenium and nitrate mass loadings to the River Arkansas in a 55,200 ha area downstream of John Martin reservoir in the LARV were explored and analyzed using 18 scenarios. The UZF-MODFLOW and UZF-RT3D numerical models, calibrated against extensive sets of field data in the region, were used to simulate groundwater flow and the physical and chemical processes

governing the fate and transport of Se and N species. Specific BMPs include reduction in the seasonal application of N fertilizer; decrease in concentration of selenate (C_{SeO_4}) and nitrate (C_{NO_3}) in canal water, representing treatment of water before application as irrigation water; reduction in irrigation application volumes; and combinations of these practices, along with fallowing of irrigated land. These practices are applied for a long term period (40 years) to observe the effects of each BMP on groundwater C_{SeO_4} and C_{NO_3} and on mass loadings from the aquifer to the Arkansas River. The BMPs are applied at varying levels: less aggressive (20%) to very aggressive (40%) of each practice.

Results indicate that the highest aggressive combined scenario 40% reduction in N fertilizer reduction, 40% reduction in canal concentration, and 35% reduction in irrigation volume, with 25% irrigated land fallowing result in the highest decrease of mass loadings of SeO_4 into the Arkansas River with 22.7%, followed by the less aggressive and highest aggressive combined scenarios of N fertilizer reduction, canal concentration reduction, and irrigation volume reduction with land fallowing showing decrease of mass loadings from 15% to 21%. For individual scenarios: the irrigation volume reduction scenario (13.1% to 13.4%) is followed by the canal concentration reduction scenario (3% to 6%); whereas the N fertilizer reduction scenario shows a minimum percent reduction (1.5% to 2.7%) as compared to the Baseline ("do-nothing" scenario).

Similarly for NO_3, results show that the highest aggressive combined scenario 40% reduction in N fertilizer reduction, 40% reduction in canal concentration, and 35% reduction in irrigation volume, with 25% irrigated land fallowing result in the highest decrease of mass loadings of NO_3 to the Arkansas River with 34.7% followed by the less aggressive and very aggressive combined scenarios of N fertilizer reduction, canal concentration reduction, and irrigation volume

reduction with land fallowing showing reduction of mass loadings from 15.5% to 30%. The results of individual BMPs is as follows: 35% irrigation volume reduction scenario (14.9%) is followed by 40% N fertilizer reduction scenario (14.5%); 20% irrigation volume reduction scenario (12%); 20% N fertilizer reduction scenario (8.3%); whereas 20% and 40% canal concentration reduction scenarios show minimum percent reduction (0.6% to 1.1%). The results are compared with results from a similar study recently performed in the Upstream Study Region of the LARV to observe the differences in BMP practices and their reduction of Se contamination in the study areas.

TABLE OF CONTENTS

LIST OF TABLES

LIST OF FIGURES

CHAPTER NO: 1

1 LITERATURE REVIEW AND RESEARCH OVERVIEW

1.1 INTRODUCTION

Selenium (Se) is an important element for animal and human nutrition. However, Se is termed the "double-edged sword" element (Fernandez – Martinez and Charlet, 2009) and an "essential toxin" (Stolz et al., 2002) because of its very small gap between daily dietary deficiency and toxic levels in cases of over consumption for both humans and animals (Levander and Burk, 2006). In fact, high concentrations and bio- accumulation of Se can prove detrimental to both humans and animals (Winkel et al., 2012). Lavender and Burk, (2006) report that the narrow range between dietary deficiency and toxic levels is 40 µg/day to 400 µg/day respectively for humans. Lakin and Davidson, (1973) estimate that Se deficiency diseases and toxicity diseases appear when dietary intake falls below 0.04 mg/kg and exceeds 4 mg/kg respectively for animals.

Rosenfeld and Beath, (1964) state that Se poisoning cases have been reported in cattle, sheep, or humans in China in 1295, in Columbia in 1560, in Mexico in 1764, in South Dakota in 1857 and 1893, and in Wyoming in 1907 and 1908. Oldfield, (1972) specifies that the concentration of Se ingested by animals and humans and the exposure time determines the symptoms and type of disease.

ATSDR (2003) states that an excess of Selenium will lead to Selenosis, which causes brittle hair, deformed nails, and may also cause loss of feeling and control in arms and legs. This has been seen in several villages in China where people were exposed to selenium rich foods for longer periods of time. In addition, it has been seen that insufficient~~ly~~ uptake of Se causes the disease known as Keshan, which causes heart problems (Beck et al., 2003) and muscle pain.

Most of these cases occur in some regions of China. On the other hand, ATSDR (2003) states that no human populations in the United States have been reported with long term selenium poisoning, including populations in the western part of the country where selenium levels are naturally high in the soil, as well as in food ~~is~~ sufficient to meet the Recommended Daily Allowance (RDA).

The primary pathway of human exposure to selenium is through the food we eat. Since farmers irrigate their crops with groundwater or surface water containing high levels of selenium, they probably grow and eat plants that contain high levels of selenium. Fishermen and hunters of waterfowl who regularly eat fish and game from waterways with high selenium content may also consume above average levels of selenium.

1.2 SELENIUM OCCURRENCE

Selenium occurs in nearly all materials of the earth's crust, and it's occurrence in various rock types is presented in Table.1.1.

Table 1.1: Selenium Concentration in Magmatic and Sedimentary rocks (after Mayland et al., 1989).

Rock Type	Se Conc., mg/kg
Magmatic Rocks	
Ultramafic rocks (Dunites, Pendotites, Pyroxeuties)	0.02 - 0.05
Mafic rocks (Basalts, Gabbros)	0.01-0.05
Intermediate rocks (Diorites, Syenites)	0.02-0.05
Acid rocks (Granites, Gueissas)	0.01-0.05
Acid rocks -volcanic (Rhyolites, Trachytes)	0.02-0.05
Sedimentary Rocks	
Argillaceous sediments	0.4-0.6
Shales	0.6
Sandstones	0.05-0.08
Phosphorites	1-100
Limestones, dolomites	0.03-0.10

Igneous rocks are usually low in Se because it escapes in high temperature-volatile gases during volcanic activity (Reuter, 1975). Sedimentary rocks have the highest Se concentration, from 0.03 to 100 mg/kg where it is associated with clay fractions. Thus higher concentrations of Se are found in shale rather than limestone or sandstone. For Cretaceous black shales in Wyoming, values ranges from <1 to nearly 300 mg/kg (NAS-NRC,1983); whereas in Cretaceous Pierre, related shales have approximately 2 mg/kg where these shales are the parent material for much of the seleniferous soil in the northern Great Plains of the USA and the Prairie region of Canada (Mayland et al, 1989).

The various processes involved in the distribution of Se in the environment include volcanic activity, burning of fossil fuels, weathering of rocks and soils, groundwater transport, precipitation of minerals, adsorption, chemical or bacterial reduction and oxidation, and metabolic uptake and release by plants and animals (Mc Neal et al, 1989). The seleniferous soils in the northern Great Plains of the USA and the Prairie region of Canada may have higher Se concentrations in the subsoil due to the process of chemical weathering of rocks and soils (Mayland et al, 1989). In Ireland, Australia, Israel and several other countries, shales are the primary sources of Se toxic soil (Abuereish and Lahham, 1987; Anderson et al, 1961; Lakin, 1948; Rosenfeld and Beath, 1964; Swaine, 1955; NAS-NRC, 1983).

1.3 SELENIUM STUDIES WORLDWIDE

For the past three decades (Gates et al, 2009), elevated Se concentrations in surface and groundwater have emerged as a serious issue in northern Europe (Alfthan et al., 1994; Bye and Lund, 1982), Asia (Afzal et al., 2000; Mizutani et al., 2001; Zhang et al., 2008), and in the western part of the United States (Engberg and Sylvester, 1993).

Oldfield, 2002, in the *Se World Atlas*, shows where selenium related problems exist along with its deficiency and toxic areas world wide.

Australia has had areas of both inadequacy and toxicity of selenium for some years. The Neptunia amplexicaulis seeds from seleniferous soil areas in central Queensland contain 123 μg Se/seed (Peterson and Butler, 1962); whereas, in the same area, "change hoof disease" has been attributed to horses grazing on a known Morinda reticulate selenium accumulator (Knott and McCray, 1959).

In India, the occurrence of toxic levels of selenium has been identified in Punjab by the Punjab Agricultural University (Dhillon and Dhillon, 1991). Toxicity in animals, in wheat, and involved analyses of soils, irrigation water, plants and animal tissues have also been identified. Dhillon and Dhillon, 1997 present the selenium analyses of soils in identified sampling sites in northwest India. The seleniferous and non-selenifeorus areas ~~are~~ range from 0.31 – 4.45 μg/kg and 0.08 – 0.55μg/kg respectively, where soils containing 0.5μg Se/kg or more are considered as toxic areas.

In China, biological effects of selenium have continued on a broad scale for many years. In fact, China is considered a selenium rich country, unlike known selenium-low countries such as Finland and New Zealand. China is also the first world site to record selenium deficiency disease in humans. Keshan disease, an endemic cardiomyopathy, was first reported in 1935 in Keshan county, in the northeast corner of China (Yang et al, 1984). As a result, medical interest was heightened by its discovery in a number of different locations in China (Riley, 1996). The Keshan disease-suffering individuals contained an average of 0.074 μg Se/g as compared with

0.343 μg Se/g in non-Keshan disease areas (Wang et al, 1979). Sufferers of Keshan disease responded positively to selenium supplementation.

In South America, seleniferous areas exist in Venezuela and have led to the accumulation of data on selenium levels in humans in the Venezuelan Andes (Bratter et al, 1991). Furthermore, for 16 years, selenium deficiency areas have been surveyed in Argentina. White muscle disease, another manifestation of selenium deficiency, has been identified in Argentinian cattle (Ruksan et al, 1993). A map showing areas of Se deficiency for livestock in Argentina is presented in Ruskan and Zanelli, 1992.

With regard to Japan, a map of the selenium status of soils for 150 sampling sites throughout the Japanese islands, including adequate levels of selenium in soil ~~is~~ was published by Mizutani et al, 2001. High levels of selenium have been reported in dolphins, seals, and whales which feed on fish and represent the highest position in the marine food chain (Shibata et al, 1992).

1.3.1 SELENIUM STUDIES IN THE UNITED STATES

Since 1856, problems associated with Se toxicities for many areas of the western USA have been reported; in fact, most of the occurrences of Se toxicity in the western states are associated with known seleniferous geological formations (Boon, 1989). Concerns about livestock poisoning involving excess Se (Moxon, 1937) and later concerns about Se deficiencies evident in White Muscle Disease have been reported (Muth et al, 1958).

Seleniferous soils occur from Canada to Mexico, and those are frequently associated with Se-containing geological formations. Most notable are Cretaceous sedimentary deposits of the Niobrara and portions of the Pierre shale, which outcrop or underlie > 700000 km^2 of the western USA. The chalky and calcareous marls and shales of the Niobrara formation are the most

persistent seleniferous beds of the Great Plains region (Moxon et al., 1939). ~~The~~ Niobrara or its equivalent is widespread in many western states, including North Dakota, South Dakota, Montana, Wyoming, Colorado, Kansas, and New Mexico.

Supplementation is shown to bring positive results to health, as well as to animal production in cases of selenium deficiency. In the 1980's, Se excess abnormalities in young ~~of~~ waterfowl were noted including mortality incidents, congenital deformities, and reproductive failures in aquatic birds at the Kesterson National Wildlife Refuge in the western San Joaquin Valley in California . The occurrences of these abnormalities are identified due to poisoning by selenium carried in irrigation drainage into areas used by wildlife (Ohlendorf et al, 1986 and 1988). In 1985, the U.S. Department of Interior (DOI) implemented the National Irrigation Water Quality Program (NIWQP) to study the effects of irrigation drainage on water resources and on fish and wildlife (Deason, 1986). The NIWQP screened DOI data and identified 26 sites for the study; the results were published by the United States Geological Survey (USGS). The maps of areas identified in the western United States as having seleniferous rocks from bedrock, and areas identified as susceptible to irrigation-induced selenium contamination are shown in Figures 1.1, 1.2 and 1.3 respectively.

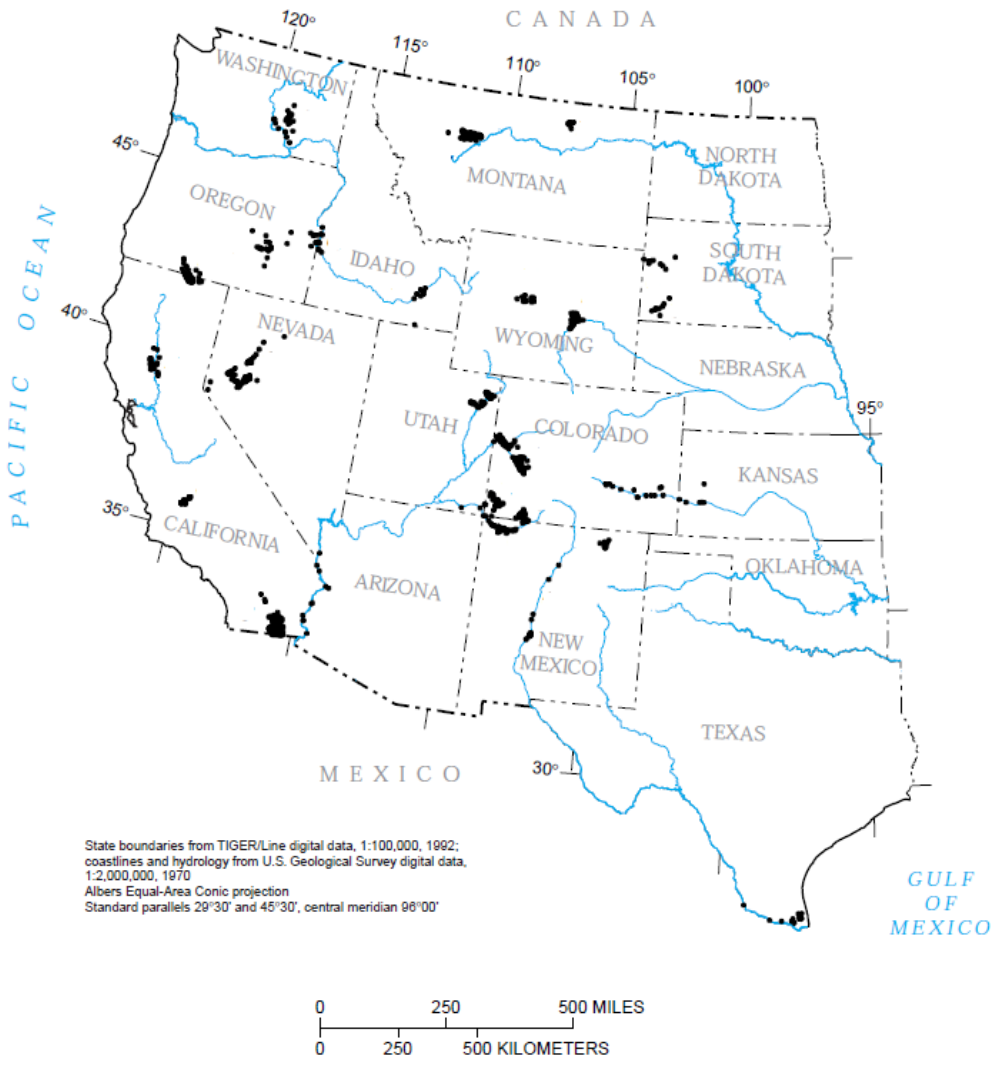

Figure 1.1: Location of Study Area of National Irrigation Water Quality Program (NIWQP) (Siler, 1997)

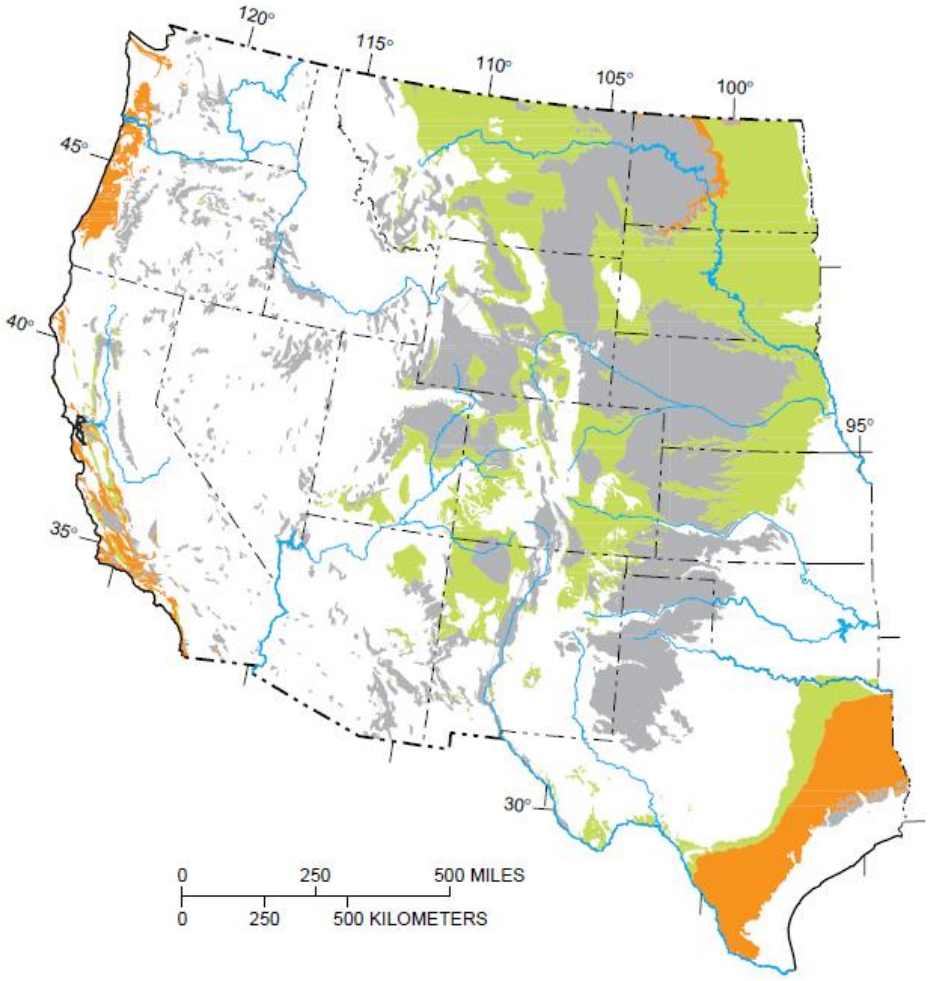

Figure 1.2: Spatial distribution of Upper Cretaceous marine (green) and Tertiary marine and continental (orange and grey) sedimentary deposits (Seiler, 1997).

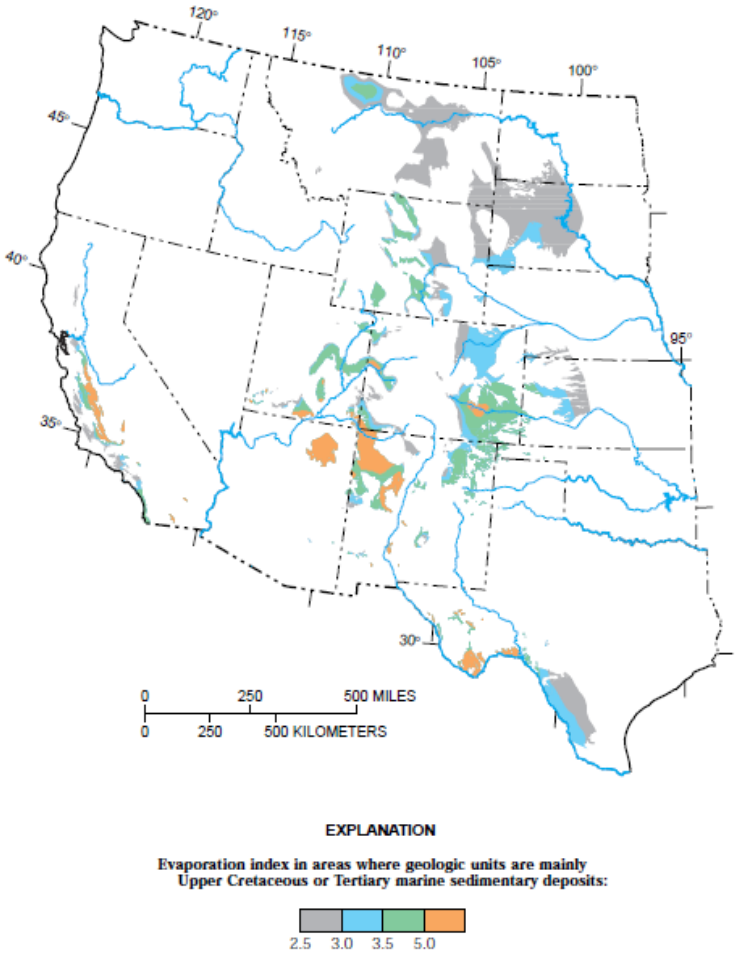

Figure 1.3: Locations of regions in the western United States those are susceptible to irrigation-induced Se contamination (Seiler, 1997).

1.4 RESEARCH OBJECTIVE

The overall goal of this research is to **investigate the best remediation strategies to reduce Selenium and Nitrate mass loadings into the Arkansas River and their concentrations in the groundwater system of the stream-aquifer system in the Lower Arkansas River Valley (LARV) of southeastern Colorado.**

1.5 OVERVIEW OF METHODOLOGY

This section provides a brief description of each chapter of the report where the models involved and the results of the study are detailed. There is also a flow chart of the study.

Chapter 2 provides a description of the study region, including location and extent, climate and geological details, as well as aquifer properties, irrigation, cultivated crops , topography, and land use.

Chapter 3 discusses the methods used to achieve the objective of the study which includes a groundwater flow model (MODFLOW) and a reactive transport model (RT3D) along with their application to the study region and crop parameters. The limitations of the RT3D model also are discussed.

Chapter 4 discusses the sensitivity analysis which is used to identify the influential parameters to calibrate the RT3D model.

Chapter 5 discusses the investigation of best management practices applicable to the study region to reduce the Se and NO_3 mass loadings into the Arkansas River and their concentrations in groundwater. Results also are presented.

Chapter 6 discusses the conclusions of the study, future research, and compares the Downstream Study Region results with the findings from the Upstream Study Region.

The flow chart shown in Figure 1.4 represents the steps involved in the research.

1.5.1 FLOW CHART OF RESEARCH STUDY

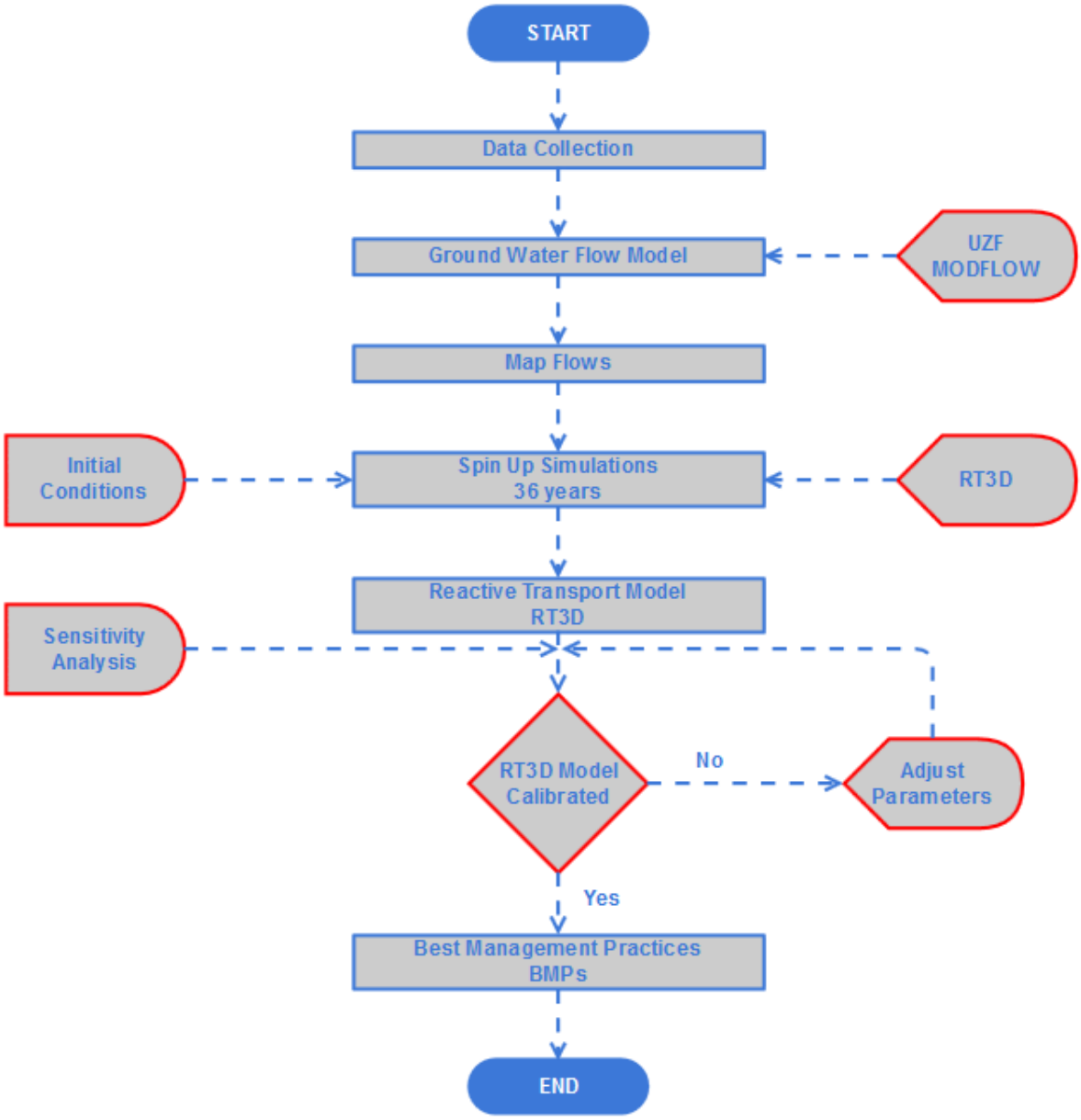

Figure 1.4: Flow Chart of the research study.

CHAPTER NO: 2

2 STUDY REGION DESCRIPTION

2.1 STUDY SITE

The study region, termed as the Downstream Study Region (DSR) is located downstream of John Martin Reservoir and approximately 30 km east of the eastern edge of the Upstream Study Region (USR) (located upstream of the reservoir) as shown in Fig: 2.1. The DSR falls under the Lower Arkansas River Valley (LARV) and stretches from the city of Lamar, eastward to the Colorado - Kansas state line. The DSR covers the valley that extends approximately to a total of 55,200 ha (136,000 acres), of which about 33,000 ha (81,600 acres) are irrigated from canals that divert water from the river or from alluvial pumping wells in the DSR. This area stretches 71 km along the river from the May Valley Drain to the Colorado – Kansas border. A total of 47 groundwater observation wells, 12 locations in tributaries and drains and 6 locations along the river have been routinely monitored for Se and related constituents. In addition, 59 observation wells were sampled periodically (Gates et al, 2009). The cities, shale, the Arkansas River, tributaries, canals, irrigation fields, pumping wells, and observation wells, along with the Downstream Study Region boundaries are presented in Figure 2.1.

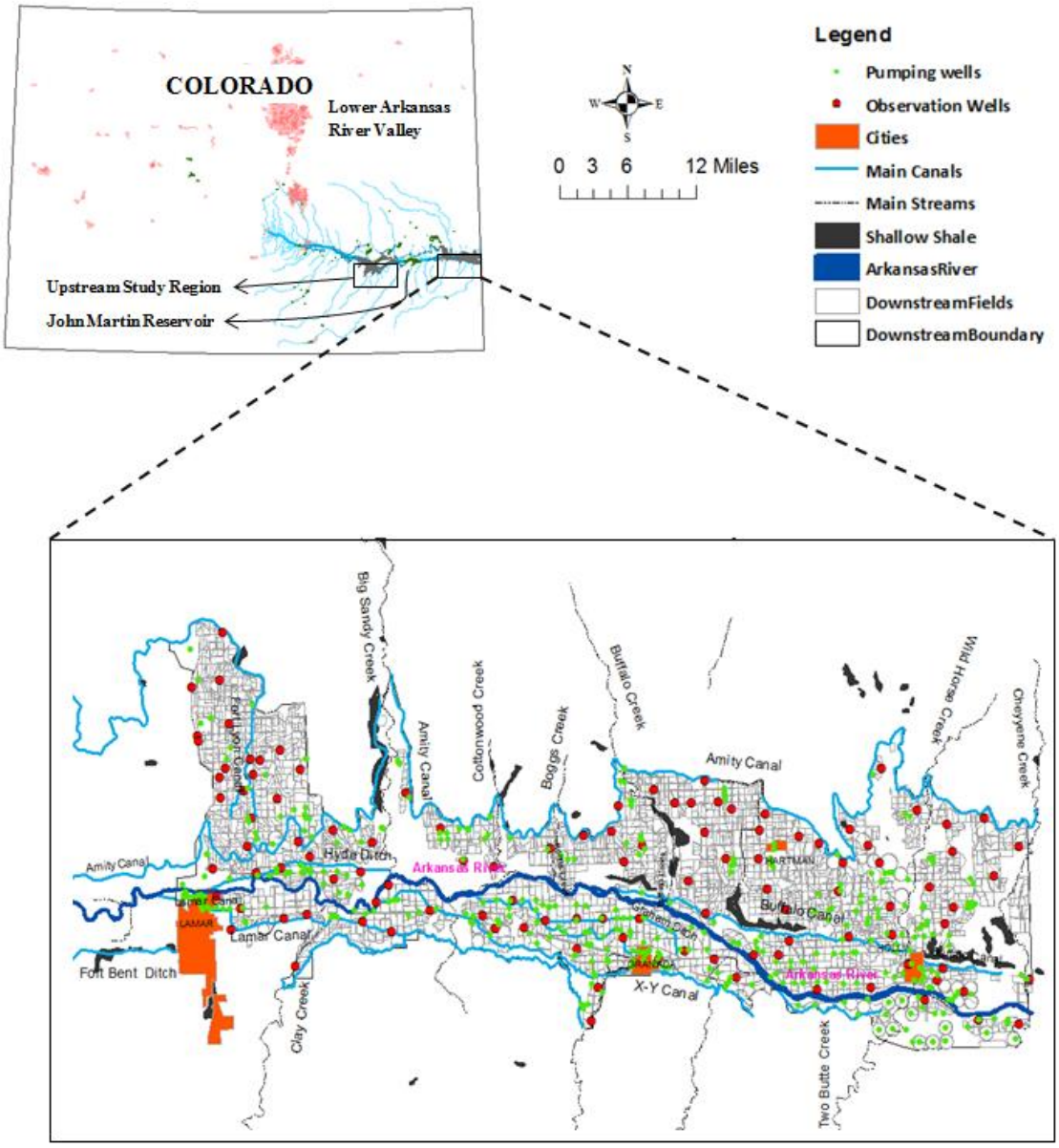

Figure 2.1: Detailed view of the Location and Surface features of Downstream Study region of the Lower Arkansas River Valley.

This study region was chosen for the following reasons:

(a) it is a designated as a seleniferous river basin, as determined through NIWQP (Seiler, 1997);

(b) all river segments have been identified as impaired by Se by the Colorado Department of Public Health and Environment (CDPHE);

(c) since the last decade, Colorado State University has monitored both hydrologic and chemical species components in the region; hence, yielding an extensive data-set of measured groundwater and surface water species concentrations; and

(d) a groundwater flow model for the Downstream Study Region has been constructed, calibrated, and tested (Morway et al, 2013).

2.2 CLIMATE AND LANDUSE

The climate is semi-arid, with average monthly temperatures during winter and summer months ranging from -1^{o}C to 25^{0}C respectively, and precipitation ranges from 0.7 cm and 5.0 cm during winter and summer months respectively.

Land use in the Lower Arkansas River Valley is heavily agricultural , with both surface and groundwater having been utilized to grow crops for more than 10 decades (Colorado Geological Survey website).

2.3 CITIES

There are 4 small cities: Lamar, Granada, Holly, and Hartman, as shown in Figure 2.1. These cities fall under the study region and their locations are shown in figure 2.1. All the cities ~~falls~~ fall under the Prowers County seat. The town of Lamar is located in an area of 4.24 sq. ~~M~~

miles at an elevation of 3622 feet. Of the four cities, it has the largest population, with 7776 people in 2013. Holly is located in an area of 0.8 sq. miles at an elevation of 3387 feet; it has the next highest population of 780 people. Granada covers 0.72 sq. miles and stands at an elevation of 3484 feet; its population is 501. Finally, Hartman covers 0.3 sq. miles and is situated at an elevation of 3600 feet with a population of 75 people. U.S. Highway 50 passes from Lamar through Granada and Holly. Holly is situated at the border between Colorado and Kansas, with lowest elevation of the four cities. The Arkansas River flows from Lamar to Holly as shown in Figure 2.1.

2.4 IRRIGATION

Agricultural production in LARV in Colorado has gone on for more than 10 decades. A total of about 109,000 ha of irrigated lands has required crop water well in excess of the mean average precipitation, so the supplement has had to come from locally pumped and diverted river water to achieve full crop production (Morway et al. 2013). Irrigation has been practiced on 14,000 fields, where water supply is provided by 25 canals that divert water from the river in accordance with the Colorado Water Law and from about 2400 wells that pump from alluvial groundwater (Gates et al, 2012). The majority of the fields in the LARV are irrigated using surface–irrigation methods, and less than 5% of the fields are irrigated using sprinklers or drip lines (Gates et al, 2012). The DSR has 33,000 ha of irrigated lands that cover approximately 30% of the total LARV irrigation lands (Morway et al. 2013). To maintain the imbalance in water requirements, the Pubelo and John Martin Reservoirs storage capture is released during the irrigation season. Alfalfa, corn, grass, wheat, and sorghum are major crops, whereas dry beans, oats, onions, and pumpkin, etc. are minor crops under irrigation in the DSR. Figure 2.2 shows the irrigated crop types for each cultivated field for 2003.

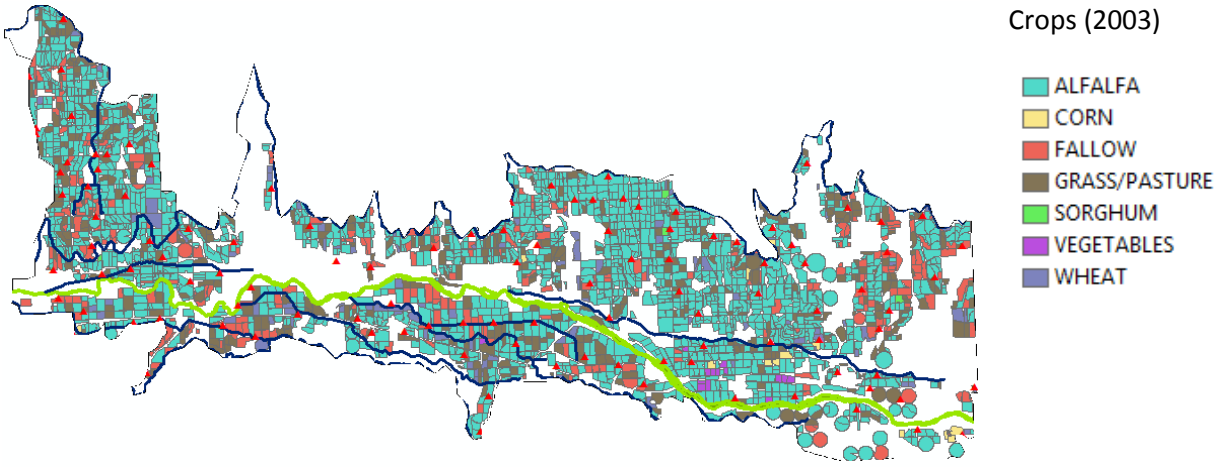

Figure 2.2: Crop types for each cultivated field for the year 2003.

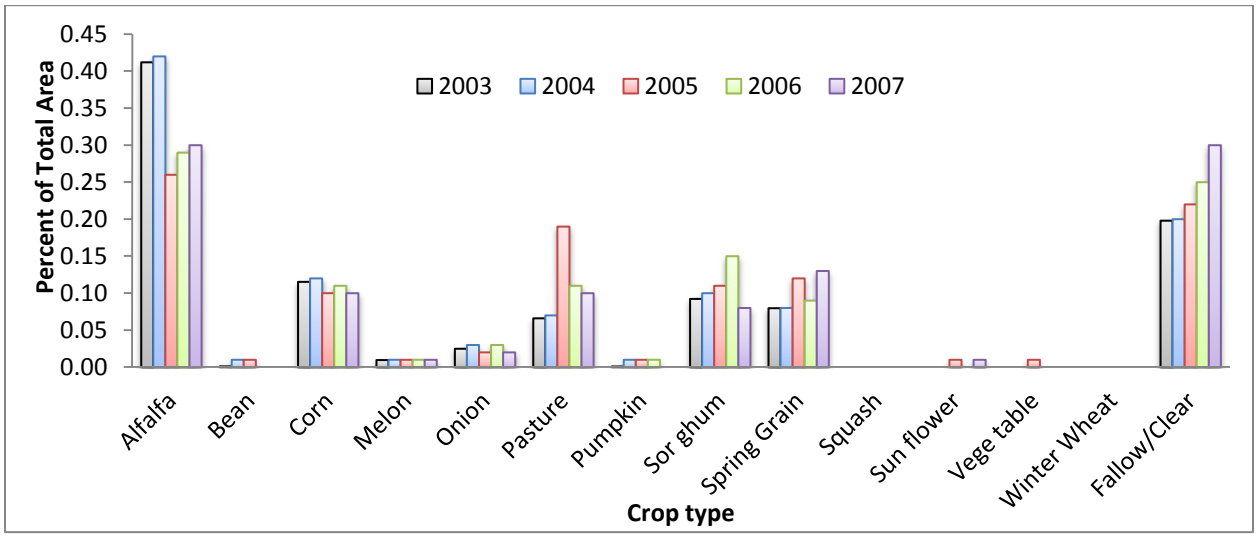

Figure 2.3: Percent of each crop type for each cultivated field from 2003 to 2007 with respect to total area in the study region.

Figure 2.3 shows that alfalfa is the dominant crop, followed by sorghum, corn, grass/pasture, spring grains, onions, melons, sunflowers, soybeans, and vegetables. Principal cash crops such as onions and melons receive the most irrigation water per unit of cultivated

area. The growing season commences mid- to late-March and ends in early November, with un-lined irrigation canals receiving water from the Arkansas River during the period from March 15th to November 15th. Irrigation water is derived from either one of eight main irrigation canals (Amity, Buffalo, Fort Bent, Fort Lyon, Hyde Ditch, Lamar, South Side and XY Graham) or from groundwater pumps, as shown in Figure 2.1. The command areas associated with each canal, i.e., where the cultivated fields receive irrigation water from the same canal, are shown in Figure 2.5. The Amity Command area is subdivided into 3 areas: Amity 1, Amity 2, and Amity 3. The Buffalo Command area is subdivided into 2 areas: Buffalo 1 and Buffalo 2. Similarly, Fort Lyon has been divided into Fort Lyon 1 and Fort Lyon 2, and Lamar is divided into Lamar 1, Lamar 2, and Lamar 3. The XY Graham is divided into XY Graham 1 and XY Graham 2, so the entire study region is divided into a total of 16 command areas, as shown in Figure 2.5. More than 100 years of irrigation in the area has resulted in salinization and water logging because of canal seepage and poor drainage, so a decrease in crop production has resulted (Burkhalter and Gates, 2005).

2.5 GEOLOGY AND AQUIFER

The Arkansas River Basin drains a total area of 28,273 sq. miles in the southeastern part of Colorado, as shown in Figure 2.4. This covers both the Upper and Lower Arkansas River Valleys, but our main target is the Lower Arkansas River Valley where the study region is situated. This basin shows Water Division 2 with the divisional office in Pueblo. A total of 5,450 alluvial wells- have been recorded in the Arkansas River basin as of early 2001 (Colorado Geological Survey website). Agriculture is the main land-use in the Lower Arkansas River Valley. Surface and groundwater are used for crop production with the alluvial aquifer being the source of groundwater, as shown in Figure 2.4.

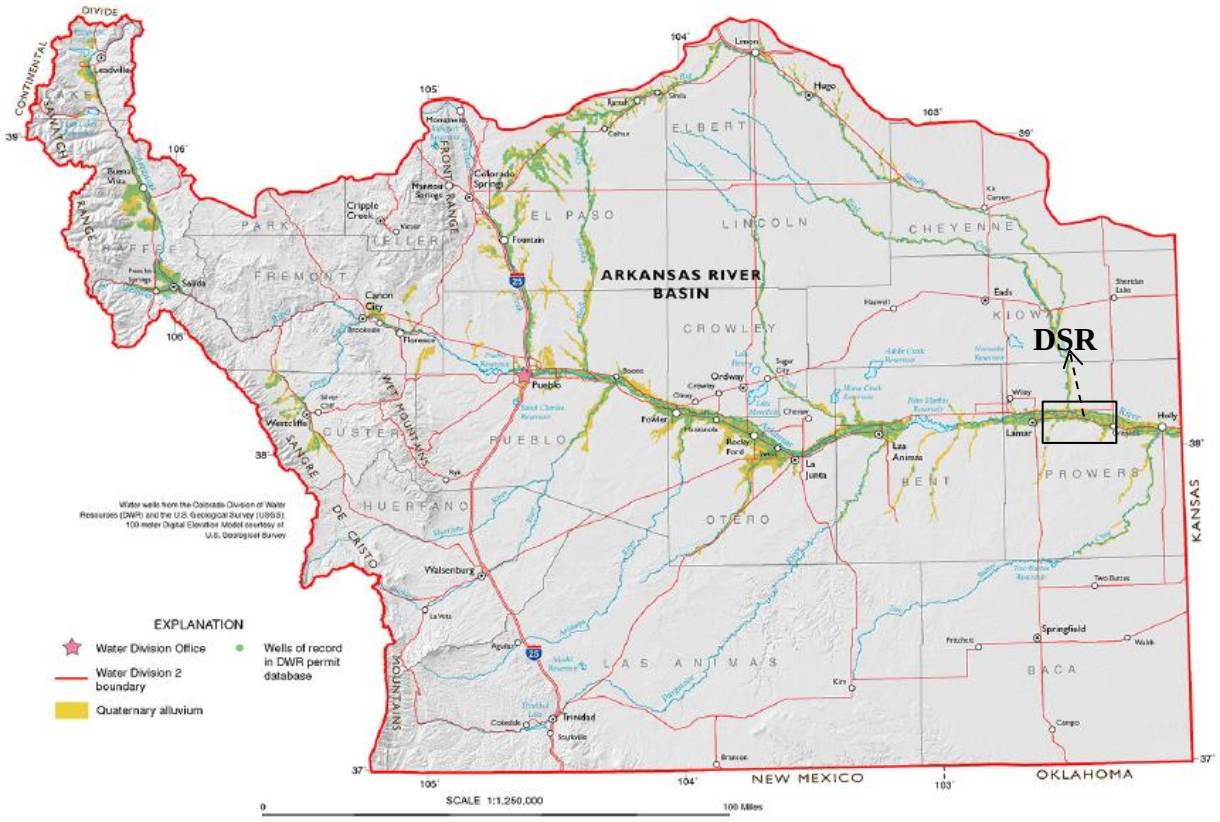

Figure 2.4: Location of Arkansas River basin showing the extent of mapped alluvium from Colorado Geological Survey website.

In LARV, the soils consist of a variety of clay loam, loam, silty clay loam, silty loam, and sandy loam textural classes (Gates et al, 2012). The study region consists of fertile alluvial aquifer ranging from approximately 0 to 45.5 m in thickness; this is underlain by Cretaceous shale in both solid and weathered forms. Figure 2.5 shows the spatial pattern of the aquifer depth in the DSR. The recharge to the alluvial aquifer is mainly through infiltration of surface water through the stream bed of the Arkansas River, as well as through significant infiltration from the unlined irrigation canals and surface application of irrigation water to the alluvial aquifer.

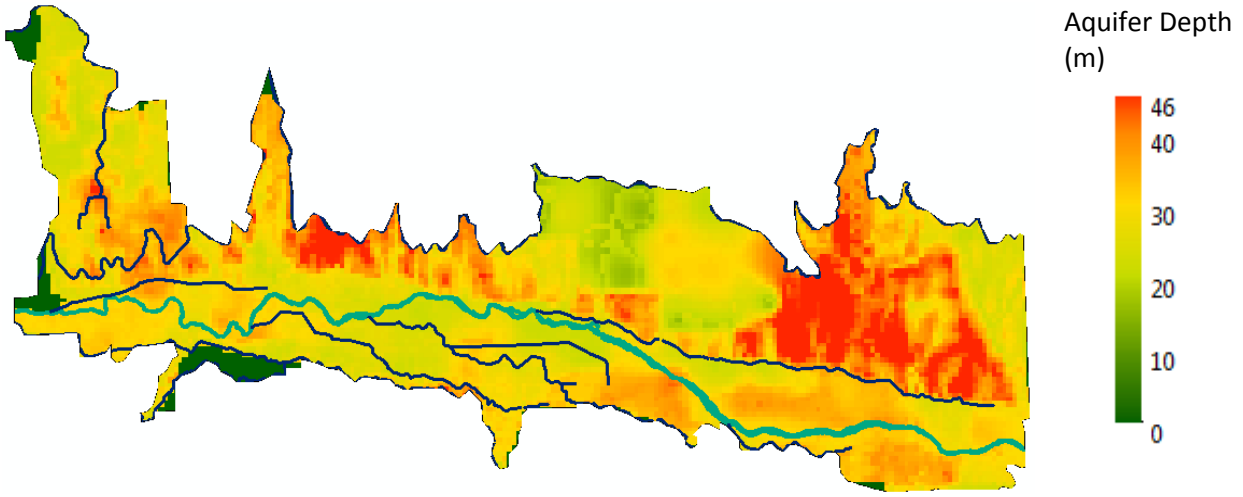

Figure 2.5: Spatial Pattern of Alluvial Aquifer depth (m) in the study region.

The most important hydraulic properties of the aquifers are their ability to store and transmit water. Hydraulic Conductivity (K, L/T) is the measure of ~~its~~ an aquifer's ability to transmit water, and this is mainly dependent on material properties such as permeability and fluid properties. Hydraulic Gradient is the driving force for the transmission of water. The volume of water that can be transmitted by the aquifer is determined by the transmissibility (T, L^2/T)) of the aquifer, where the transmissivity is the product of the hydraulic conductivity and thickness of the aquifer.

The ability to store or release water in the aquifer depends on its storage coefficient. This storage coefficient depends on the type of the aquifer; for example, note unconfined and confined aquifers shown in Figure 2.6. The storage coefficient is usually associated with the storativity of the confined aquifer, where water release depends upon the elasticity of the aquifer and compressibility of the water. In contrast, an unconfined aquifer releases water by physical dewatering of the material which reduces the water table in the aquifer. The specific yield (Sy) is

usually applied to the unconfined aquifer for its storativity. The storage coefficient is higher for unconfined than for confined aquifers.

From Colorado Geological Survey website, the hydraulic characteristics in the Lower Arkansas River Valley are presented in Table 2.1.

Table 2.1: Hydraulic Characteristics in the LARV aquifer from Colorado Geological Survey website.

S.No	Hydraulic Characteristic	Value
1	Transmissivity (ft^2/day)	2,000 – 60,000
2	Hydraulic Conductivity (ft/day)	70 – 1200
3	Discharge (gpm)	10- 4,000
4	Specific Capacity (gpm/ft drawdown)	7 – 54
5	Specific yield	0.13 – 0.20

The LARV covers a total of 14,000 fields in southeastern Colorado. For this research, the hydraulic properties are taken from Morway et al., (2013) for both the Upstream and Downstream Study Regions specifically. The Downstream Study Region hydraulic properties ranges are tabulated in Table 3.1.

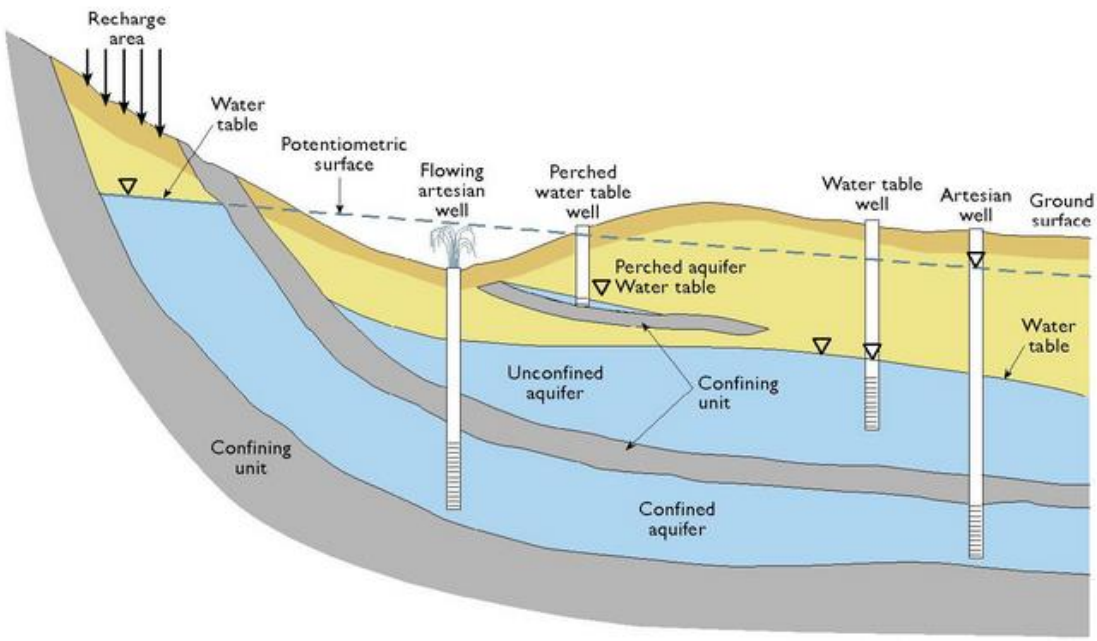

Figure 2.6: Schematic cross section of aquifer types (Colorado Geological Survey Website).

2.6 WATER QUALITY

GroundWater in the alluvial aquifer in the Lower Arkansas River Valley is classified as sodium-calcium, sulfate-bicarbonate in character and is typically fair to good quality (Colorado Geological Survey website). Due to its high irrigation use, the water quality becomes saline and unusable downstream of the LARV. The summary of the hydraulic characteristics and water quality in the Lower Arkansas River valley is tabulated in Table No.2.2.

Table 2.2: Information on water quality and hydraulic characteristics in the LARV.

S.No	Type	Lower Arkansas River Valley
1	Aquifer Characteristics	A heterogeneous mix of interbedded sands, gravels, silts and clays. Width varies from 1 to 10 miles; 30 to 200 thick. Designated groundwater basins include the Upper Black Squirrel and Big Sandy.
2	Primary Uses	Agriculture
3	Water levels	5 - 30 ft.
4	Well data	3400 completed wells 90% < 120 ft. deep mean depth - 58 ft.
5	Yield	variable = 10 - 4,000 gpm
6	Water Quality	Degrades downstream from good in the upper reaches to saline near the Kansas state line. Nitrates and herbicides are periodically detected in shallow alluvial wells in the areas of intense agricultural use.

Being that agriculture is the primary land use in the study region, as clearly shown in Figure 2.7, agriculture only is considered as a non-point source polluting the groundwater and the Arkansas River.

Figure 2.7: Imagery view of the study region on May 2015.

CHAPTER NO: 3

3 METHODOLOGY AND MODELS

3.1 GROUNDWATER FLOW MODEL

MODFLOW is the United States Geological Survey (USGS) modular finite difference flow model which solves the 3-dimensional groundwater equation as shown in Eq. (3.1). USGS has released four major versions of MODFLOW since 1980. This computer code is public domain software and is also considered to be the *defacto* standard code for aquifer simulations and predictions of groundwater flow.

The partial 3D groundwater equation for an unconfined aquifer, heterogeneous, and anisotropic is shown in Eq. (3.1).

$$\frac{\partial}{\partial x}\left[K_{xx}\frac{\partial h}{\partial x}\right]+\frac{\partial}{\partial y}\left[K_{yy}\frac{\partial h}{\partial y}\right]+\frac{\partial}{\partial z}\left[K_{zz}\frac{\partial h}{\partial z}\right]+W=\ S_s\frac{\partial h}{\partial t} \qquad \text{Eq. 3.1}$$

Where

- K_{xx}, K_{yy} and K_{zz} – Hydraulic Conductivity Values along the x, y and z coordinate axes (L/T)
- h is the potentiometric head (L)
- W is a volumetric flux per unit volume representing sources and/or sinks of water (T^{-1}). If W> 0 for flow into the system and where W <0 for flow out of the groundwater system
- S_s is the Specific storage of the aquifer (L^{-1})
- t is time (T)

The finite difference form of the partial differential for a cell (i,j,k) in a discretized aquifer domain is represented by using rows, columns and layers as shown in Figure 3.1, and cell indices are shown in Figure 3.2 in Eq. 3.2.

$$CR_{i,j-1/2,k}\left(h^{m}_{i,j-1,k}-h^{m}_{i,j,k}\right)+\ CR_{i,j+1/2,k}\left(h^{m}_{i,j+1,k}-h^{m}_{i,j,k}\right)$$

$$+ CC_{i-1/2,j,k}\left(h^m_{i-1,j,k} - h^m_{i,j,k}\right) + CC_{i+1/2,j,k}\left(h^m_{i+1,j,k} - h^m_{i,j,k}\right)$$

$$+ CV_{i,j,k-1/2}\left(h^m_{i,j,k-1} - h^m_{i,j,k}\right) + CV_{i,j,k+1/2}\left(h^m_{i,j,k+1} - h^m_{i,j,k}\right)$$

$$+ P_{i,j,k}h^m_{i,j,k} + Q_{i,j,k} = S_{s_{i,j,k}}\left(\Delta r_j \Delta c_i \Delta v_k\right)\frac{h^m_{i,j,k} - h^{m-1}_{i,j,k}}{t^m - t^{m-1}} \qquad \text{Eq. (3.2)}$$

Where

- $h^m_{i,j,k}$ is the hydraulic head at cell (i,j,k) at time step m
- CV, CR and CC are the hydraulic conductance's between node i, j, k and a neighboring node.
- $P_{i,j,k}$ is the sum of coefficients of head from source and sink terms
- $Q_{i,j,k}$ is the sum of constants from source and sink terms
- $Ss_{i,j,k}$ is the specific storage
- $\Delta r_j \Delta c_i \Delta v_k$ are the dimensions of cell i,j,k , represents volume of the cell when multipled.
- t^m is the time at step m

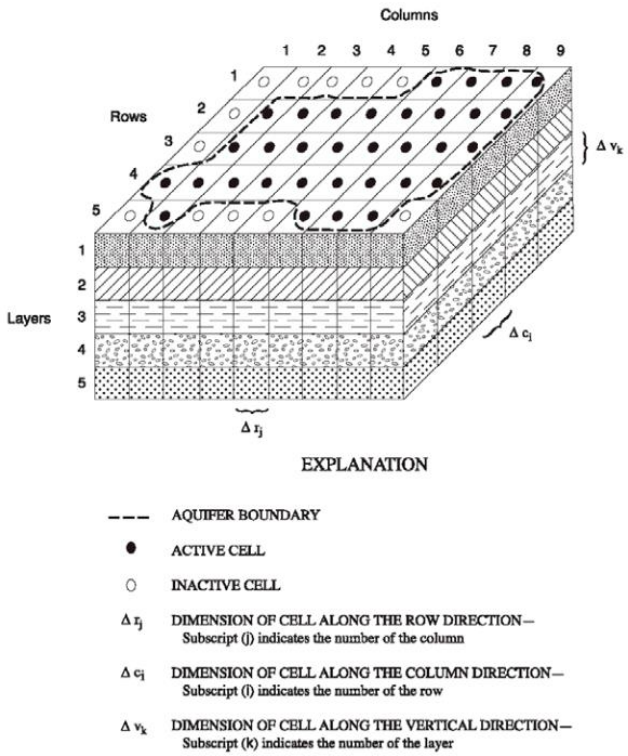

Figure 3.1 Hypothetical discretized aquifer system (McDonald and Harbaugh, 1988, USGS)

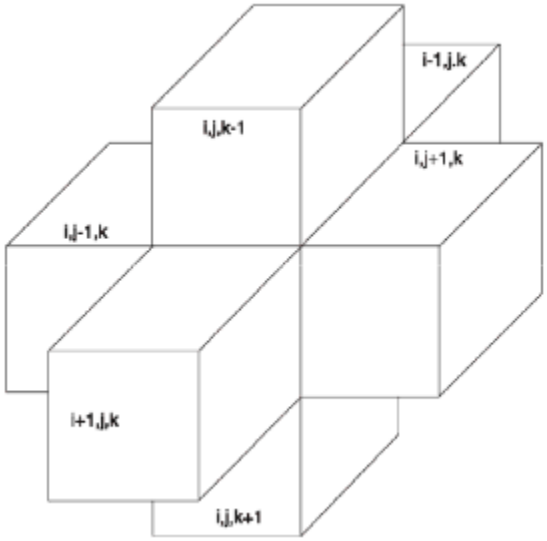

Figure 3.2 Showing six indices for the six adjacent cells surrounding cell i, j, k (McDonald and Harbaugh, 1988, USGS)

One of the major MODFLOW releases is MODFLOW-2005 which is a new version of the finite-difference groundwater model commonly known as MODFLOW-2000. MODFLOW-NWT (Niswonger et. al, 2011) solves the equation with Newton formulation of MODFLOW-2005, and it has the ability to solve difficult unconfined groundwater-flow problems and surface water/groundwater interactions. MODFLOW – NWT is a standalone program that solves the nonlinearities in drying and rewetting of unconfined groundwater flow equations. This software is used with the Upstream – Weighting (UPW) Package, which treats nonlinearities of cell drying and rewetting by using a continuous function of groundwater head. This UPW package calculates inter-cell conductance's with an upstream-weighting approach rather than in Block-centered Flow (BCF) or Layer Property Flow (LPF) packages in which heads in two adjacent cells are used to calculate the inter-cell horizontal conductance. The difference in the 2005 and NWT versions of MODFLOW is the numerical solver. The Newton linearization approach solver is used in NWT, which improves the convergence and computational efficiency because

of applied nonlinear boundary conditions to the groundwater flow. This approach generates an asymmetric matrix, whereas all other solvers of MODFLOW generate a symmetric matrix where all linear solvers solve these symmetric matrices. The Generalized–Minimum-Residual Solver (GMRES) and Orthomin/Stabilized Conjugate-Gradient Solver (CGSTAB) are the two developed asymmetric matrix-solver options included in the MODFLOW –NWT. For details about the GMRES and CGSTAB numerical solvers, refer to Kipp et al, 2008 and Niswonger et al, 2011 respectively.

The Unsaturated Zone Flow (UZF1) (Niswonger et al., 2006) package solves the unsaturated zone flow process by replacing the Recharge and Evapotranspiration (ET) packages of MODFLOW-2005. UZF1 package applies the infiltration rate at land surface instead of specified recharge rate to groundwater directly as in the Recharge package. Precipitation and snow melt are partitioned into different pathways of runoff, evapotranspiration, infiltration, unsaturated–zone storage, and recharge. Firstly, the evaporation losses are taken from the unsaturated zone, which is above the evapotranspiration extinction depth; whenever the demand is not met, the losses are removed directly from the groundwater if the water table is lower than the extinction depth. The process in the unsaturated-zone linked to the saturated-zone is shown in Figures 3.3 and 3.4.

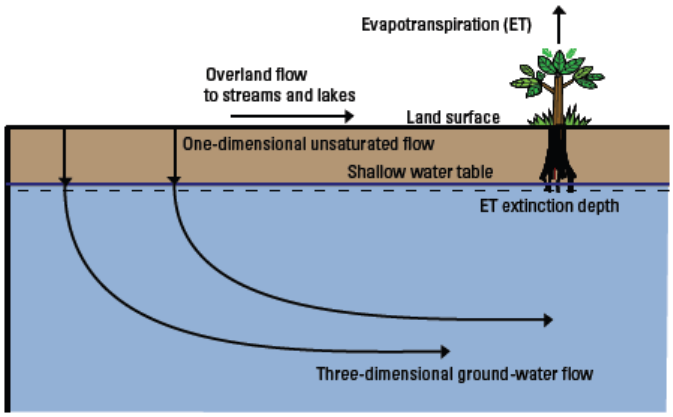

Figure 3.3: One Dimensional unsaturated-zone flow coupled to three-dimensional groundwater flow for shallow water table aquifer (Niswonger et al, 2006)

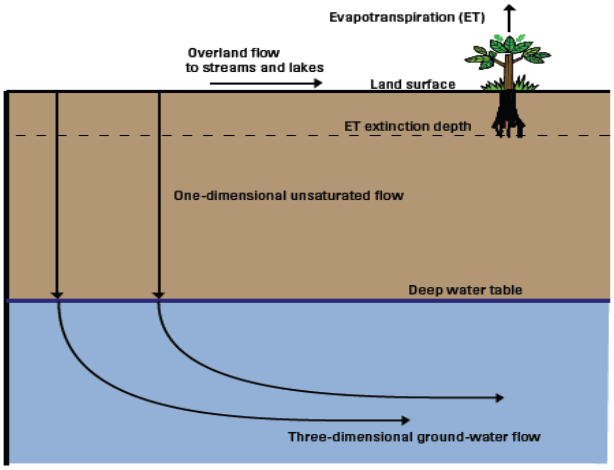

Figure 3.4: One Dimensional unsaturated-zone flow coupled to three-dimensional groundwater flow for deep water table aquifer (Niswonger et al, 2006)

The vertical flow in the unsaturated zone as shown in Figures 3.3 and 3.4 is simulated using the one dimensional form of Richard's equation which is approximated by the kinematic wave equation solved by Method of Characteristics (Niswonger et al, 2006). This approach assumes that the flow in an unsaturated zone occurs due to gravity potential gradients only and ignores the negative potential gradients. It also assumes the homogenous hydraulic properties in the unsaturated zone for each vertical column of model cells. The one-dimensional downward

flow in the unsaturated zone is derived by neglecting the diffusive term in the Richard's Equation, as discussed in Niswonger et al, 2006.

3.1.1 UZF- MODFLOW-NWT MODEL FOR THE DOWNSTREAM STUDY REGION

To model the groundwater flow in the 55,200 ha study area, the MODFLOW–2005 version with the Newton solver (NWT) was used and linked to the UZF1 package. A description of the model construction, modeling methods, and model simulations is presented in Morway et al., (2013). Only the basic details of the model are presented here. The study area was converted to a finite difference surface grid with 102 rows and 217 columns with 250 m spacing in each direction and active cells covering the study region, as shown in Figure 3.5. In MODFLOW simulations, the aquifer is divided into two layers with marine shale bed rock as the 3rd layer, as shown in Figure 3.9. The hydraulic properties for the study region are taken from Morway, et al., 2013 and tabulated in Table No: 3.1. Figure 3.6 and 3.7 shows the spatial pattern of the hydraulic conductivity and specific yield in layer 1 of the aquifer.

Table 3.1: Range of Parameter values employed in the models (Morway et al, 2013).

S.No	Model Parameter	Range of values
1	Layer 1 (K_H)	0.3 - 160 md^{-1}
2	Layer 1 (K_S/K_H)	7.0e-5 - 2.9e-2
3	Layer 2 (K_H)	1.4 - 75 md^{-1}
4	Layer 2 (K_V/K_H)	0.1
5	Layer 1 (Sy)	0.01 - 0.33
6	Layer 2 (Sy)	0.01 - 0.34
7	Layer 1 and 2 Specific Storage	1.70e-05
8	Canal Conductance	1.7e-3 - 8.6 $m^2d^{-1}m^{-1}$
9	Saturated K in UZF1	1.1e-2 - 0.26 md^{-1}
10	ε (Brooks- Corey exponent)	3.5
11	θ_s (UZF1)	0.18 - 0.39
12	Extinction depth	1.3 - 4.5 m

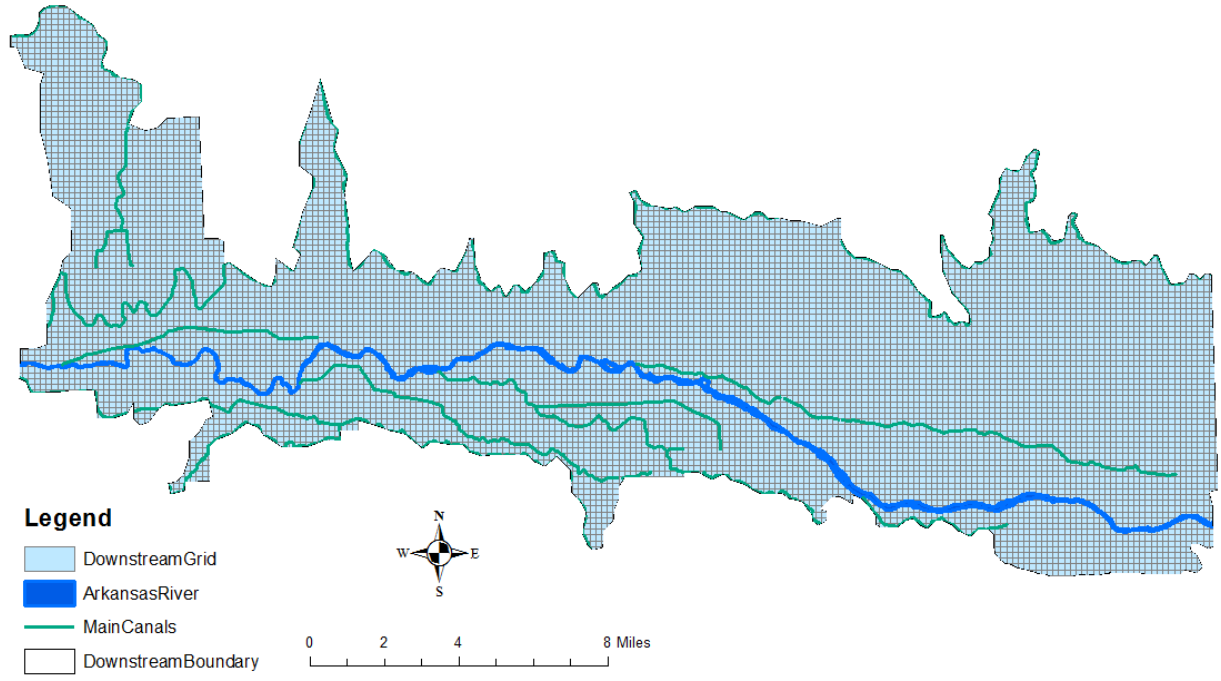

Figure 3.5: Finite Difference surface grid of the study region.

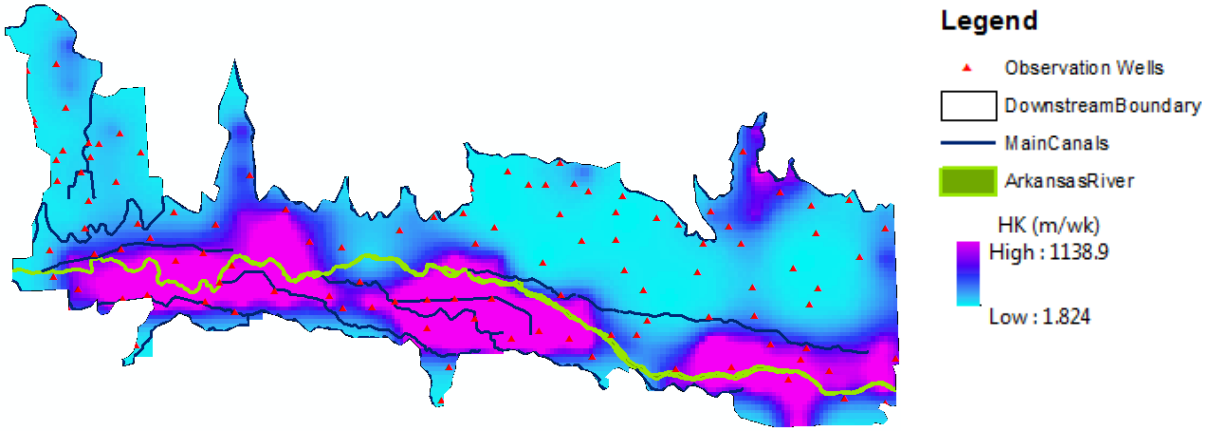

Figure 3.6: Spatial Pattern of Hydraulic Conductivity (m/wk) of layer 1 of the MODFLOW model in the study region.

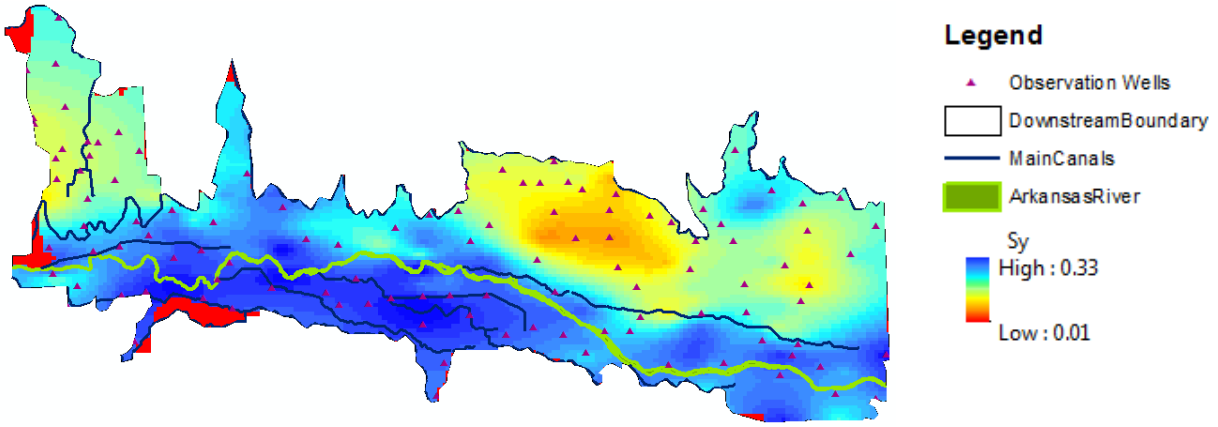

Figure 3.7: Spatial Pattern of Specific Yield of layer 1 of the MODFLOW model in the study region.

The explanation of MODFLOW input and output files, the flow chart showing how the model works, and a sample of the model output are incorporated in Appendix A.

3.2 FATE AND TRANSPORT PROCESSES FOR SELENIUM AND NITROGEN

Selenium involves in many inorganic and biochemical processes on earth extensively. Naturally, selenium behaves similarly to sulfur and follows much of that element's geochemistry (Severson. et al, 1990, USGS). Se occurs primarily in four oxidation states as described below:

Selenate, SeO_4 (+6): SeO_4 is one of the soluble species of Se and a weak sorbent. Selenate is a highly mobile inorganic Se species (Severson et al, 1990) which makes it the most toxic of the Se species. Thus, our primary target is to find remediation strategies to reduce the selenium.

Selenite, SeO_3 (+4): SeO_3 is also a soluble and mobile Se species, but it has a stronger adsorption rate than the selenate (Cantrell et al, 2014).

Elemental Selenium, Se (0): Se is very insoluble in an aqueous system and is naturally resistant to oxidation or reduction (Severson et al, 1990).

Selenide, Se (-2): Se^{-2} is also insoluble in an aqueous system. This species occurs as Organic-Selenomethionine (SeMet) and is a product of the volatilization of SeMet, also called Dimethyl-selenide (DMSe), which is in gaseous form.

As discussed, Se behaves similarly to sulfur, the solid Se found as seleno-pyrite ($FeSe_2$) in geological formations as it replaces the sulfur in pyrite (FeS_2) (Bye and Lund, 1982). Redox and Sorption reactions control the transport of Se species in soil and aquifer systems. Depending on pH, the selenate is reduced to selenite, which further reduces to Se(0), further to SeMet and nontoxic DMSe through volatilization (Bailey et al, 2013a). These process are mediated through a microbial population which is a generic organic carbon compound (CH_2O). These reactions are shown in Eq.(3.3).

$$CH_2O + 2SeO_4^{2-} \longrightarrow CO_2 + 2SeO_3^{2-} + H_2O$$

$$CH_2O + 2SeO_3^{2-} + 2H^+ \longrightarrow CO_2 + Se_{(s)} + 2H_2O \qquad \text{Eq. (3.3)}$$

The Se reduction requires the presence of microbial populations having the required metabolic capacity, the presence of e^- - donors like organic carbon compounds and restricted presence of oxygen (O_2) and nitrate (NO_3) because of e^- - acceptor processes.

The following equations show how SeO_4 can be released from marine shale that consists of seleno-pyrite through oxidation of available Se through autotrophic reduction of O_2 or NO_3 (Bailey et al, 2013a).

$$2FeSe_2 + 7O_2 + 2H_2O \longrightarrow 2Fe^{2+} + 4SeO_4^{2-} + 4H^+$$

$$5FeSe_2 + 14NO_3^- + 4H^+ \longrightarrow 5Fe^{2+} + 10SeO_4^{2-} + 7N_2 + 2H_2O \qquad \text{Eq. (3.4)}$$

The primary target is to reduce the Se contamination in the SeO_4 anion which depends on the presence of O_2 and NO_3. Thus the reduction in NO_3 will simultaneously lead to reduction of SeO_4 in the aquifer (Gates et al, 2009 and Bailey et al, 2013a).

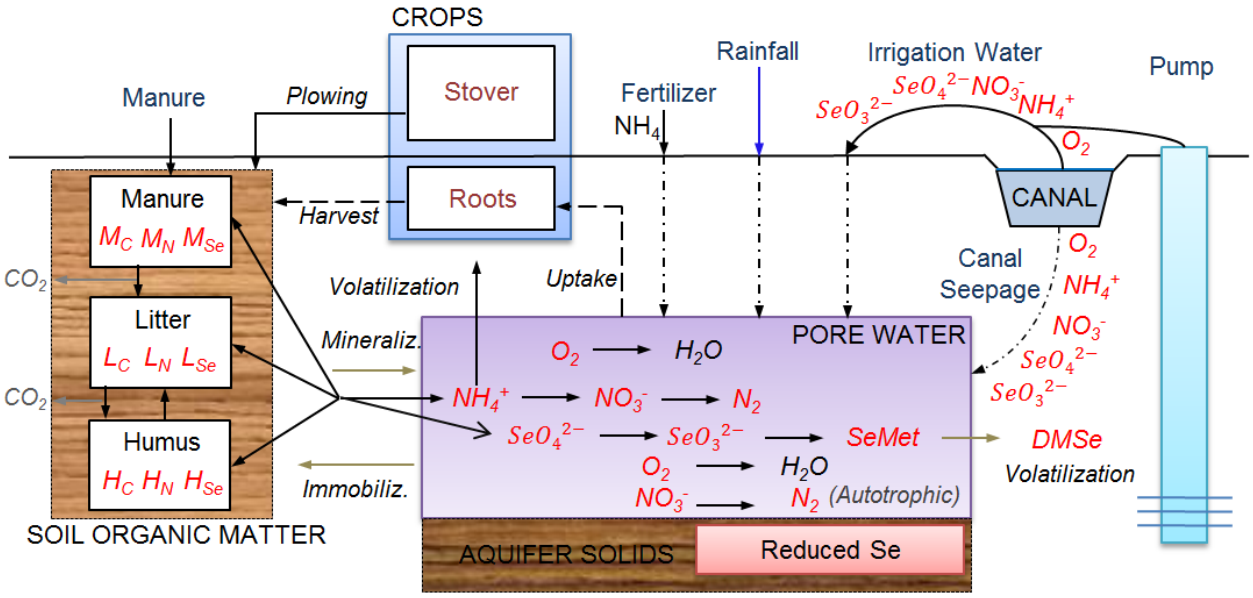

Figure 3.8: Fate and Transport process of Selenium, Nitrogen and Carbon solid – phase and dissolved – phase species in agricultural groundwater systems (after Bailey et al., 2014).

Figure 3.8 shows the concept of the fate and transport process of selenium and nitrogen in solid and dissolved phases. The chemical reactions include organic matter decomposition, mineralization/immobilation, heterotrophTic and autotrophic reduction, volatilization and sorption.

The model includes the six mobile dissolved phase species which are O_2, NH_4-N, NO_3-N, SeO_4 – Se, SeO_3-Se and SeMet, where in solid phase the humus (H), litter (L), and manure (M) which represent the soil organic matter are included. For simplicity, NH_4-N, NO_3-N, SeO_4-Se, SeO_3-Se will be written as NH_4, NO_3, SeO_4, SeO_3 throughout the report. Like other nutrients,

crops require Se to be distributed to the entire plant and then deposited back into the soil by decaying root mass or above the ground (stover) when it has not been removed ~~at~~ during the previous harvest (Bailey et al, 2013a). This is ~~as~~ shown in Figure 3.8. The litter pool includes the dead root mass after the harvest, the remaining root mass at plowing, and stover after the harvest.

The soil's organic matter is mineralized to inorganic SeO_4 or SeO_3, which can further leach into the soil profile, be sorbed or reduced to Se, SeMet, or DSMe, or used by the crops in the next season. The microbes convert inorganic Se species to the organic Se forms to fulfill the Se cellular requirements; this is known as Immobilization (Ajwa et al, 1998). Plants take up the SeO_4 more often than the SeO_3 from the soil (Sors et al, 2005, Bisbjerg and Gissel-Nielsen, 1969 and Sager 2006). The species enters the groundwater system through fertilizer, irrigation water, and canal seepage, as shown in Figure 3.8.

3.3 REACTIVE TRANSPORT MODEL (UZF-RT3D)

The reactive transport model for the Se and N is UZF- RT3D, presented in Bailey et al. (2013b) and Bailey et al. (2014). The UZF-RT3D model was developed by linking the RT3D model of Clement, (1997) and Clement et al, (1998) and adjusted to simulate the variably – saturated reactive transport with the Unsaturated Zone Flow (UZF1) package of MODFLOW-NWT (Niswonger et al, 2011). The UZF1 package was discussed in Section 3.1; it neglects the diffusive term in the one dimensional Richard's Equation. The RT3D uses a one-dimensional downward flow in the unsaturated zone, ET from the saturated and unsaturated zones, three dimensional flow in the saturated zone, as shown in Figures 3.3 and 3.4, and flow sources and sinks from MODFLOW-UZF1. UZF-RT3D solves the advection-dispersion reaction (ADR) for

the dissolved and solid phase as shown in Eq. (3.5) and Eq. (3.6) respectively by using the operator split strategy (Yeh and Tripathy, 1989; Clement, 1997; Bailey et al, 2013b)

$$\frac{\partial(C_k\theta)}{\partial t}R_k = \frac{\partial(\theta\vartheta_i C_k)}{\partial x_i} + \frac{\partial}{\partial x_i}\left[\theta D_{ij}\frac{\partial C_k}{\partial x_j}\right] + q_f C_{fk} + \theta r_f \quad k = 1,2,\dots m \qquad \text{Eq. (3.5)}$$

$$\frac{\partial(C_l\varepsilon)}{\partial t} = \alpha_l P_s + \varepsilon r_s \quad l = 1,2,\dots n \qquad \text{Eq. (3.6)}$$

Where

- m and n are the total number of dissolved and solid phase respectively
- C_k and C_l are the concentrations of k^{th} dissolved and l^{th} solid phase species respectively ($M\ L^{-3}$)
- D_{ij} is the hydrodynamic dispersion coefficient (L^2T^{-1});
- ϑ is the pore velocity (LT^{-1}) from MODFLOW-UZF1;
- θ and ε is the volumetric water content and volumetric solid content respectively
- q_f is the volumetric flux of water representing source/sinks from MODFLOW
- C_{fk} is the concentration of the source/sink for the k^{th} dissolved –phase species
- P_s is the mass application rate of all solid-phase sources for the l^{th} solid-phase species
- α_l is the fraction of P_s attributed to species l
- r_f and r_s is the rate of all reactions that occur in the dissolved and solid phase species respectively
- R_k is the retardation factor for the k^{th} dissolved-phase species, equal to $1+(\rho_b K_{d,k})/\theta$;
- ρ_b is the bulk density of the porous media (ML^{-3}) and $K_{d,k}$ is the partitioning coefficient for the k^{th} species ($L^{-3}M$)

Using the Eq. (3.5) of the ADR equation and the fate and transport mechanism, the Se dissolved phase species equations are written as in Eq. (3.7).

$$\frac{\partial(C_{SeO4}\theta)}{\partial t}R_{SeO4} = \frac{\partial(\theta\vartheta_i C_{SeO4})}{\partial x_i} + \frac{\partial}{\partial x_i}\left[\theta D_{ij}\frac{\partial C_{SeO4}}{\partial x_j}\right] + q_f C_{fSeO4} + F_{SeO4} - U_{SeO4} + \varepsilon\left(r_{s,se}^{min} - r_{s,se}^{imm}\right) + \theta\left(r_{f\,SeO4}^{auto} - r_{f\,SeO4}^{het}\right)$$

$$\frac{\partial(C_{SeO3}\theta)}{\partial t}R_{SeO3} = \frac{\partial(\theta\vartheta_i C_{SeO3})}{\partial x_i} + \frac{\partial}{\partial x_i}\left[\theta D_{ij}\frac{\partial C_{SeO3}}{\partial x_j}\right] + q_f C_{fSeo3} - U_{SeO3} + \varepsilon\left(r_{s,se}^{min} - r_{s,se}^{imm}\right) + \theta\left(r_{f_{SeO4}}^{het} - r_{f_{SeO3}}^{het(se_s)} - r_{f_{SeO3}}^{het(SeMet)}\right)$$

$$\frac{\partial(C_{SeMet}\theta)}{\partial t}R_{SeO4} = \frac{\partial(\theta\vartheta_i C_{SeMet})}{\partial x_i} + \frac{\partial}{\partial x_i}\left[\theta D_{ij}\frac{\partial C_{SeMet}}{\partial x_j}\right] + q_f C_{fSeMet} - U_{SeMet} + \theta\left(r_{f_{SeO3}}^{het(SeMet)} - r_{f_{SeMet}}^{het}\right)$$

Eq. (3.7)

Similarly, the mathematical equations for the NH_4, NO_3 and O_2 are shown in Eq. (3.8)

$$\frac{\partial(C_{NH4}\theta)}{\partial t}R_{NH4} = \frac{\partial(\theta\vartheta_i C_{NH4})}{\partial x_i} + \frac{\partial}{\partial x_i}\left[\theta D_{ij}\frac{\partial C_{NH4}}{\partial x_j}\right] + q_f C_{fNH4} + F_{NH4} - U_{NH4} + \varepsilon\left(r_{s,N}^{min} - r_{s,N}^{imm}\right) + \theta\left(-r_f^{nit} - r_f^{vol}\right)$$

$$\frac{\partial(C_{NO3}\theta)}{\partial t} = \frac{\partial(\theta\vartheta_i C_{NO3})}{\partial x_i} + \frac{\partial}{\partial x_i}\left[\theta D_{ij}\frac{\partial C_{NO3}}{\partial x_j}\right] + q_f C_{fNO3} + F_{NO3} - U_{NO3} + \theta\left(r_f^{nit} - r_{f,NO3}^{het} - r_{f,NO3}^{auto}\right)$$

$$\frac{\partial(C_{O2}\theta)}{\partial t} = \frac{\partial(\theta\vartheta_i C_{O2})}{\partial x_i} + \frac{\partial}{\partial x_i}\left[\theta D_{ij}\frac{\partial C_{O2}}{\partial x_j}\right] + q_f C_{fO2} + \theta\left(-r_{f,O2}^{het} - r_{f,O2}^{auto}\right)$$

Eq. (3.8)

Where

min and *imm* defines the mineralization and immobilization respectively; and *auto* and *het* represents autotrophic and heterotrophic chemical reduction respectively.

The solid phase equations are written using the Eq. (3.6) for humus pool, litter pool and manure as shown in Eq. (3.9)

$$\frac{\partial(C_{L_{se}}\varepsilon)}{\partial t} = \alpha_{Rt,Se}P_{Rt} + \alpha_{St,Se}P_{St} + \varepsilon\left(r^{dec}_{s,Se(H\to L)} + r^{dec}_{s,Se(M\to L)} + r^{dec}_{s,Se(L\to L)} - r^{dec}_{s,Se(L)}\right) + \varepsilon\left(r^{imm}_{s,Se(L)} - r^{min}_{s,Se(L)}\right)$$

$$\frac{\partial(C_{H_{se}}\varepsilon)}{\partial t} = \varepsilon\left(r^{dec}_{s,Se(L\to H)} - r^{dec}_{s,Se(H)}\right) + \varepsilon\left(r^{imm}_{s,Se(H)} - r^{min}_{s,Se(H)}\right)$$

$$\frac{\partial(C_{M_{se}}\varepsilon)}{\partial t} = M_{se} - \varepsilon\left(r^{dec}_{s,Se(M)}\right) + \left(r^{imm}_{s,Se(M)} - r^{min}_{s,Se(M)}\right) \quad \text{Eq. (3.9)}$$

Where

P_{Rt} and P_{St} are the application rates of root and after- harvest stover mass respectively;

dec represents organic matter decomposition; and

L, *H* and *M* represent the litter pool, humus pool and manure respectively with direction shows the mass flow.

The explanation of RT3D input and output files and the flow chart show how the model works, and a sample of the model output was incorporated in Appendix B.

3.4 APPLICATION OF MODFLOW AND UZF-RT3D TO STUDY REGION

As discussed in the sections about groundwater flow, (MODFLOW – UZF1) and reactive transport (UZF-RT3D) are applied to the study region in LARV. The 55,200 ha study region consists of 33,000 irrigated ha, which covers 30% of the irrigated land in LARV.

The study region consists of alluvial aquifer with varying thickness of 0 to 45.5 m. The study area is divided into a finite difference grid with a total of 22,134 cells out of which 9313 are active cells covering the study region as shown in Figure 3.5.

In the groundwater flow model (Morway et al., 2013), the aquifer is divided into 3 layers with marine shale bed rock as the third layer. The model calculates the spatial hydraulic heads in

each layer, whereas in the RT3D, the aquifer was divided into 7 layers with bed rock of marine shale as the 7th layer, and the remaining layers covering the 2 layers of MODFLOW, as shown in Figure 3.9.

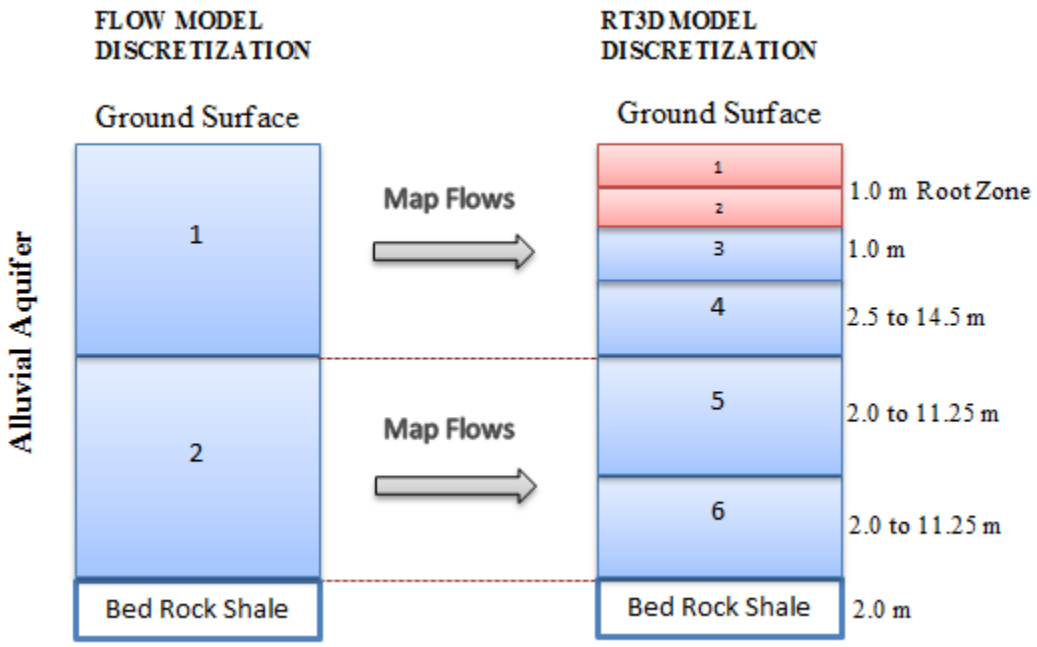

Figure 3.9: Mapping from MODFLOW to RT3D layers of the alluvial aquifer depth in the study region.

In order to preserve the groundwater flow field as established through the calibration procedure performed by Morway et al, 2013, Figure 3.9 explains how the volumetric flow rates, volume of water sources, and groundwater sinks are mapped from the three-layer grid to the seven-layer grid using Map Flows which convert the MODFLOW output to use as an input file for the RT3D. The conversion rules are stated below:

- Volumetric water content is mapped directly, with values from the original first layer given to layers 1-4, and values from the original second layer given to layers 5-6.
- The flux of infiltrated water for the original first layer is given to the first layer of the new grid to preserve the infiltration of water at the ground surface; for all other layers, the flux of infiltrated water is mapped according to the layer thicknesses of the new grid, e.g., the infiltrated flux in the first layer of the original grid is divided and given to the top four layers in the new grid according to the thicknesses of the four layers
- The saturated thickness for each layer of the seven-layer grid is calculated using the location of the water table in the three-layer grid
- Volumetric flow rates in the horizontal directions are mapped according to the location of the water table in the three-layer grid, i.e., a layer in the new grid does not receive lateral flow if the water table is below the bottom of the layer
- For vertical flow rates in the upward direction, i.e., flowing from the second layer to the first layer in the original grid, the flow is added only to the fourth layer in the new grid
- Pumping volumes are assigned to layer 5 in the new grid (assigned to layer 2 in the original grid)
- Layers corresponding to designated river cells (cells that exchange water between the aquifer and surface water bodies) are determined in accordance with the bed of the surface water channel (canal, tributary, or Arkansas River)

The MODFLOW simulates 292 stress periods, each consisting of a week from May 2002 to August 2007, so the volumetric flow rates are divided by 7 in the RT3D model to convert from weekly rates into daily rates. So the daily flow rates and sources/sinks

remain constant for the entire given week, where RT3D simulates the reactive transport for 252 stress periods from June 2003 to August 2007.

3.4.1 CROP PARAMETERS

For the Downstream Study Region, the crop types and corresponding crop parameters are contained in Tables 3.2 to 3.5. Table 3.2 contains parameters concerning crop cultivation (planting, harvesting, plowing, root mass, and stover mass). Table 3.3 contains parameters concerning root growth. Table 3.4 contains parameters concerning nitrogen fertilizer and crop uptake, and Table 3.5 contains parameters concerning selenium root mass, stover mass, fertilizer, and crop uptake. The crop parameters are taken from the similar study of the Upstream Study Region research done by Bailey, 2012. Figure 3.11 shows the scheduling of cultivation practices (fertilizer loading, planting, irrigation application, harvesting, and plowing) for a typical growing season. Typically, 40% of the annual fertilizer load is applied one week before planting, with the remaining 60% applied six weeks after planting.

Each surface grid cell receives a set of crop parameter values depending on the crop type cultivated during the current growing season with the possibility that crop type may change from year to year. See Figure 3.10 for the crop type of each cultivated field in the Downstream Region for the 2006 growing season. In the event that portions of multiple cultivated fields reside in a single grid cell, a weighting scheme is used to calculate composite crop parameter values according to the spatial area of each field contained within the grid cell. A similar weighting scheme is used to determine the concentration of chemical species in infiltrating water for each grid cell, since each field contained within a grid cell may have a different source of irrigation

water (e.g., canal water, pumped aquifer water) with accompanying species mass, and, hence, a composite species concentration must be determined.

Table 3.2: General crop parameters for each crop type cultivated in the Downstream Study Region (Refer to List of Abbreviations for the abbreviation of the parameters).

Crop	PLDY (d)	HVTP (yr)	FYR (yr)	HVDY (d)	PGDY (d)	PGDP (m)	RTHV (kg/ha)	CBRT (-)	STPG (kg/ha)	CBST (-)	FLR (-)
Alfalfa	120	5	3	273	293	1	500	0.4	561.6	0.4	0.8
Bean	140	1	1	273	293	0.8	500	0.3	561.6	0.3	0
Corn	121	1	1	298	318	1	500	0.4	5616	0.4	0
Melon	135	1	1	222	242	1	500	0.4	561.6	0.4	0
Onion	79	1	1	258	278	1	500	0.4	561.6	0.4	0
Pasture	242	5	3	273	293	1	500	0.4	0	0.4	0.8
Pumpkin	152	1	1	273	293	1	500	0.4	561.6	0.4	0
Sorghum	140	1	1	288	308	1	500	0.4	1684.8	0.4	0
SpringGrain	91	1	1	196	216	1	500	0.4	1684.8	0.4	0
Squash	140	1	1	206	226	1	500	0.4	561.6	0.4	0
Sunflower	152	1	1	283	303	1	500	0.4	561.6	0.4	0
Vegetable	115	1	1	242	262	1	500	0.4	561.6	0.4	0
WinterWheat	273	1	1	186	206	1	500	0.4	1684.8	0.4	0
Clear	0	0	0	0	0	0	0	0	0	0	0

Table 3.3: Root growth parameters for each crop type.

Crop	RTDP (m)	RTB (-)	RTC (-)	RBETA (-)
Alfalfa	1.829	0.1	0.05	5
Bean	0.914	0.05	0.05	5
Corn	1.219	0.07	0.05	5
Melon	1.219	0.1	0.07	5
Onion	0.457	0.05	0.045	5
Pasture	0.914	0.05	0.045	5
Pumpkin	0.914	0.08	0.06	5
Sorghum	0.914	0.1	0.05	5
SpringGrain	0.914	0.1	0.07	5
Squash	0.914	0.05	0.1	5
Sunflower	0.914	0.05	0.06	5
Vegetable	0.914	0.05	0.06	5
WinterWheat	0.914	0.05	0.06	5
Clear	0	0	0	0

Table 3.4: Nitrogen Plant Parameters.

Crop	CNRT (-)	CNST (-)	FNO3 (kg/ha)	FNH4 (kg/ha)	FUREA (kg/ha)	NUP (kg/ha)	NB (-)	NC (-)	NBETA (-)	MNCN (-)
Alfalfa	25	50	0	22.4	0	22.4	1	0.08	5	20
Bean	25	45	0	140	0	84.2	1	0.08	5	20
Corn	70	50	0	252	0	224.6	2	0.06	5	20
Melon	25	50	0	112	0	112.3	2	0.1	5	20
Onion	25	50	0	140	0	78.6	1.3	0.055	5	20
Pasture	70	50	0	0	140	112.3	1.2	0.055	5	20
Pumpkin	25	50	0	140	0	84.2	1	0.08	5	20
Sorghum	70	50	0	0	112	112.3	1	0.07	5	20
SpringGrain	70	50	0	0	112	112.3	2	0.09	5	20
Squash	25	50	0	140	0	84.2	3	0.12	5	20
Sunflower	25	50	0	140	0	84.2	2	0.11	5	20
Vegetable	25	50	0	140	0	84.2	2	0.11	5	20
WinterWheat	70	50	0	0	112	112.3	2	0.09	5	20
Clear	0	0	0	0	0	0	0	0	0	0

Table 3.5: Selenium Plant Parameters

Crop	SEST (-)	SERT (-)	FSE (g/ha)	SEUP (g/ha)	MNSE (-)
Alfalfa	0.0001	0.0002	0	1.3	0.003
Bean	0.00005	8E-05	0	0.3	0.003
Corn	0.0013	0.0022	0	10.8	0.003
Melon	0.00005	8E-05	0	1.3	0.003
Onion	0.00005	8E-05	0	2.7	0.003
Pasture	0.0032	0.0053	0	10.7	0.003
Pumpkin	0.00005	8E-05	0	2.7	0.003
Sorghum	0.0013	0.0022	0	10.4	0.003
Spring Grain	0.0013	0.0022	0	8.7	0.003
Squash	0.00005	8E-05	0	2	0.003
Sunflower	0.00005	8E-05	0	0.1	0.003
Vegetable	0.00005	8E-05	0	2.7	0.003
Winter Wheat	0.0013	0.0022	0	8.7	0.003
Clear	0	0	0	0	0

The general, root, nitrogen, and selenium crop parameters are mapped to the cells of the surface grid using cell crop arrays:

Table 3.6: A sample of cell wise distribution of various crops in the study region for 2004 year.

	Alfalfa	Bean	Corn	Melon	Onion	Pasture	Pumpkin	Sorghum	Spring Grain	Squash	Sunflower	Vege table	WinterWheat	Clear
Cell1	0.42	0	0	0	0	0	0	0.58	0	0	0	0	0	0
Cell2	1	0	0	0	0	0	0	0	0	0	0	0	0	0
Cell3	1	0	0	0	0	0	0	0	0	0	0	0	0	0
Cell4	0.39	0	0	0	0	0	0	0	0	0	0	0	0	0.61
Cell5	1	0	0	0	0	0	0	0	0	0	0	0	0	0
Cell6	1	0	0	0	0	0	0	0	0	0	0	0	0	0
Cell7	0.82	0	0.18	0	0	0	0	0	0	0	0	0	0	0
Cell8	0.11	0	0.89	0	0	0	0	0	0	0	0	0	0	0
Cell9	0.08	0	0.57	0	0	0	0	0	0.36	0	0	0	0	0
Cell10	0.52	0	0	0	0	0	0	0	0.48	0	0	0	0	0
Cell11	0.89	0	0.11	0	0	0	0	0	0	0	0	0	0	0
Cell12	0.06	0	0.94	0	0	0	0	0	0	0	0	0	0	0
Cell13	1	0	0	0	0	0	0	0	0	0	0	0	0	0
Cell14	1	0	0	0	0	0	0	0	0	0	0	0	0	0
Cell15	1	0	0	0	0	0	0	0	0	0	0	0	0	0

For each surface cell in the model grid, the portion of the grid cell occupied by each crop type is specified for each year of the simulation. A scenario with multiple fields residing in a single grid cell is shown in Figure No. 3.10. For example, Cell 1 contains portions of two fields, with one field growing alfalfa and occupying 42% of the cell area; another field is growing sorghum, occupying 58% of the cell area. Cell 15 is completely encompassed by a field growing alfalfa; hence, the Alfalfa term is given a value of 1.00. For cells encompassing more than one field, the subroutines within the NTR package apply a weighting scheme that calculates composite crop parameters for the grid cell depending on the crop type of the fields within the cell.

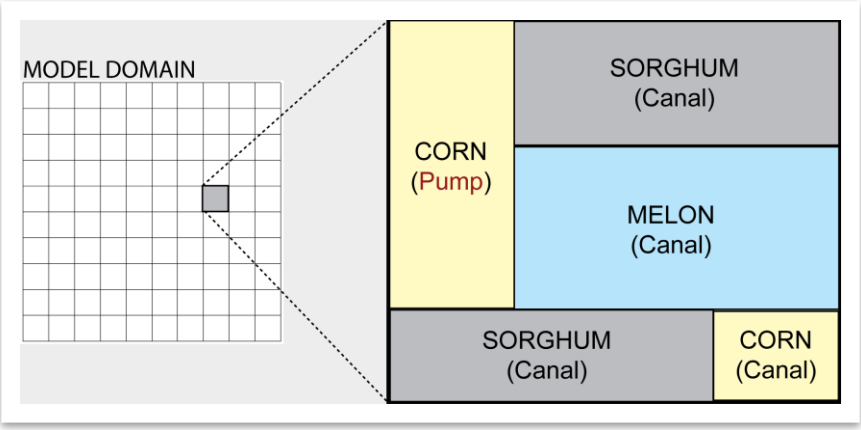

Figure 3.10: Situation of multiple irrigated fields comprising a single grid cell. The fields also receive irrigation water from different sources (canal vs. pumping well), and, hence, the species concentration associated with the infiltrating water also must be weighted (from Bailey.et al., 2014).

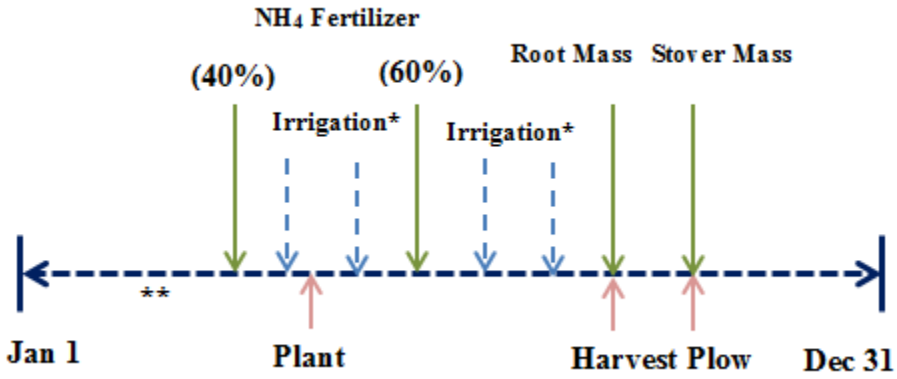

*Irrigation Water contains all mobile solutes

**Sources and Sinks of solutes during irrigation season include canal seepage, pumping, flow to and from rivers and tributaries, and crop uptake.

Figure 3.11: Scheduling of fertilizer loading, planting, irrigation water application, harvesting, and plowing during a typical growing season. Root mass and stover mass are incorporated into the pool of organic soil matter during the harvest and plowing events, respectively (from Bailey et al., 2014).

3.4.2 CHEMICAL REACTION PARAMETERS

As explained in Sec 3.2, the fate and transport of Selenium and Nitrogen depends on the chemical parameters which are grouped based on their effect on species as general reaction parameters for Carbon (C) species and O_2; Nitrogen reaction parameters, for N species; and Selenium reaction parameters, for Se species as listed in Table 3.7.

Table 3.7: General, Nitrogen, Selenium Reaction Parameter values used for pre-calibration

GENERAL		NITROGEN		SELENIUM	
λL	0.25	I_{O_2}	1	BC/Se	122.5
λM	0.11	I_{NO_3}	0.5	HC/Se	175
λH	0.003	BC/N	8	$\lambda_{SeO_4}^{het}$	0.02
fe	0.5	HC/N	12	$\lambda_{SeO_3}^{het(Se_2)}$	0.02
fh	0.2	λnit	0.8	$\lambda_{SeO_3}^{het(SeMet)}$	0.02
K_{CO_2}	0.75	λvol	0.1	λ_{SeMet}^{het}	0.02
K_{O_2}	1	K_{NO_3}	10	KSe	1000
Diff Air	1.52	$\lambda_{NO_3}^{het}$	0.2		
O2 Unsat Cons.	0.9	$\lambda_{NO_3}^{auto}$	0.1		
$\lambda_{O_2}^{het}$	2				
$\lambda_{O_2}^{auto}$	0.4				

The values of reaction parameters are derived from a similar study in LARV for the Upstream Study Region (Bailey et al., 2013a), and these values are used for the pre-calibration of the RT3D model. The chemical reaction rates can be considered as spatially constant or spatially variable throughout the study region, whereas for pre calibration, spatially constant chemical reaction rates are considered. However, the influential chemical reaction rates needed to be spatially varied for the model calibration. Therefore, a sensitivity analysis was carried out to identify influential chemical reaction rates on the species concentration in the aquifer. The detailed explanation of sensitivity analysis is provided in Chapter 4.

3.5 LIMITATIONS OF RT3D

The limitations of the used RT3D model are summarized as follows:

(i) The model can be used primarily for large-scale systems because the UZF1 package for MODFLOW uses a kinematic-wave approximation for unsaturated flow that neglects the diffusive terms in the Richards equation , thus capillary-pressure gradients can be neglected and soil parameters can be treated as homogeneous where this type of approach is reasonable.

(ii) The River package in MODFLOW is used for calculating the mass exchange of specified species concentrations for the surface water, and simulated groundwater concentrations between the aquifer and the surface water. Therefore, the surface water flow and chemical transport capabilities are not currently included in the model. As a result, species concentrations in surface water currently cannot be estimated from the model.

(iii) The average crop parameters for each crop type are supplied to the model to simulate root growth, daily uptake of N and Se, dead root mass at the end of the growing season, and the amount of above-ground stover that is incorporated into the soil layers at plowing because growth of crops is not simulated explicitly. The climatic and land-management practices for a given crop type remains the same throughout the model simulation. However, the heterogeneity in the system has been maintained where the parameter values are perturbed stochastically for each grid cell in the model domain.

(iv) The model assumes limitless supply of microbial populations which are required for oxidation-reduction reactions, and does not take into account the various microbial

species responsible for different reaction types. However, growth and death of microbial populations are simulated.

(v) Phosphate (PO_4) and sulfate (SO_4) influence are not taken into account. PO_4 is a strong sorbent and typically competes with SeO_3 for soil surface sites; it can even displace SeO_3 from soil surface sites, and crop uptake of SO_4 may limit the crop uptake of SeO_4.

The limitations (ii) and (iii) have a direct influence on the analysis of the scenario testing results in Chapter 5. Since mass loadings to surface water are not coupled with resulting surface water concentrations, and since these concentrations influence seepage of species mass into the aquifer that may occur in downstream locations along the canal, or river, the influence of best-management practices cannot be assessed completely.

The other limitation in using the model is the same as for any numerical model. No numerical model can incorporate the exact field scenario process; thus it must be recognized that the physical and chemical processes incorporated into the model are gross approximations of the actual processes. This is especially true for reactive transport models, which are comprised of various transport and chemical reaction parameters that provide concentrations that can range over orders of magnitude, so the models are more useful as investigatory tools than as prediction tools.

As a result, the objectives of models should be to investigate the governing processes on species concentration and to capture the principal spatial trends (Konikow, 2011) and inter-species relationships within the aquifer system rather than ~~not~~ to duplicate species concentrations at field observation wells and predict their exact values during the coming decades.

CHAPTER NO: 4

4 SENSITIVITY ANALYSIS AND MODEL CALIBRATION

The UZF - RT3D model was setup based on each grid cell for various crop types and parameters and chemical reaction rates on which the fate and transport of Selenium and Nitrate depend as discussed in Chapter 3. The detailed input and output files of the UZF-RT3D model were presented in Appendix B. The model was set up for 2003 to 2007, whereas to maintain the initial conditions as field conditions, the model was simulated for 36 years known as spin-up simulations using the chemical parameter values from Bailey et al., (2013a) before 2003. The 2003 to 2007 model results are compared to observed field data concentrations (command averages) and mass balance loading rates ~~to~~ for the Arkansas River for Se and NO_3 in order to calibrate the model. Figure 4.1 shows the categorized command areas of the study region along with the observation wells in the respective command area. So, all the observation wells in each command area are the averages for Se and NO_3 from 2003 to 2007 and are compared to simulated concentration values with the respective command area. The 8 command areas are subdivided into 16 areas as shown in Figure 4.1 to make precise command averages and compare these to the respective field data instead of comparing to the average data of the total wells in the study region. Comparatively, Amity command area (Amity 1, Amity 2 and Amity 3) has the most wells (49 out of 112 total wells), followed by Fort Lyon (18 wells, Fort Lyon 1 and Fort Lyon 2). Lamar has 17 wells (Lamar 1, Lamar 2 and Lamar 3); Buffalo has 8 wells (Buffalo 1 and Buffalo2); XY Graham has 8 wells (XY Graham 1 and XY Graham 2). Outside has 7 wells; Hyde Ditch and South Side each have 2 wells; and Fort Bent has1 well. The area in the study region where there are no agriculture practices falls under the Outside command area.

Although the chemical parameters are used from Bailey et al., (2013a) where the parameter rates are estimated using Parameter Estimation (PEST) and from literature, the calibration is not convincing with the observed field data. Therefore, sensitivity analysis was carried out to determine which parameter is affecting the Se and NO_3 concentration and mass loadings into the Arkansas River. This was discussed in Section 4.1. Based on this analysis, the model was calibrated enough compared with observed data and the details are discussed in Section 4.2.

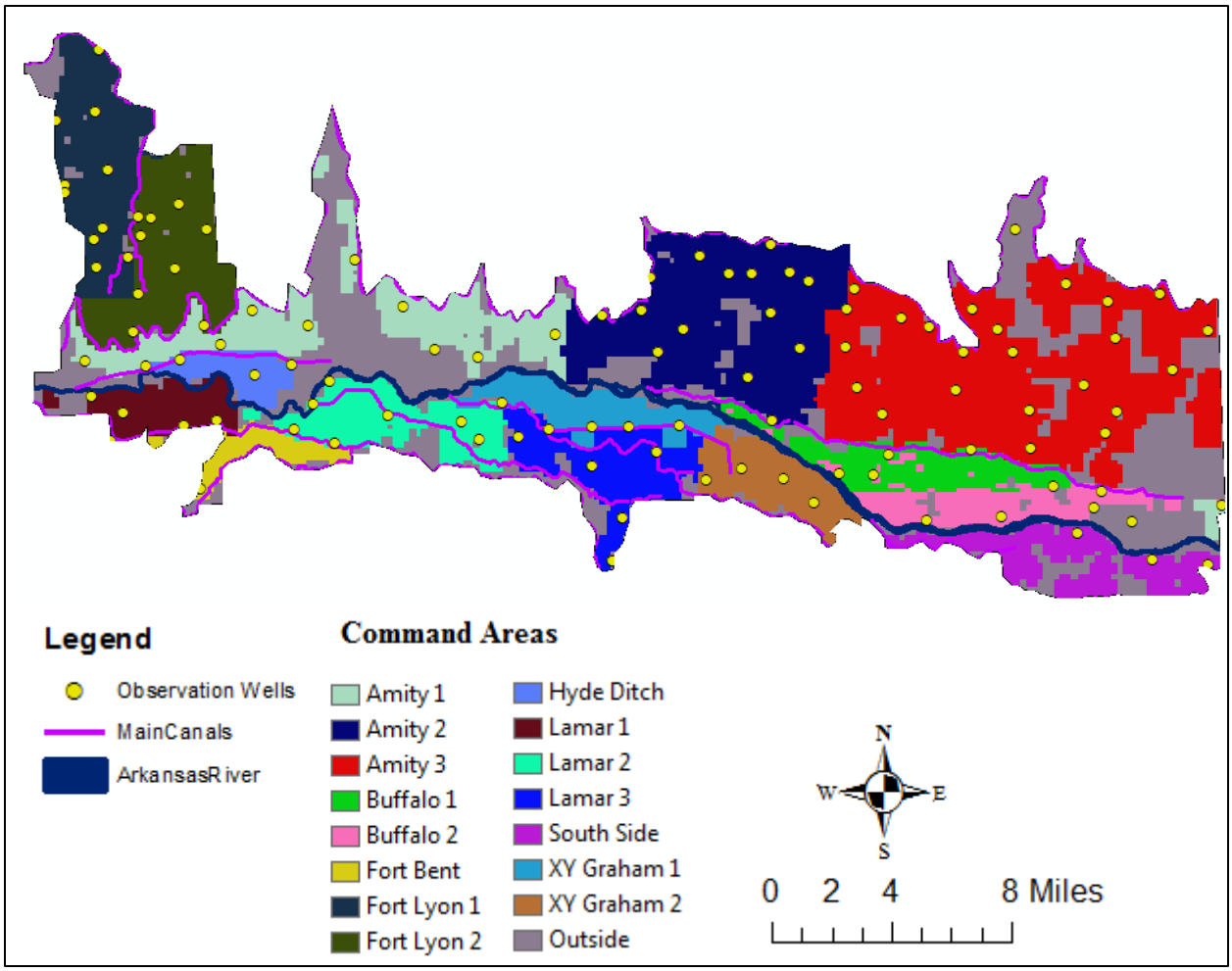

Figure 4.1: Division of command areas with their observation wells in the study region.

4.1 SENSITIVITY ANALYSIS

Initially, a 36 year spin up simulation was carried out to achieve the steady state fluctuations of the species concentration and also provide the initial conditions for the upcoming simulations.

As discussed in Chapter 3, the model was pre-calibrated with all the crop parameters, chemical parameters, and MODFLOW source and sinks between the 2003 to 2007 simulation period by comparing the command averages of simulated results and observed data to calibrate and test the model from June, 2003 to March, 2005 and June, 2005 to August, 2007 respectively. The sensitivity analysis was carried out to identify the influential parameters to govern the impact on species concentration well enough to calibrate and test the model. A total of 16 chemical parameters are considered for the sensitivity analysis as listed below:

1. Rate of autotrophic reduction of O_2 in the presence of shale ($\lambda_{O_2}^{auto}$) (kO2A)
2. Rate of autotrophic reduction of NO_3 in the presence of shale ($\lambda_{NO_3}^{auto}$) (kDENA)
3. Rate of heterotrophic reduction of O_2 ($\lambda_{O_2}^{het}$) (kO2H)
4. Rate of heterotrophic denitrification ($\lambda_{NO_3}^{het}$) (kDENH)
5. Rate of heterotrophic reduction of SeO_4 ($\lambda_{SeO_4}^{het}$) (kSeO4)
6. Rate of heterotrophic reduction of SeO_3 ($\lambda_{SeO_3}^{het}$) (kSeO3)
7. Rate of Nitrification (λ_{nit}) (kNIT)
8. Rate of NH_4 volatilization (λ_{vol}) (kVOL)
9. Rate of Se volatilization (λ_{Sevol}) (kSevol)
10. Seasonal loading of NH_4 fertilizer (F_{NH_4})
11. Seasonal N uptake (N_{up}) (NUP)
12. Seasonal Se uptake (Se_{up}) (kUPSe)
13. Rate of litter pool decomposition (λ_L) (kL)
14. Rate of humus pool decomposition (λ_H) (kH)
15. C_{NO_3} in surface water (Canal NO_3)
16. C_{SeO_4} in surface water (Canal SeO_4)

The flow chart of the sensitivity analysis was presented in Figure 4.2. The pre-calibrated RT3D model was used to test all the chemical parameters by varying individually where all other parameters are kept constant as shown in Table 3.7, and the MODFLOW source and sinks and

crop parameters always remain the same for the entire sensitivity analysis. A total of 64 simulations were carried out where each parameter was analyzed 4 times by perturbing the initial values (Table 3.7) with increases of 100% and 200% and by decreases of 50% and 90%. The graphs are developed for Se and NO_3 based on command averages of perturbed values for all 16 chemical parameters and are shown in Figures 4.3 and 4.4. For easy representation in graphs, all 16 parameters are named with k as the starting letter for each parameter, except canal NO_3 and SeO_4 and N fertilizer, as shown in the parameters list considered for sensitivity analysis.

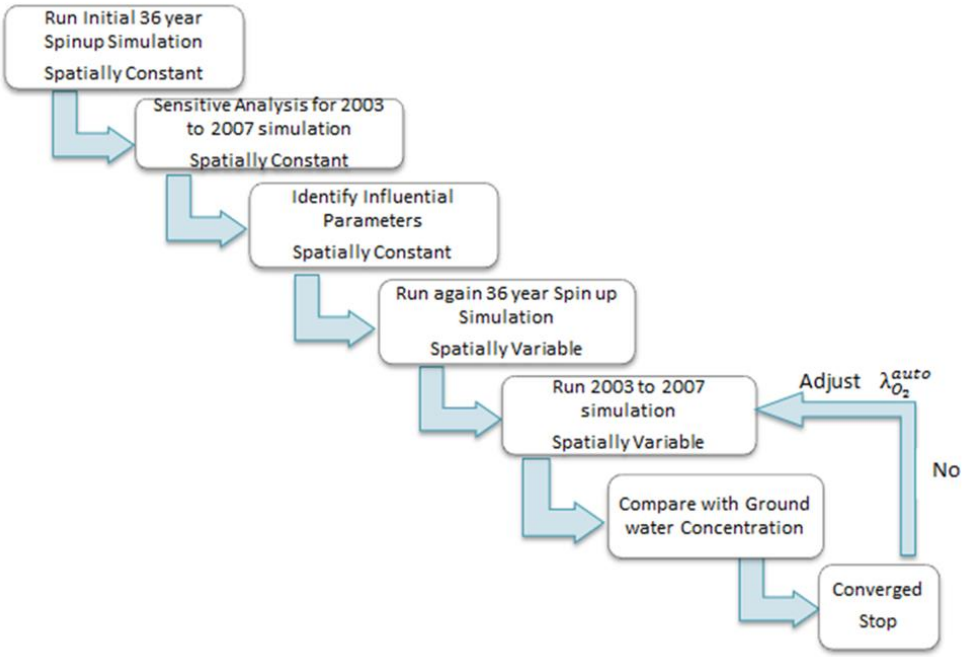

Figure 4.2: Flow Chart of the sensitivity analysis.

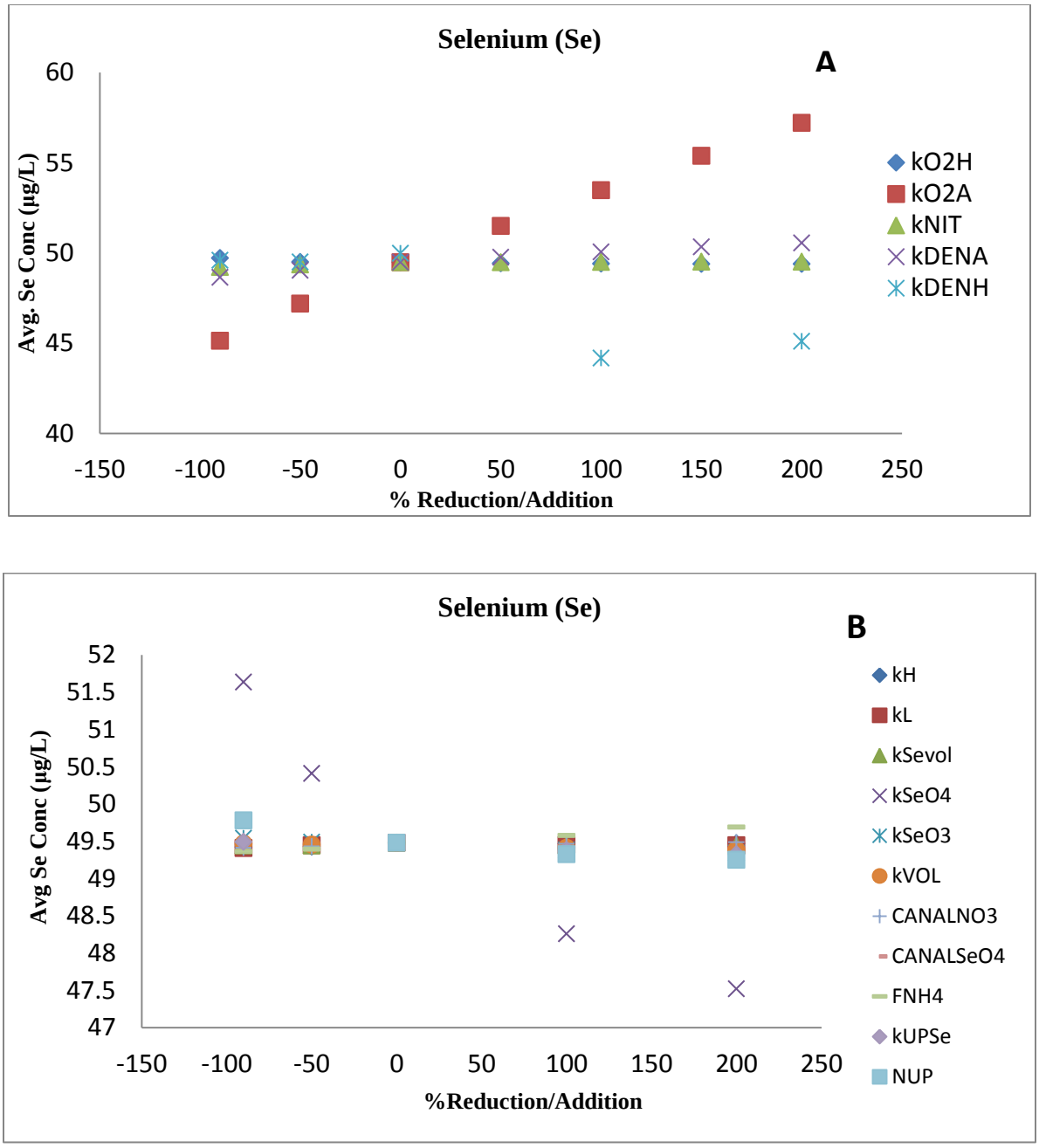

Figure 4.3: Impact on the Se concentration in sensitivity analysis for all 16 parameters.

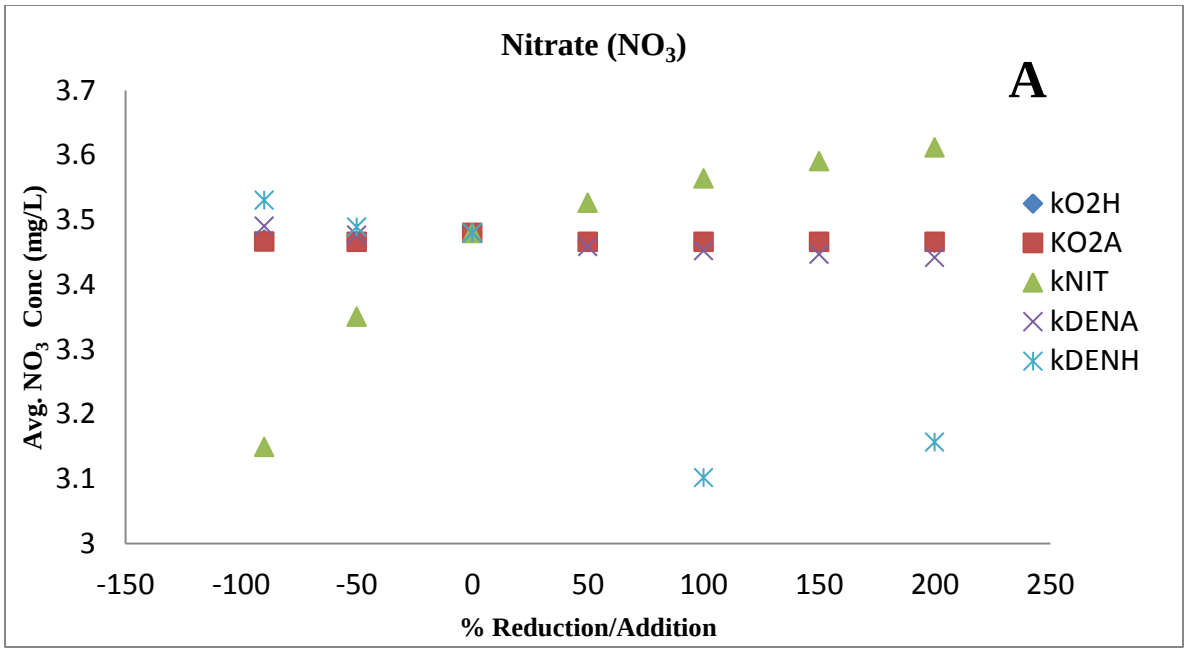

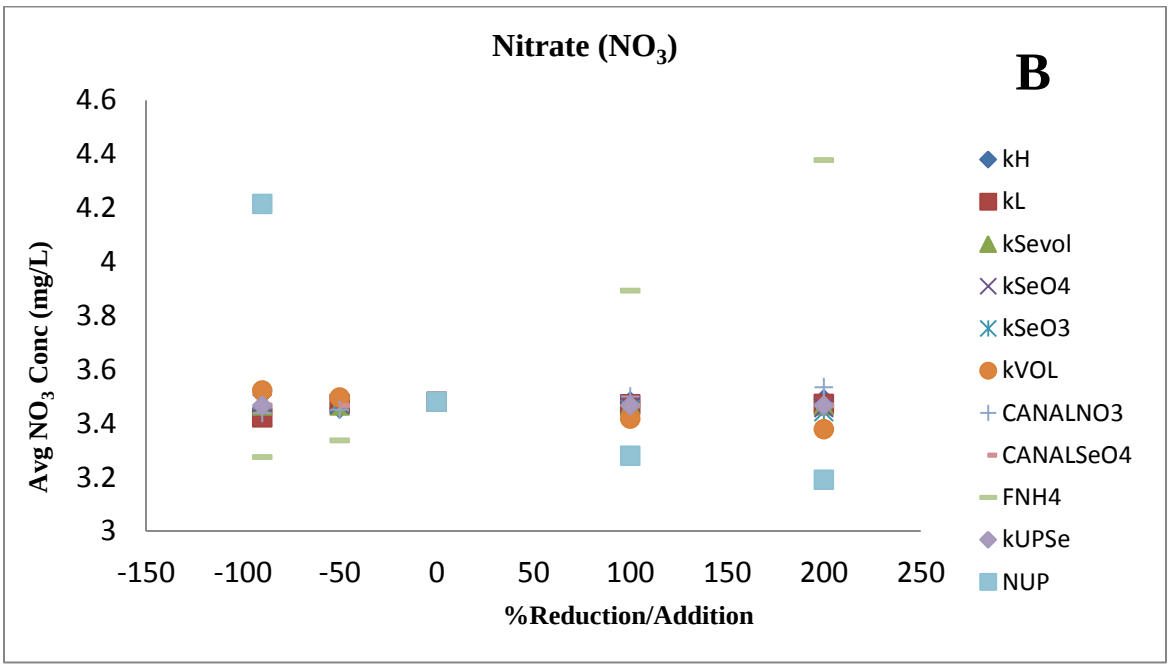

Figure 4.4: Impact on the NO_3 concentration in sensitivity analysis for all 16 parameters.

The sensitivity analysis showed that the major impact on the selenium concentration in groundwater is the rate of autotrophic reduction of O_2 in the presence of shale (kO2A) followed by rate of heterotrophic denitrification (kDENH) . Whereas for NO_3, the seasonal loading of NH_4

fertilizer (FNH_4) and seasonal N uptake (NUP) showed the major impact on the NO_3 concentrations.

The Arkansas River Basin field data has been collected by Colorado State University since the last decade, and this database is maintained by the Dr. Gates team. The data for the study region was identified from 2003 to 2012; however, 2003 to 2007 data was used for the study because the MODFLOW model was built for that period based on the research done by Morway et al., (2013). The observed Selenium and Nitrate concentrations are averaged over a month or two of each command area depending on the data availability of each command area and again averaged based on the calibration and testing periods. The command averaged observed field concentrations for Selenium, Nitrate and Dissolved Oxygen (DO) for overall simulation period ~~was~~ are presented in Appendix C. The total number of field observation values for each command area of Se, NO_3 and DO are presented here in Table 4.1. Se and DO have more observed values than the NO_3 values.

Table 4.1: Total observation values for the simulation period (2003 to 2007)

Command Area	No. of Field Observation Values		
	Se	NO_3	DO
Amity 1	73	36	72
Amity 2	116	56	116
Amity 3	192	92	187
Buffalo 1	50	24	49
Buffalo 2	52	26	53
Fort Bent	25	12	25
Fort Lyon 1	107	55	108
Fort Lyon 2	61	30	61
Hyde Ditch	27	13	27
Lamar 1	51	26	47
Lamar 2	124	62	124
Lamar 3	16	7	17
South Side	26	13	27
XY Graham 1	50	24	47
XY Graham 2	52	31	57
Outside	149	73	143

The Root Mean Square Error (RMSE) was used to measure the difference between simulated values and observed values of the species being modelled; these differences are known as residuals. The RSME serves to aggregate them into a single measure of predictive power. The RMSE values are shown in Figure 4.5 for Se and NO_3. The Normalized Root Mean Square Error (NRMSE) is a non-dimensional form which is also known as the coefficient of variation. The NRMSE can be calculated by two methods: the first uses the range of the observed data and the second uses the mean of the observed data. Using the first method, the NRMSE values for SeO_4 (0.35) and NO_3 (0.05) are calculated. The model can be said to be calibrated enough if NRMSE are close to zero, usually < 0.1. The NO_3 is very well < 0.1, whereas the Se is a little bit higher at 0.35. This is expected because some of the observed data has high concentration values for some wells; thus Se model is considered as calibrated.

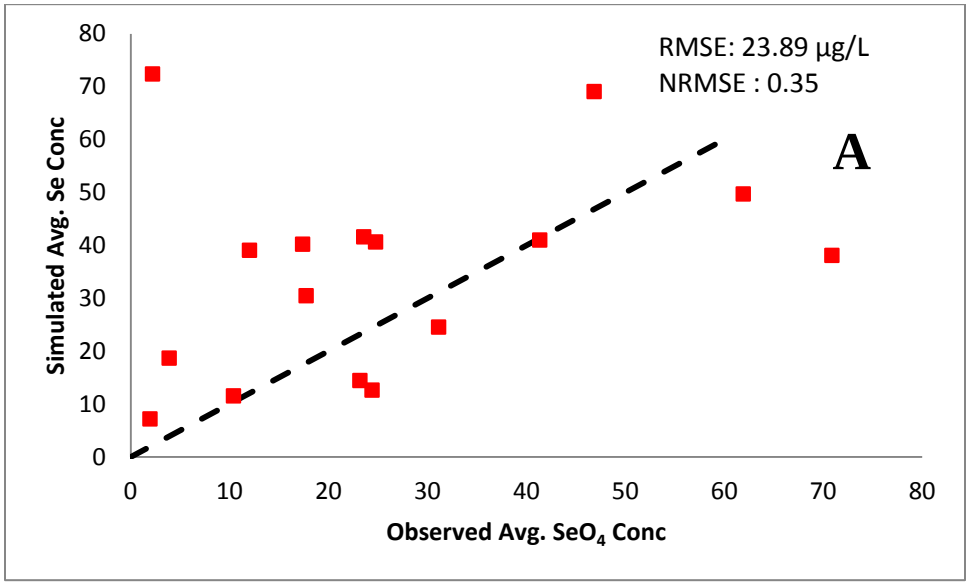

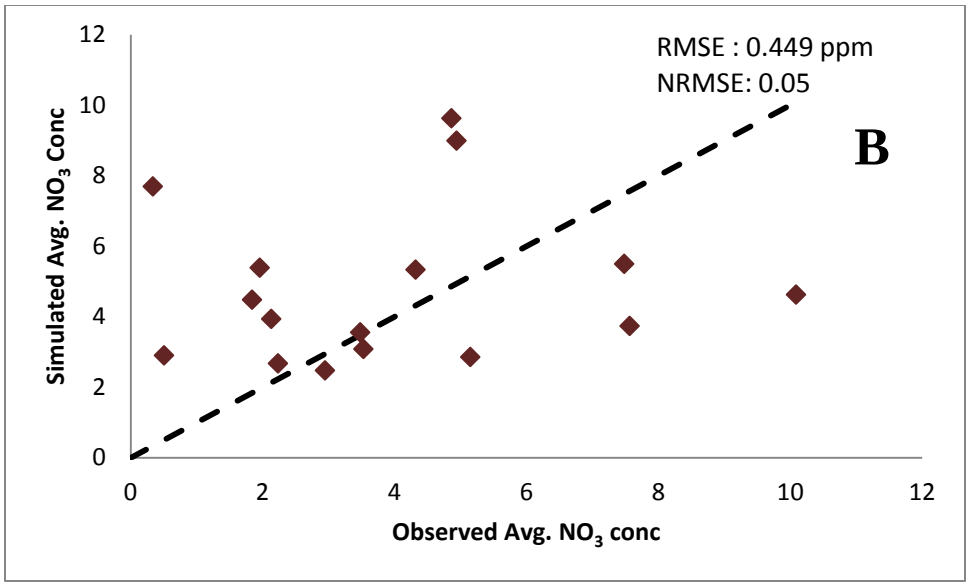

Figure 4.5: Scatter plot showing the observed and simulated concentrations for Se and NO_3 in A and B graphs respectively.

4.2 MODEL CALIBRATION

The parameter of autotrophic reduction of oxygen in the presence of shale (kO2A) shows a major impact on Se concentration in the study area, so it is spatially varied in the entire model domain from 0.04 to 0.8 d^{-1} to match the observed data as best as can be seen. On the other hand, the nitrogen fertilizer (FHN_4) and nitrogen uptake show considerable impact on the NO_3 but negligible impact on Se, so these values remain the same as initial values. Also, the remaining parameter rates are considered as the same as the initial values as shown in Table 3.7. The model was simulated from June 2003 to August 2007. The calibration period is from June 2003 to March 2005, whereas the testing period is from June 2005 to August 2007. The command averages of the groundwater concentrations of selenium, nitrate, and dissolved oxygen (DO) for each command area of both calibration and testing periods are shown in Figures 4.6 to 4.8 respectively.

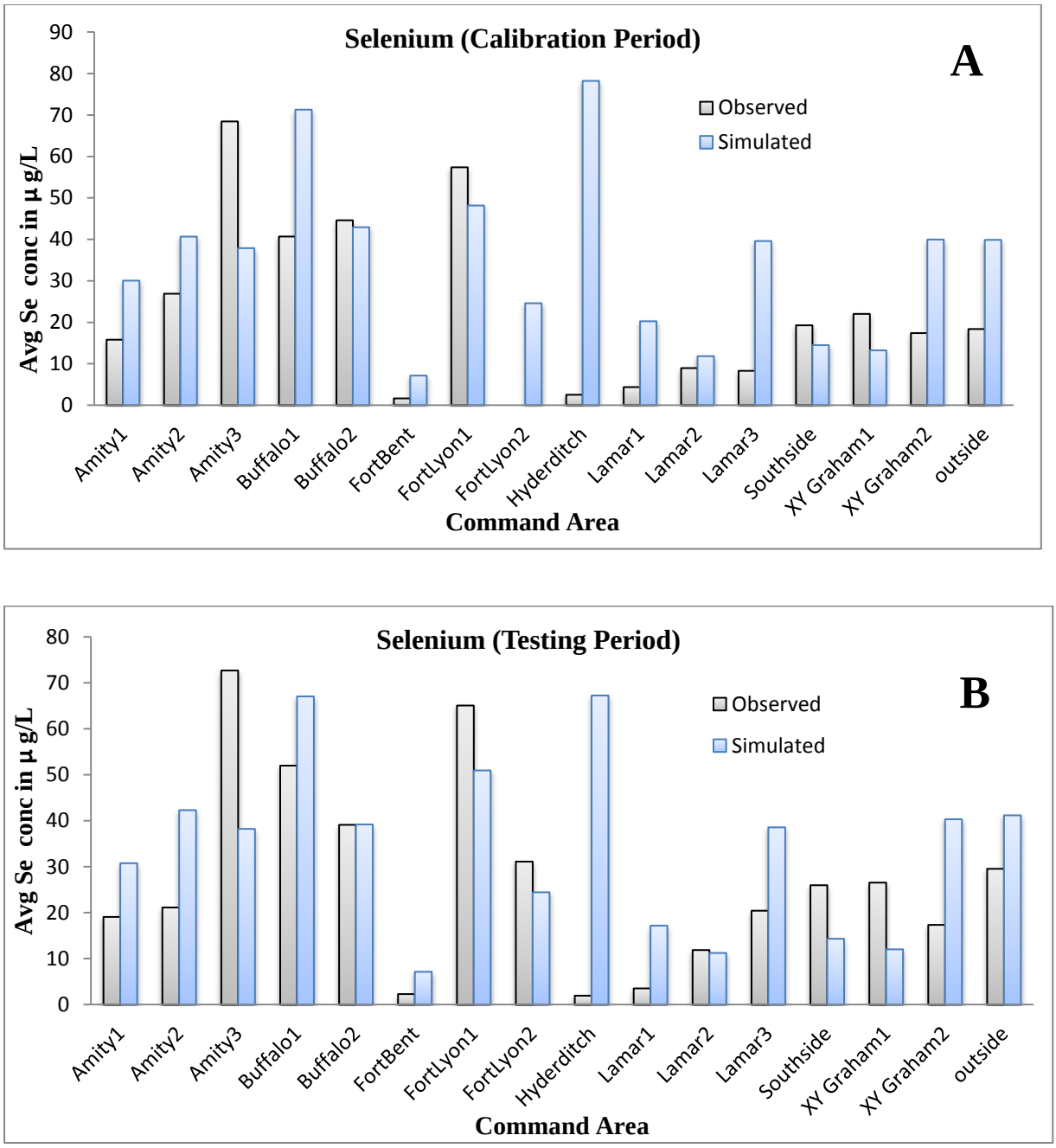

Figure 4.6: Bar chart showing the observed and simulated concentrations for calibration and testing period for Se in A and B graphs respectively.

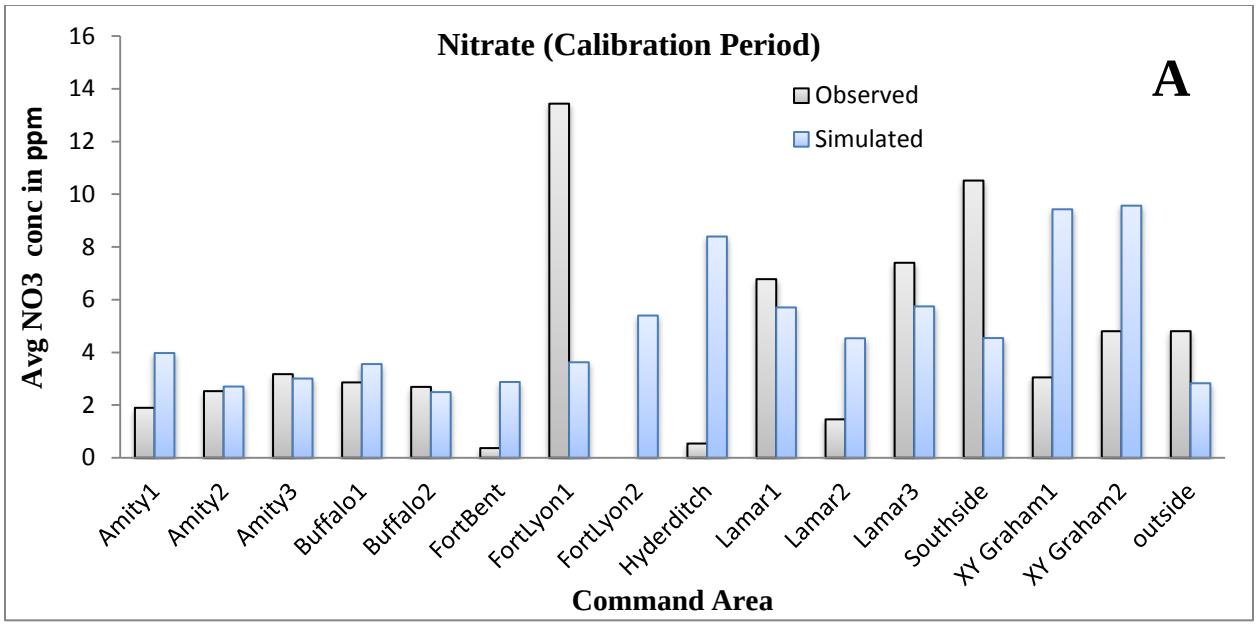

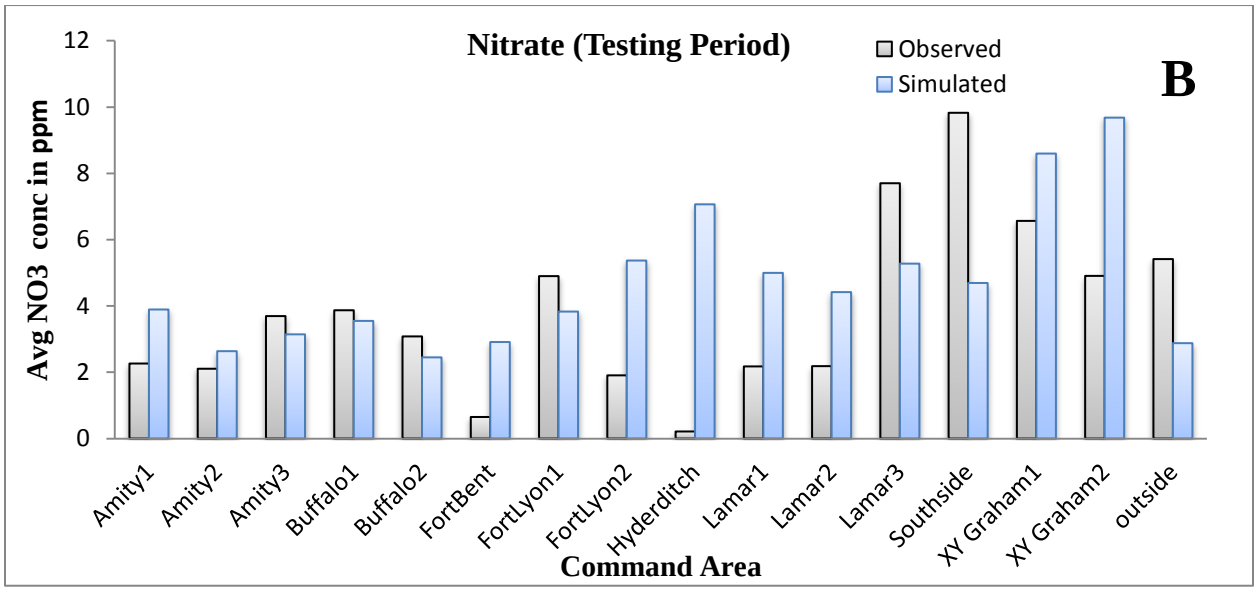

Figure 4.7: Bar chart showing the observed and simulated concentrations for calibration and testing period for NO_3 in A and B graphs respectively.

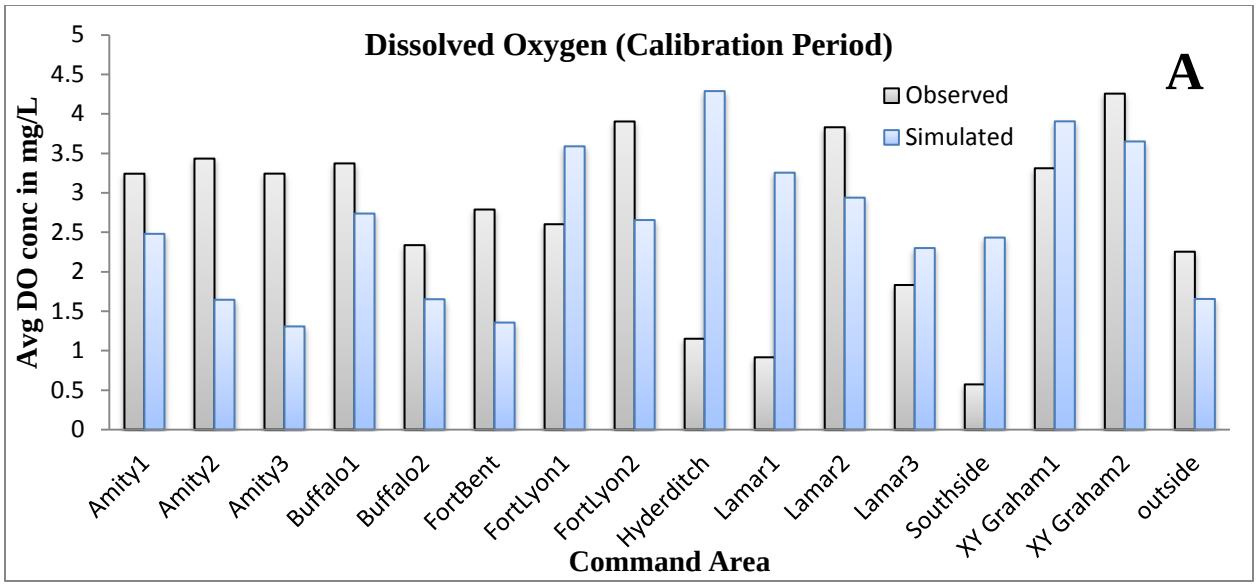

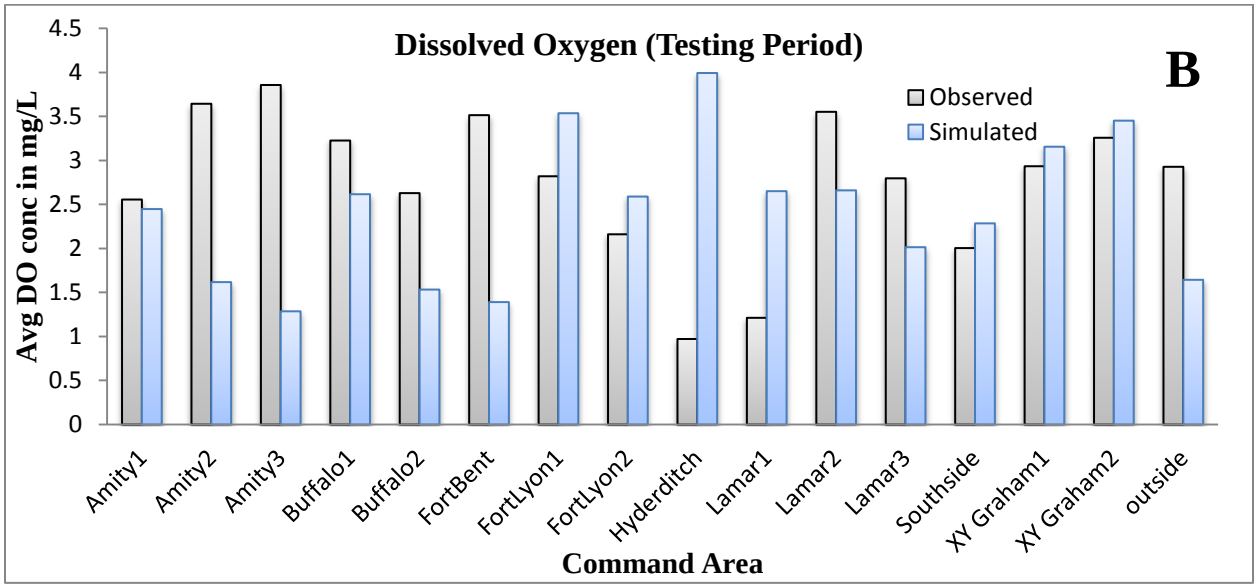

Figure 4.8: Bar chart showing the observed and simulated concentrations for calibration and testing period for DO in A and B graphs respectively.

The difference between the concentration values of the observed and calibrated models when summed up for all the command areas is less (105.93 µg/L for Se and 8.44 ppm for NO_3),

whereas the difference between the pre-calibrated (before sensitivity analysis) and observed concentration values is 346.85 µg/L for Se and 12.66 ppm for NO_3. The sensitivity analysis plays an important role in identifying which parameters has an effective impact on the species concentrations compared to the observed data. Comparatively with all of the command areas, only the Hyde Ditch command area simulated concentrations of Se, NO_3, and DO showing high variation from observed field data due to less data availability in that command area. Also, there are only 2 wells in that command area.

The observed and simulated values of C_{SeO_4} in Buffalo2 are very close for both calibration and testing period, even though it is exactly the same in the testing period. In Buffalo 1, however, the observed average values are increased from 40.7 µg/L to 52.0 µg/L, but the simulated averages are decreased from 71.3 µg/L to 67.1 µg/L. In Fort Lyon 1, the observed average is 13.4%, increased from calibration to testing period, whereas the simulated average shows only a 5% increase. The simulated averages overall match with observed averages with a considerable range deviation.

The overall match for the C_{NO_3} is good between the simulated and observed averages in all command areas for both calibration and testing periods. In the C_{NO_3} in Lamar 1 command area, the observed averages show a 67% decrease in the concentration from calibration period to testing period, from 6.7 ppm to 2.2 ppm, whereas simulated averages show a negligible decrease from 5.7 ppm to 5.0 ppm from calibration period to testing period. This is the same case with Fort Lyon 1, where the observed averages reduced from 13.5 ppm to 4.9 ppm, and the simulated averages increased from 3.6 ppm to 3.8 ppm. The C_{O_2} shows an overall good match in all command areas except Amity 2, Amity 3, Fort Bent, and Outside command areas.

Observed data in Fort Lyon 2 is presented for the calibration period for both Se and NO_3 because well 306 reported high concentrations for Se (1700 to 3690 μg/L) and NO_3 (499 to 685 mg/L); also, only partial data is available because this well was closed. Thus, those values are not considered for the analysis in the study.

Figure 4.9 shows the frequency distributions of the observed and simulated C_{SeO_4} values for both calibration and testing periods. There is a good match between the observed and simulated SeO_4 concentration values in both calibration and testing periods, but the simulated values produced relatively more values for low C_{SeO_4} which is less than 10 μg/L in both calibrated and testing periods. However, the simulated values follow a similar pattern as the actual field SeO_4 concentration values. Similarly for NO_3, Figure 4.10 shows the frequency distributions of the observed and simulated values for both calibration and testing periods. Comparatively, NO_3 shows an excellent match between the observed and simulated concentration values in both calibration and testing periods which can be seen in Figure 4.10.

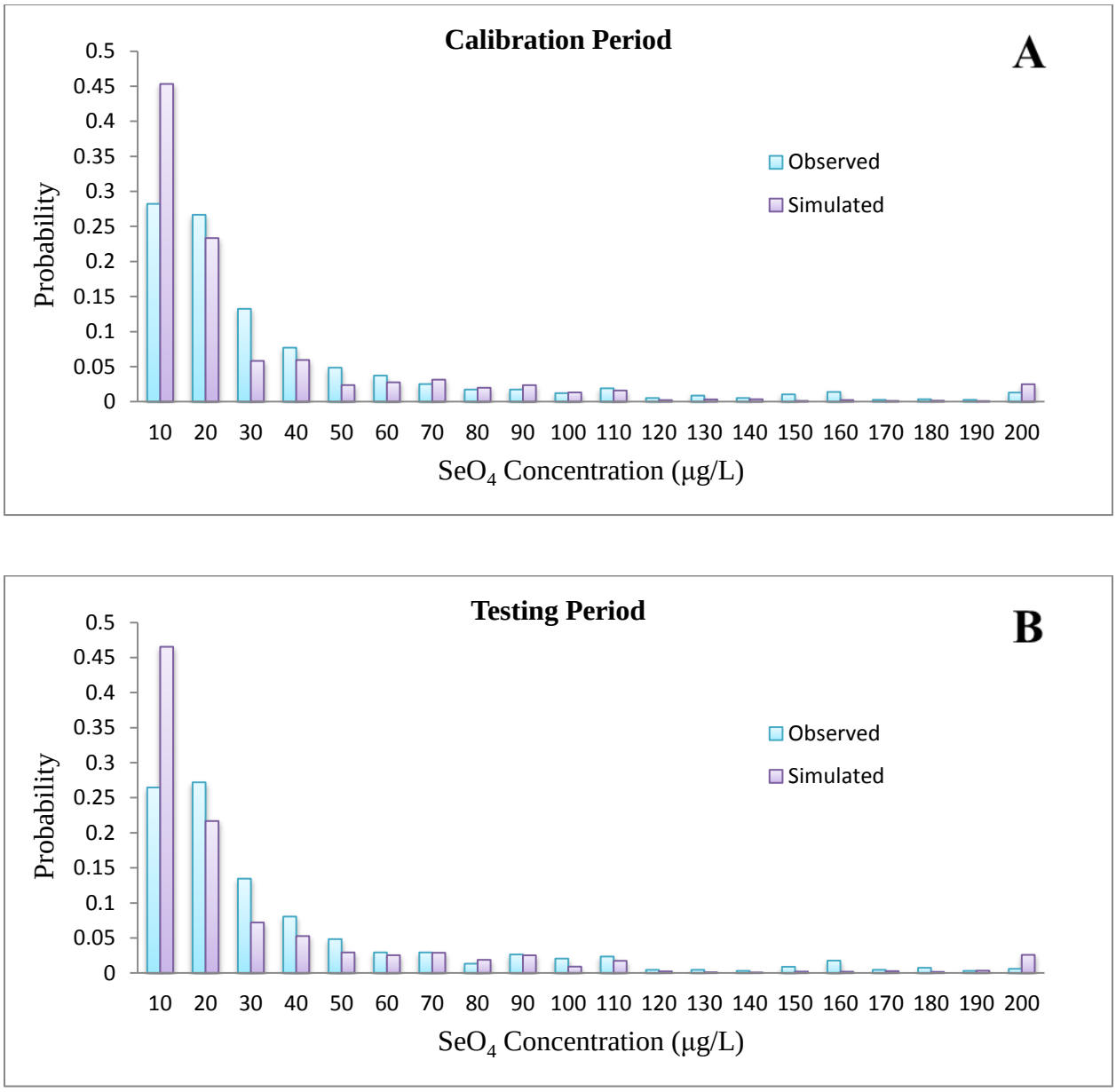

Figure 4.9: Frequency distributions of observed and simulated values of SeO_4 concentrations for the (A) calibration period and (B) testing period.

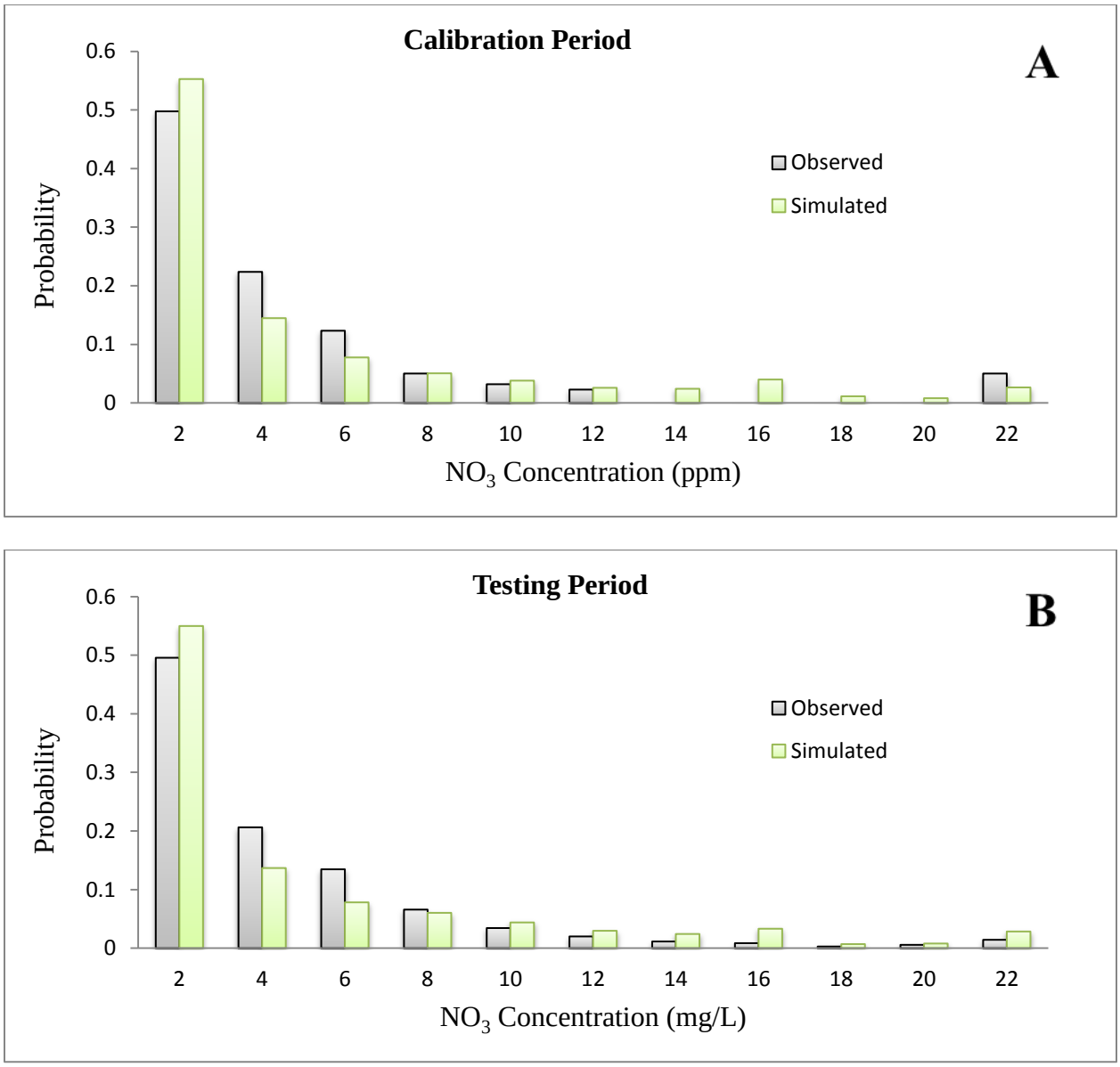

Figure 4.10: Frequency distributions of observed and simulated values of NO_3 concentrations for the (A) calibration period and (B) testing period.

The spatial Se and NO_3 concentration values are shown in Figure 4.11 and 4.12 respectively. The spatial figures show the hot spots where the concentrations are highest in the study region; these hot spots are near to the marine shale out-crops as shown in Figure 2.1. These hot spots are expected because the marine shale out crops releases SeO_4 from seleno-pyrite through the oxidation of available Se through autotrophic reduction of O_2 or NO_3 which is the toxic species of Se.

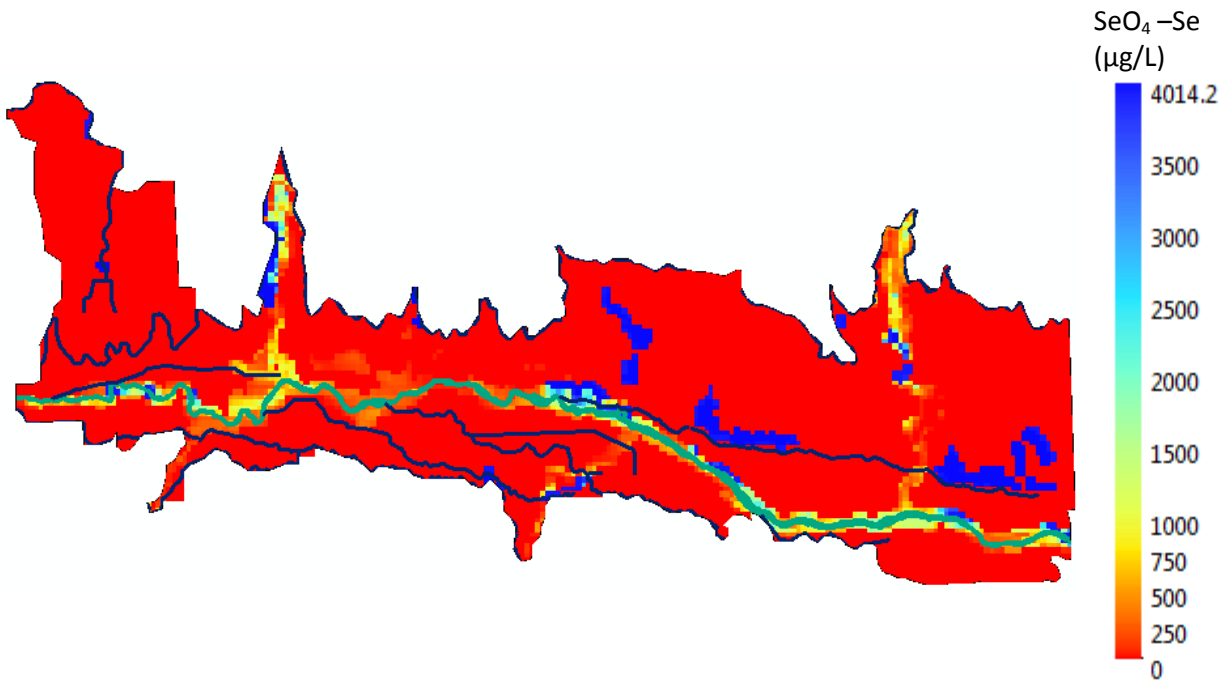

Figure 4.11: Spatial pattern of Se concentration values of calibrated model.

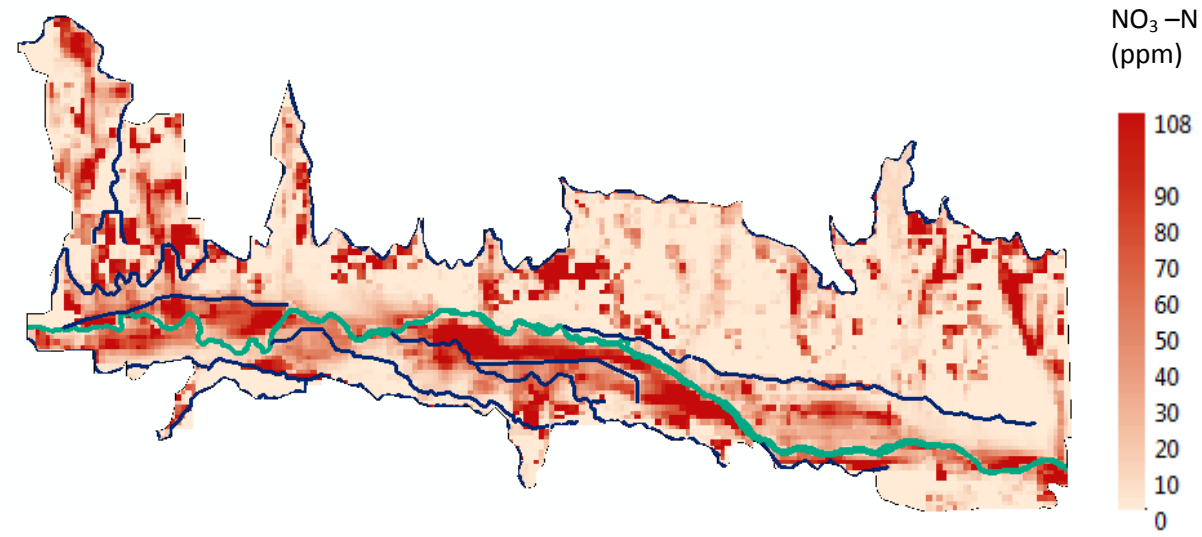

Figure 4.12: Spatial pattern of NO_3 concentration values of calibrated model.

The observed unaccounted-for and simulated mass loadings of SeO_4 (A) and NO_3(B) during the 2003-2007 period are shown in Figure 4.13, where the values of simulated during the calibration and testing periods are shown in red and green respectively. Although observed loadings of NO_3 are only available for testing, the simulated daily loadings for both calibration and testing period are shown for completeness in Figure 4.13B. Overall, the simulated daily mass loadings follow the pattern of the observed unaccounted-for mass loadings of SeO_4 and NO_3 to the Arkansas River within the study region, which was estimated by using measured stream flow rates and concentrations. The Colorado Division of Water Resources (CDWR) ARKGRACO, ARKJMRCO, ARKLAMCO gauge measures flow, stage, electrical conductivity (EC), and temperatures. ~~So~~ As a result, a mass balance was used to calculate the total unaccounted-for mass loading of dissolved species (SeO_4 and NO_3) from the study region to the Arkansas River for each day ~~on~~ of the study period (2003 to 2007). This daily unaccounted-for mass loadings includes the solute loads in unmeasured tributary flows and loads in unmeasured direct surface return flows, in addition to loads in groundwater return flow along the river reach. Hence the

observed unaccounted –for mass loads provides an upper bound estimate of loadings to the river in groundwater return flows.

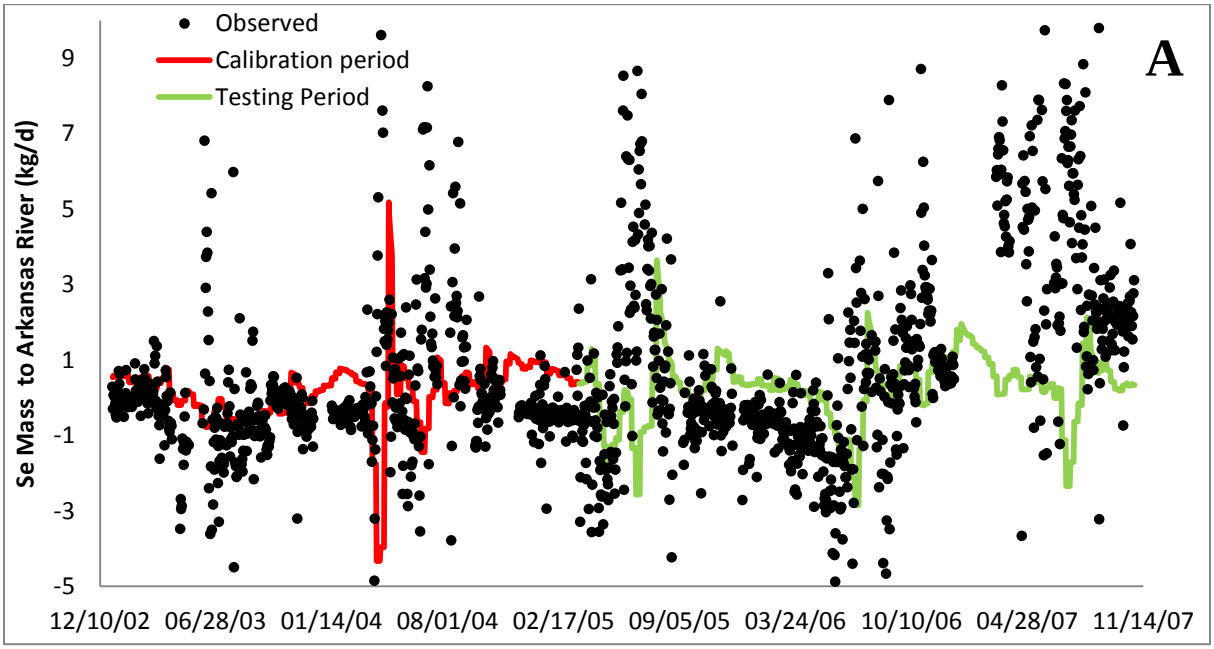

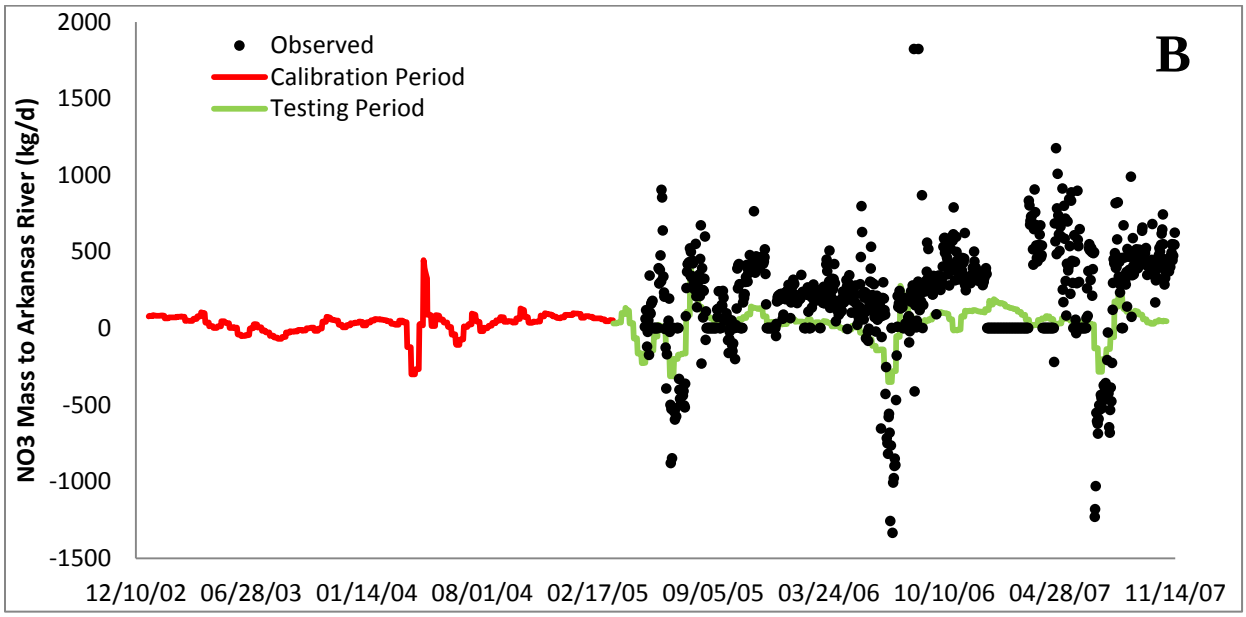

Figure 4.13: Time plot showing the observed and simulated mass loadings for Se and NO3 to the River Arkansas, the red line indicates the calibration period whereas green indicates testing period and black dots indicates the observed loadings.

Figure 4:14 and 4:15 shows the mass balance of loadings of SeO_4 and NO_3 in each layer respectively of calibrated model.

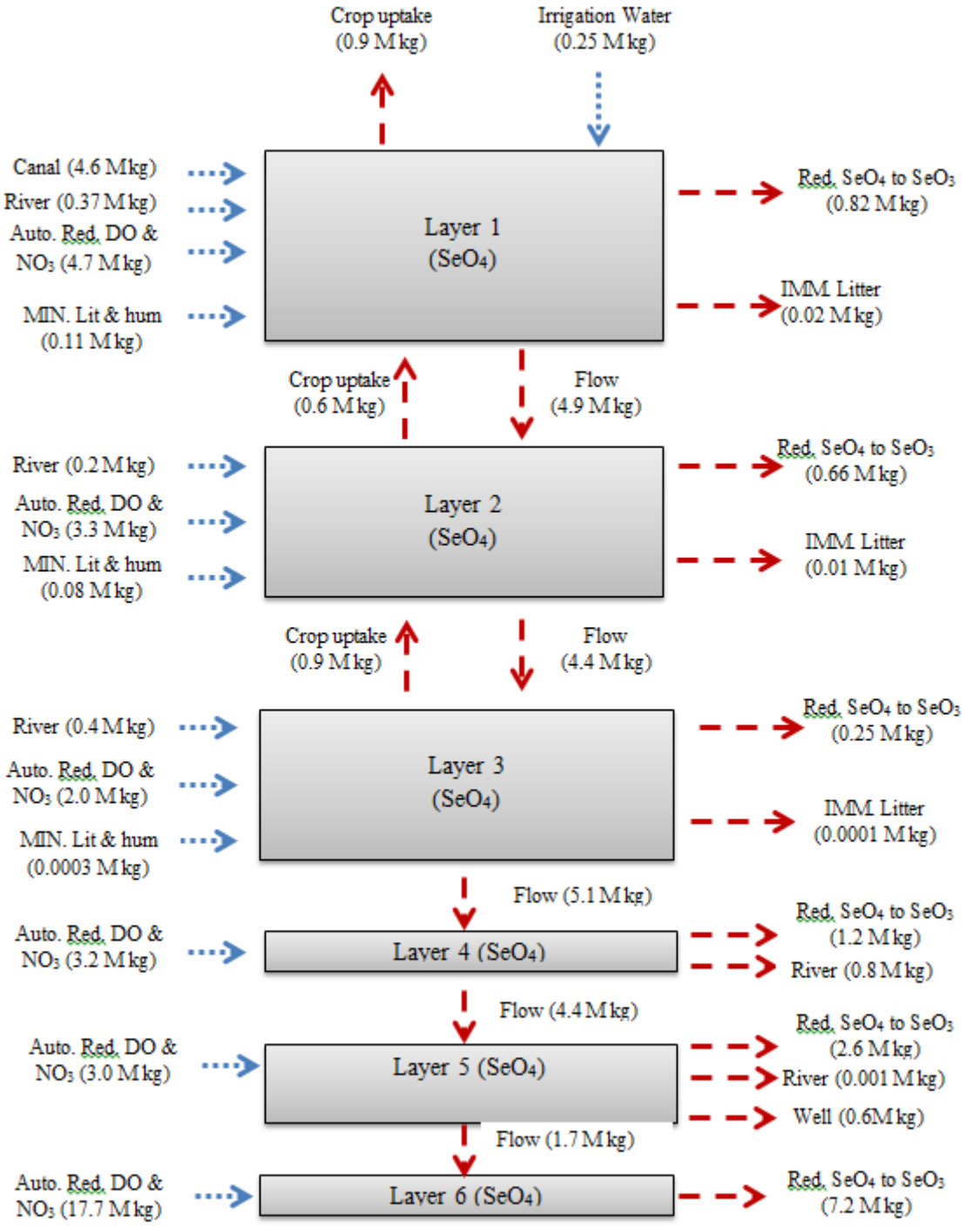

Figure 4.14: Mass Balance of SeO4 load in each layer of the calibrated model. All loads are presented in Million Kilograms (M kg). MIN (Mineralization), IMM(Immobilization). All inputs are represented by blue arrows whereas outputs are in red arrows.

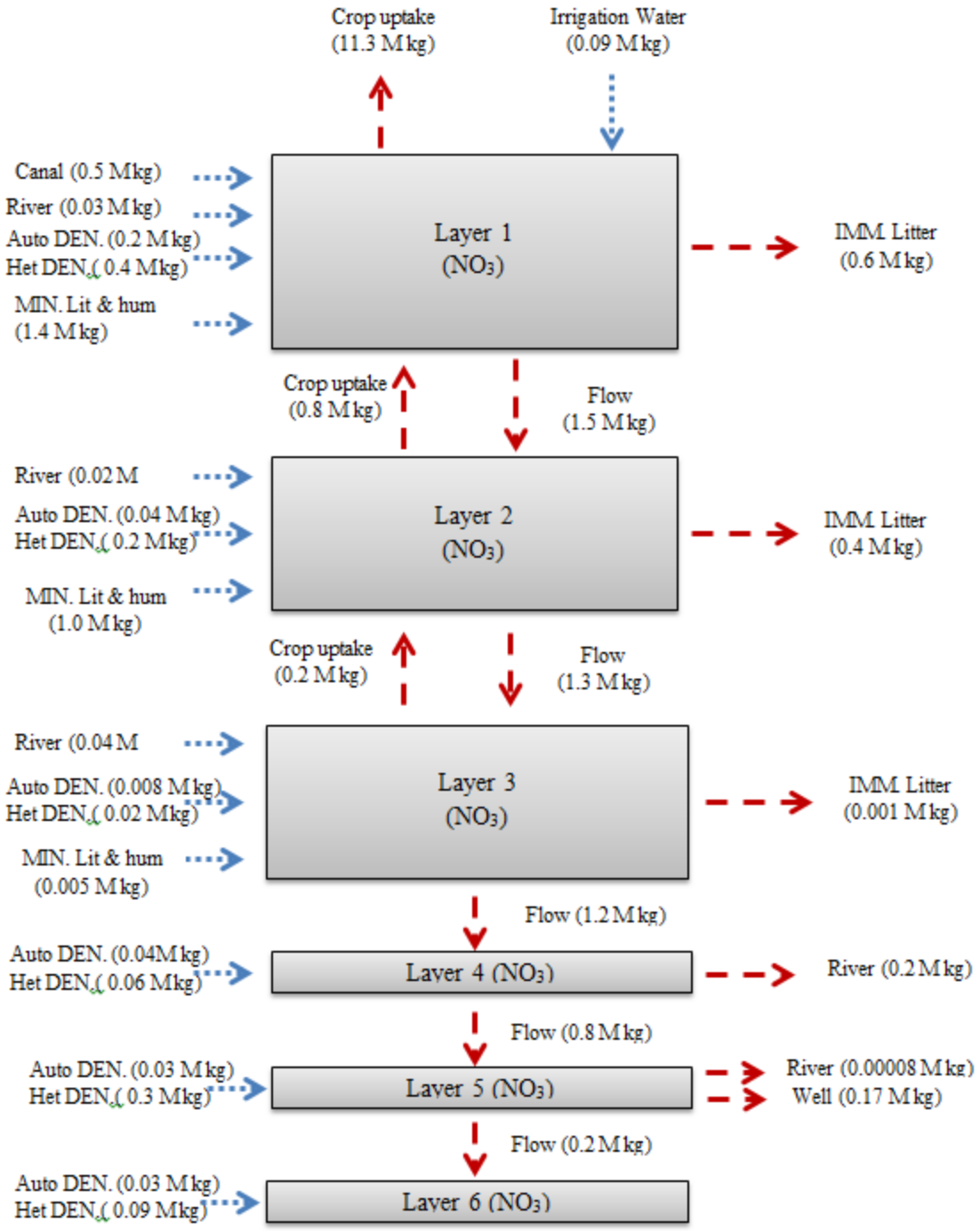

Figure 4.15: Mass Balance of NO3 load in each layer of the calibrated model. All loads are presented in Million Kilograms (M kg). MIN(Mineralization), IMM(Immobilization). All inputs are represented by blue arrows whereas outputs are in red arrows.

CHAPTER NO: 5

5 ASSESSMENT OF REMEDIATION STRATEGIES

The main importance of the numerical models is that we can predict the long term impacts of strategies by calibrating the model with current field data. Once the model is calibrated using the current field data, the long term impact can be analyzed by changing the system-response variables, for example, nitrogen fertilizer loading, rate of applied irrigation water, etc. in agricultural watersheds. The same is applied in the study for investigating the remediation of selenium and nitrate in stream –aquifer systems downstream of John Martin Reservoir, LARV, in southern Colorado.

As explained in Section 3.5, the calibrated and tested RT3D model is used to investigate the best management practices (BMP's) for C_{SeO_4} and Se mass loadings to the Arkansas River in LARV. As we know, the model also accounts for the fate and transport of N species, which is also a great nutrient problem in the LARV. Moreover, the reduction in NO_3 results in reduction of the release of C_{SeO_4} in the aquifer. Hence, the C_{NO3} and NO_3 mass loadings are also investigated for proposing the best management practices in the study region.

5.1 SIMULATING THE IMPLEMENTATION OF BMPS

The BMP's considered in this study are decreased Nitrogen (N) fertilizer, decreased C_{NO_3} and C_{SeO_4} in canal water, reduced irrigation, fallowing of irrigated land, and a combination of these. The Se and NO_3 concentrations and their mass loadings of these BMP's are compared with baseline scenario (do-nothing scenario) concentrations and loadings. The seasonal fertilizer

loadings are reduced by 20% and 40%; canal concentrations are reduced by 20% and 40%; annual applied irrigation volumes are reduced by 20% and 35%; and land fallowing by 25%.

The total 18 scenarios, excluding one baseline scenario, where the model inputs and parameters used from the calibrated model are discussed in Sec.3.5. The scenarios are applied to the study region from a range of less aggressive to very aggressive. The scenarios from 1 to 6 are considered as less aggressive, from 7 to 14 are considered as intermediate aggressive, and from 15 to 18 are considered very aggressive. Also, the scenarios from 1 to 6 are considered as independent remediation strategies, while from 7 to 18 are considered as combined remediation strategies where the independent scenarios are combined and represented as COM1 to COM12 as shown in Table 5.1.

Table 5.1: List of Best Management Practices investigated in the study.

Scenario	**Type**	**% of Canal Reduction in both NO_3 & SeO_4**	**% N Fertilizer Reduction**	**% of Irrigation water Reduction**	**Fallowing of Irrigated Land**
Base Line	Base Line	-	-	-	-
1	C1	20	-	-	-
2	C2	40	-	-	-
3	N1	-	20	-	-
4	N2	-	40	-	-
5	IR1	-	-	20	
6	IR2	-	-	35	
7	COM1 (C2+IR1)	40	-	20	-
8	COM2 (C2+IR2)	40	-	35	-
9	COM3 (N2+IR1)	-	40	20	-
10	COM4 (N2+IR2)	-	40	35	-
11	COM5 (N1+C1+IR1)	20	20	20	-
12	COM6 (N1+C1+IR2)	20	20	35	-
13	COM7 (N2+C2+IR1)	40	40	20	-
14	COM8 (N2+C2+IR2)	40	40	35	-
15	COM9 (N1+C1+IR1+F1)	20	20	20	25
16	COM10 (N1+C1+IR2+F1)	20	20	35	25
17	COM11 (N2+C2+IR1+F1)	40	40	20	25
18	COM12 (N2+C2+IR2+F1)	40	40	35	25

Scenarios 1 to 2 represent canal concentration in surface water; scenarios 3 to 4 represent fertilizer loading; scenarios 5 to 6 represent annual irrigation volumes; scenarios 7 to 8 represent

the combination of two independent scenarios of canal concentration and annual irrigation volumes; from 9 to 10 represents fertilizer loading and annual irrigation volumes. Scenarios 11 to 14 represent the combination of three independent scenarios of canal concentration, fertilizer loading and annual irrigation volumes. Scenarios 15 to 18 represent the combination of scenarios 11 to 14 along with fallowing of irrigated land.

The percentage of decrease in fertilizer loading is applied to each crop type within the Downstream Study Region; the percentage reduction in canal concentrations is applied to each canal within the Downstream Study Region; and the percentage reduction in applied irrigation water volume is applied across the model domain.

A similar study has been done in the LARV for the Upstream Study Region (USR) by Bailey et at., 2014. This research shows that the effect of BMPs will take between one to several decades before results can be observed because the water entering from canal seepage or applied irrigation water to the subsurface takes 10 to 20 years to reach aquifer – stream interaction. The approximate travel time to the river network from each point within the model domain is calculated using the average groundwater velocities and average groundwater flow paths (Bailey et al., 2014). Being that the Downstream Study Region falls under the same LARV region, the Se fate and transport was investigated using a multi-decadal simulation period where the complete effect of the BMP can be observed in terms of Se mass loading to the Arkansas River from the aquifer. So each BMP was simulated for a period of 40 years to observe the decrease in Se loadings and concentrations.

Initially, the MODFLOW model was run from 2003 to 2007 as described in Sec 3.1, and then using the final hydraulic heads as initial conditions for the further simulation of a 40 year

period to end in 2047 for each scenario. Similarly, the RT3D model was run for simulation from 2003 to 2007 as described in Sec 3.4, and then using the final concentrations as initial conditions again, with each scenario to run for a 40 year period ending in 2047. The results of the MODFLOW are mapped for the RT3D inputs using the MapFlows as described in Sec.3.4.

The results of each of the 18 scenarios are compared to the results of the baseline scenario ~~for~~ using the following measures:

(i) The difference in total daily mass loadings over the reach of the Arkansas River from aquifer for the entire simulation period.

(ii) The difference in the groundwater concentration for the 40^{th} year of the simulation period using the command averages.

5.2 RESULTS AND DISCUSSIONS

5.2.1 MASS LOADINGS TO ARKANSAS RIVER

The total mass loadings to the Arkansas River are calculated using the 313 river cells along the reach of the Arkansas River in the Downstream Study Region for each scenario compared to the baseline scenario loadings. Figures 5.1 to 5.4 show the time series of daily mass loadings of SeO_4 to the Arkansas River from the aquifer. Figure 5.1 shows independent scenarios 1 to 6; Figure 5.2 shows 2 BMPs applied concurrently 8, 10; Figure 5.3 shows 3 BMPs applied concurrently 12, 14; and Figure 5.4 shows 4 BMPs applied concurrently 16 and 18. From Figure 5.5, the overall 4 BMP combination shows greater reduction of SeO_4 mass loading to the Arkansas River as compared to the others.

From Figure 5.5, the total percentage of decrease in SeO_4 loads for all 18 scenarios is compared with the baseline scenario, where scenario 18 shows the highest degree of percentage decrease of 22.7%; this is followed by scenario 16 with 20.9%; scenario 13 with 19.3%; and scenario 14, 7 and 17 with 17.4%, 17.3%, and 17.1% respectively. The scenarios 11, 8, 9, 12, 15, and 10 show a medium degree of percentage decrease with 16.5%, 15.8%, 15.5%, 15.4%, 17.9%, and 14.7% respectively. Out of independent scenarios 1 to 6, scenario 5 and 6 show the maximum percentage of decrease with 13.4% and 13.1%. The lowest percent decrease is shown in scenario 3 with 1.5%, and scenario 2, 1 and 4 at 5.9%, 3% and 2.7% respectively. The total SeO_4 mass loadings along the Arkansas River cells is shown in Figure 5.6, and from Figures 5.6a to 5.6i the spatial total difference of SeO_4 mass loads between scenarios 2, 4, 6, 8, 10, 12, 14, 16, 18 and the baseline scenario of the 40 year simulation period along the Arkansas River are shown. The maximum and minimum differences of SeO_4 mass load ~~is~~ are observed in scenario 18 and scenario 4 respectively.

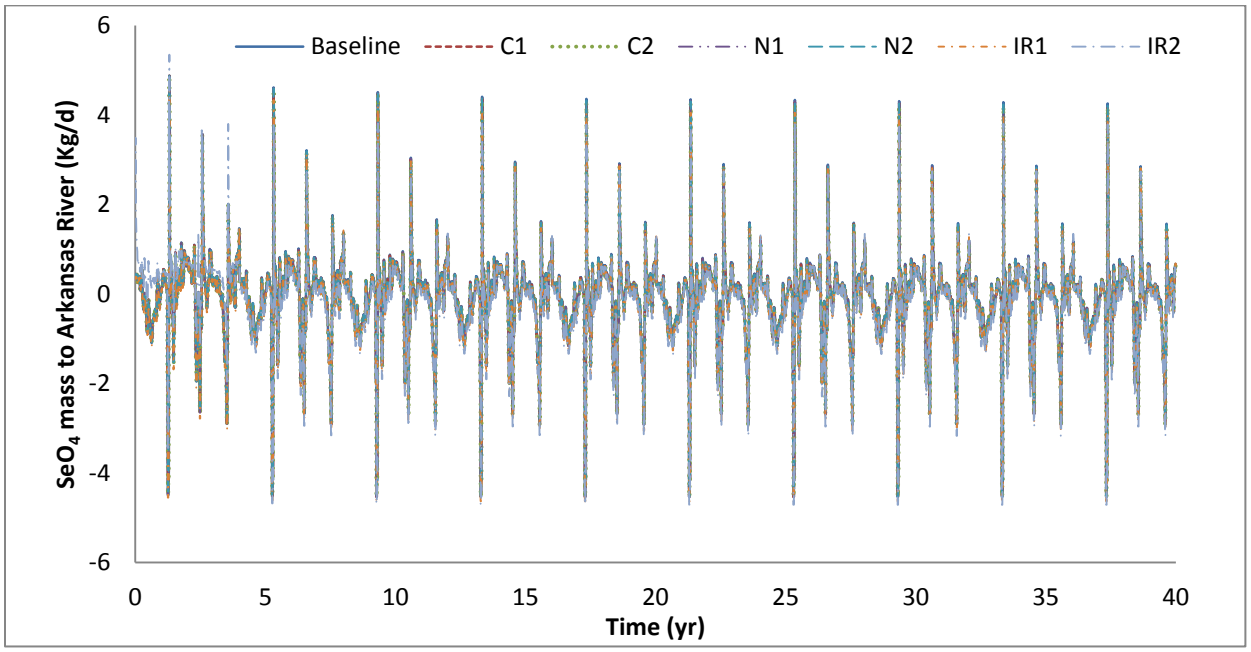

Figure 5.1: Mass Loadings of SeO_4 –Se for scenario baseline, 1, 2, 3, 4, 5 and 6

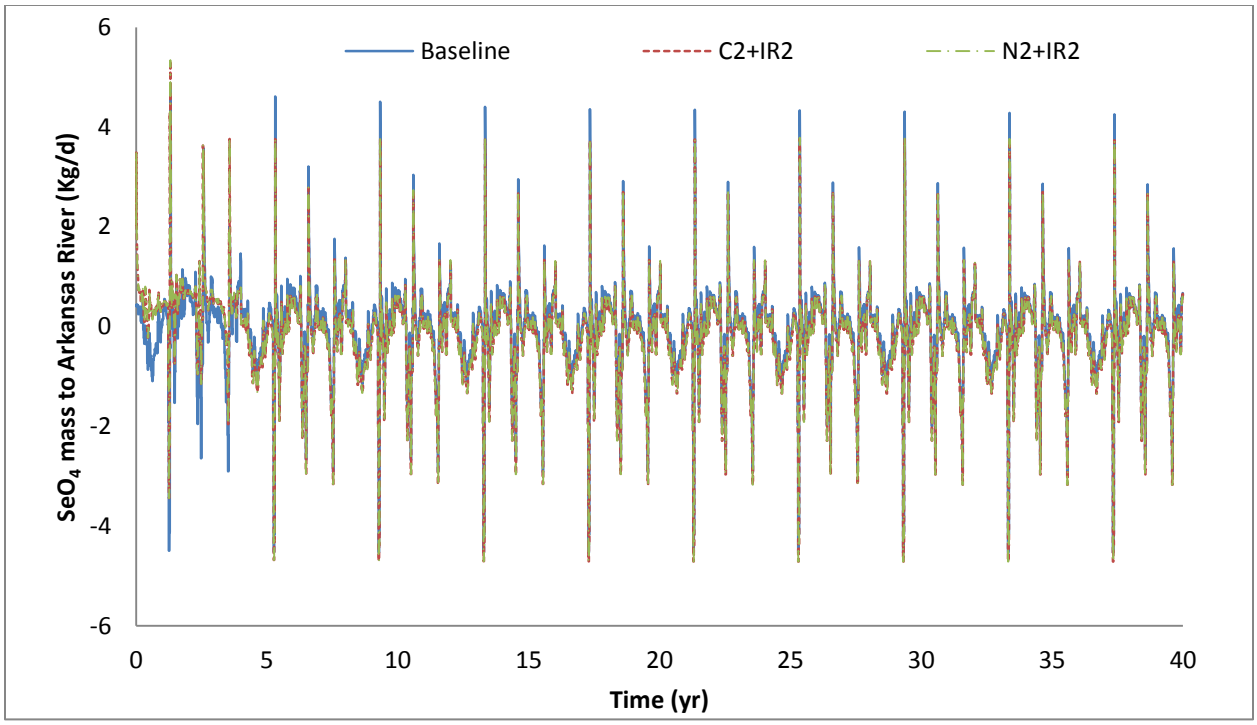

Figure 5.2: Mass Loadings of SeO_4 –Se for scenario's baseline, 8 and 10.

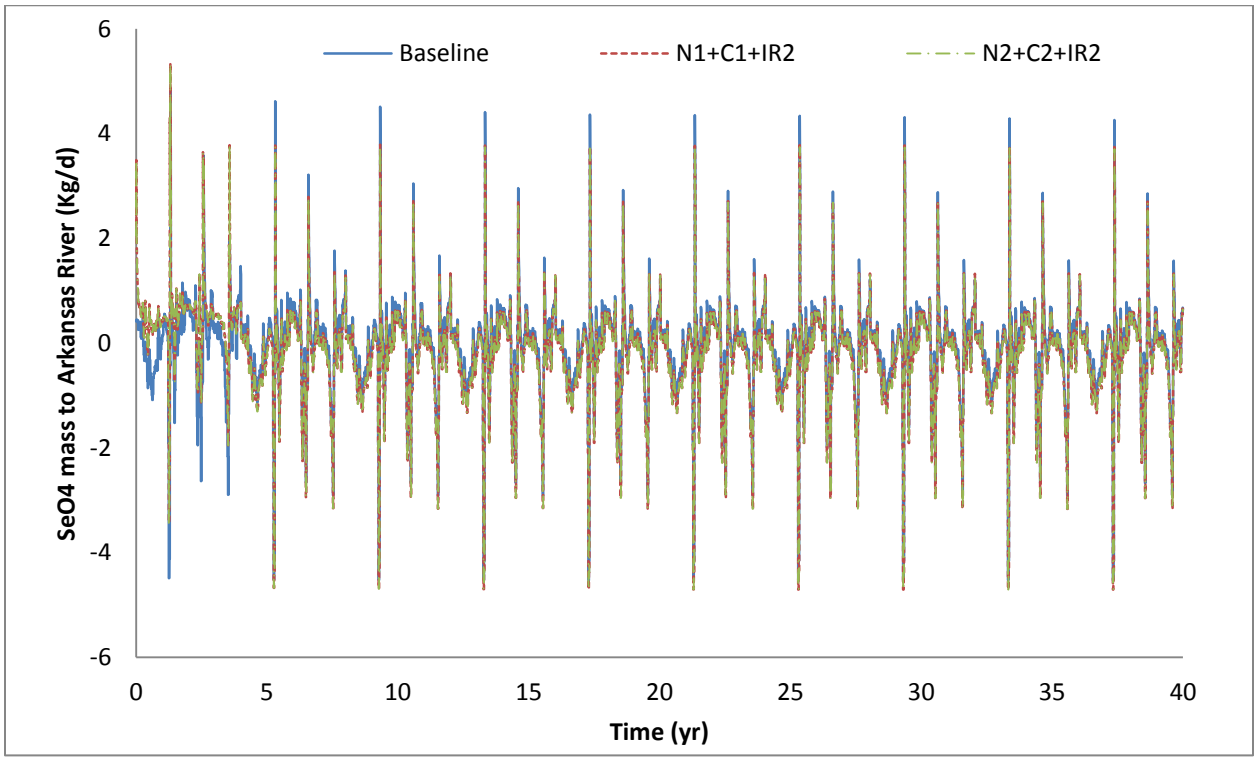

Figure 5.3: Mass Loadings of SeO_4 –Se for scenario's baseline, 12 and 14

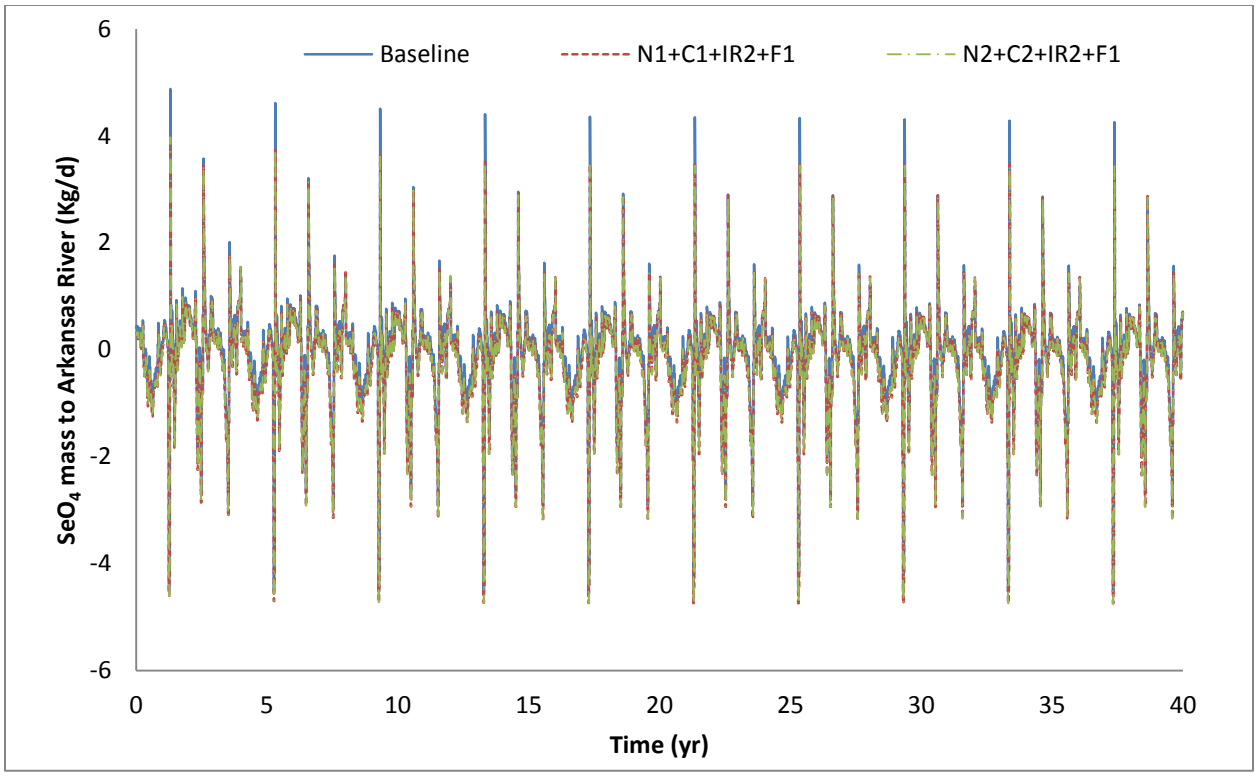

Figure 5.4: Mass Loadings of SeO_4 –Se for scenario's baseline, 16 and 18.

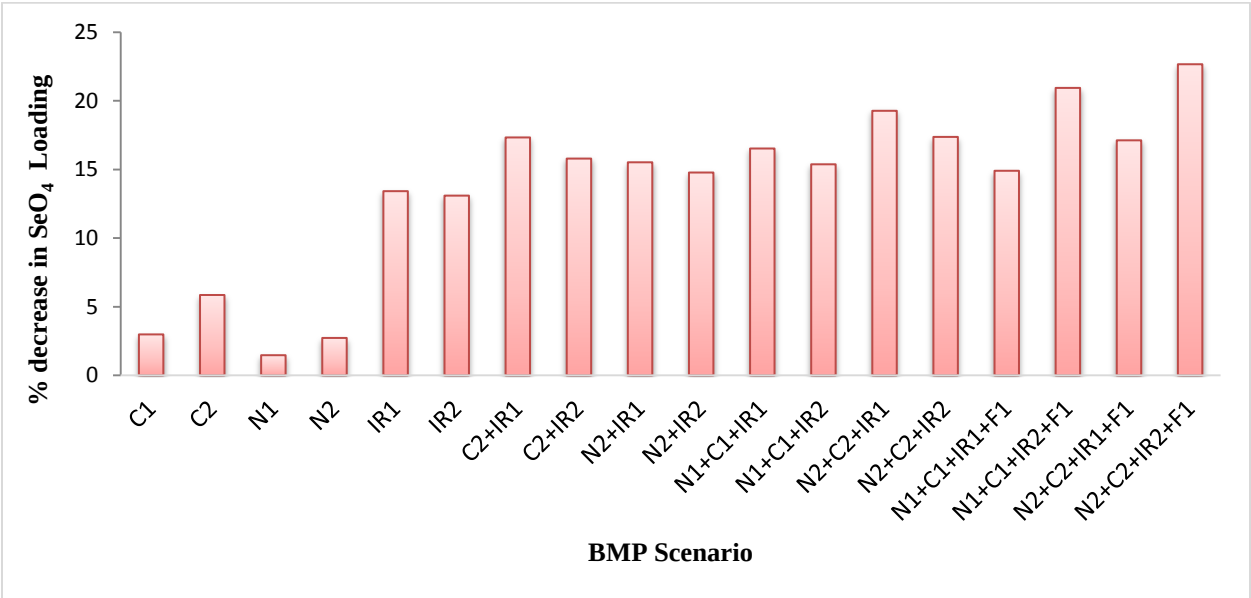

Figure 5.5: Percentage decrease of SeO_4 –Se mass loadings of all scenarios to the River Arkansas compared to baseline scenario.

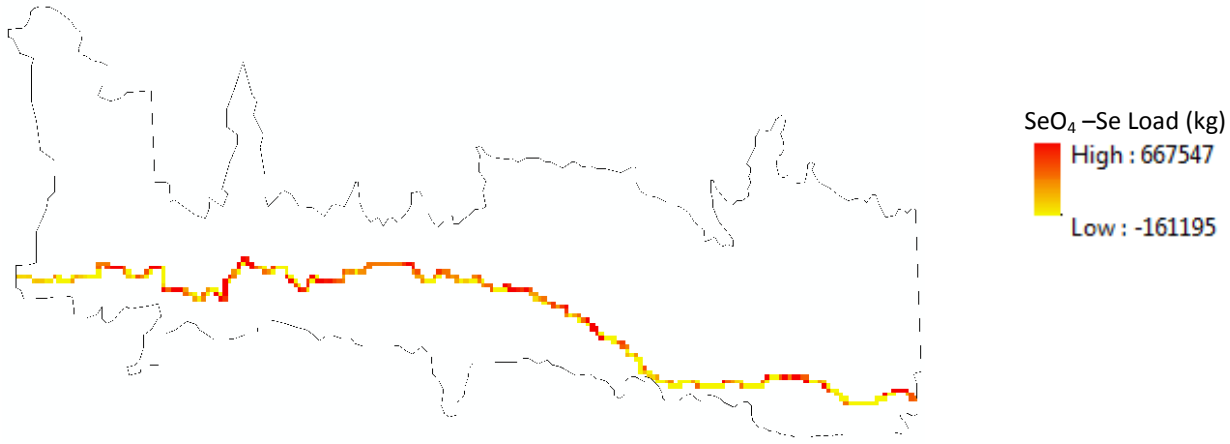

Figure 5.6: Spatial Pattern of baseline scenario total SeO_4 –Se mass loadings to Arkansas River from the aquifer for total 40 years simulation period.

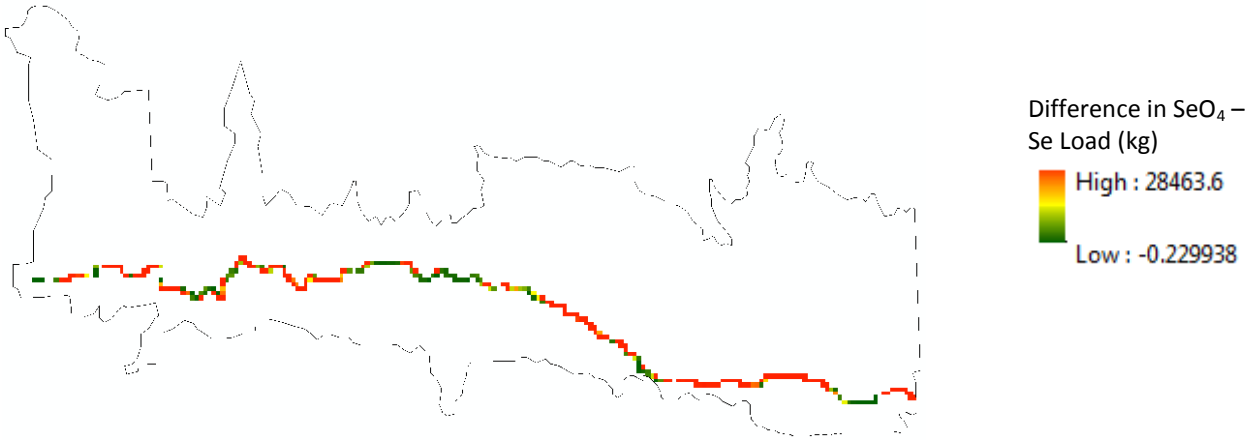

Figure 5.6a: Spatial Pattern of difference in total SeO_4 mass loadings between baseline and scenario 2.

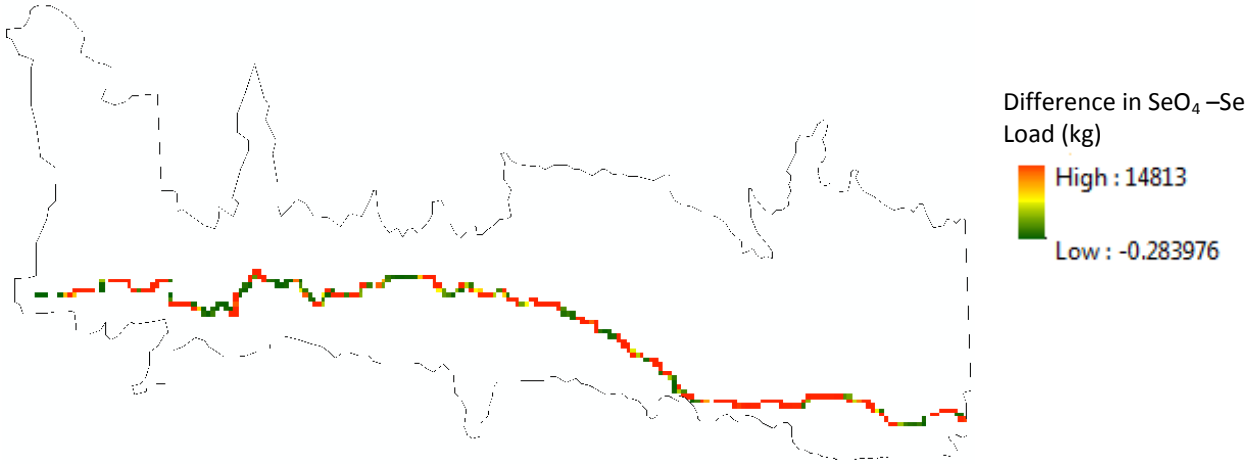

Figure 5.6b: Spatial Pattern of difference in total SeO_4 –Se mass loadings between baseline and scenario 4.

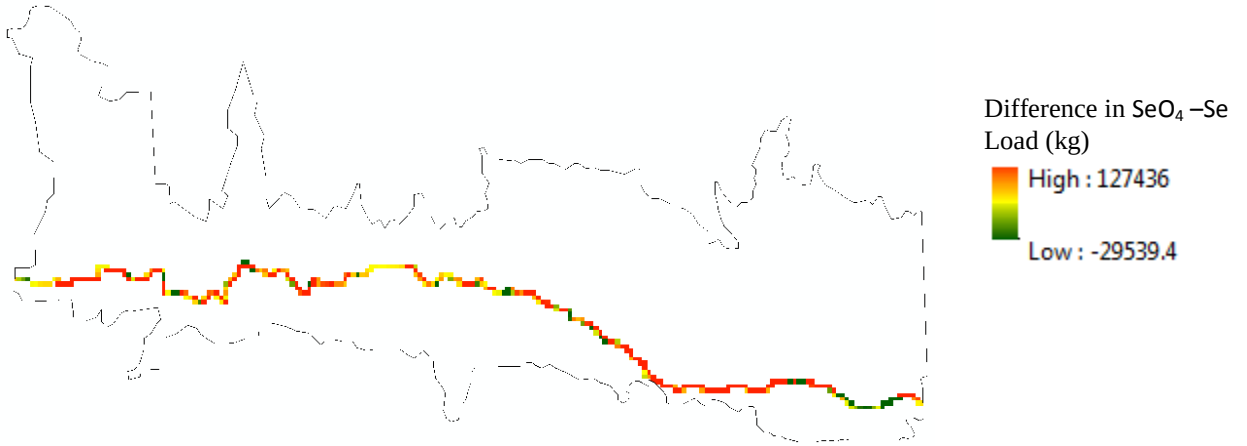

Figure 5.6c: Spatial Pattern of difference in total SeO_4 –Se mass loadings between baseline and scenario 6.

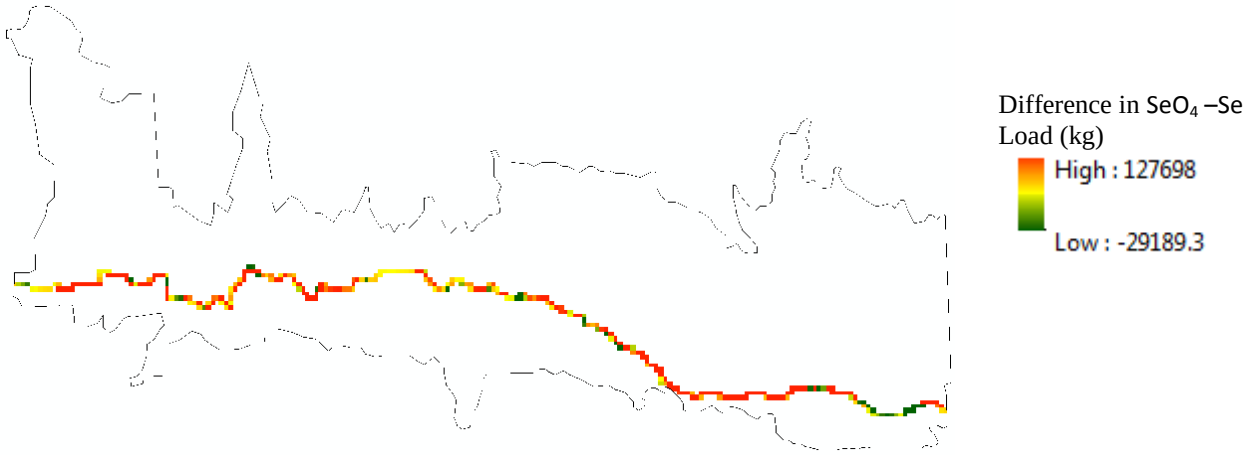

Figure 5.6d: Spatial Pattern of difference in total SeO_4 –Se mass loadings between baseline and scenario 8.

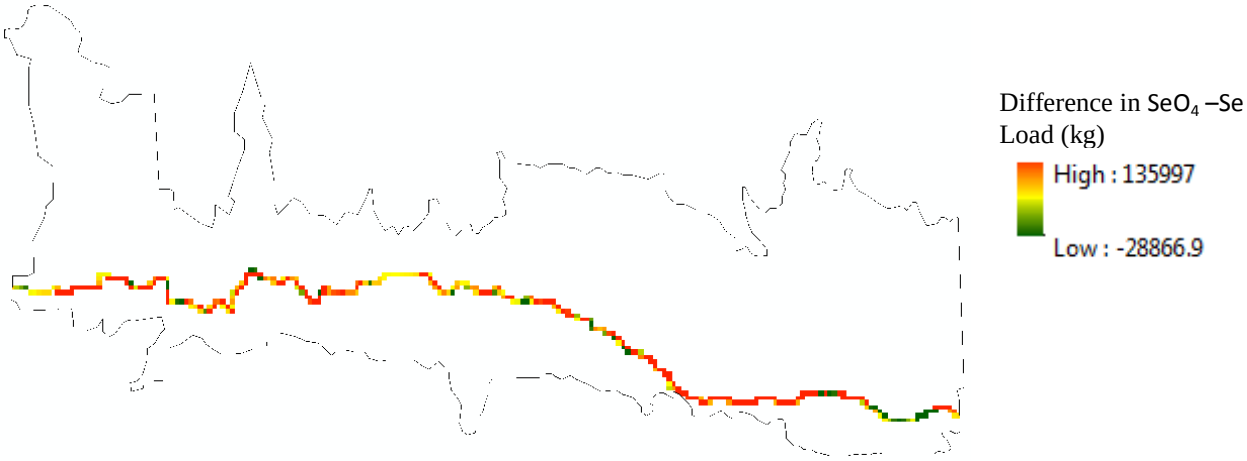

Figure 5.6e: Spatial Pattern of difference in total SeO_4 –Se mass loadings between baseline and scenario 10.

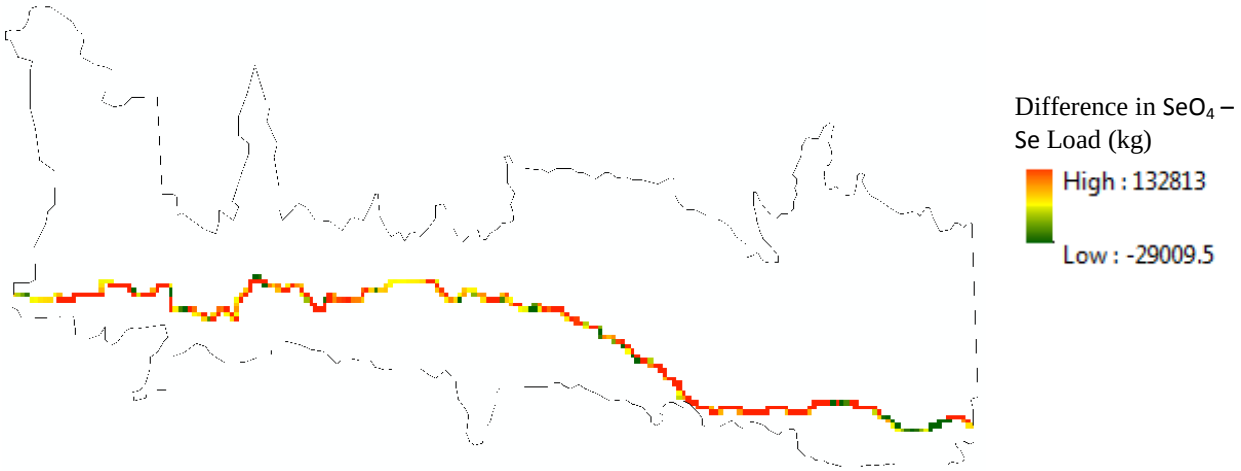

Figure 5.6f: Spatial Pattern of difference in total SeO_4 –Se mass loadings between baseline and scenario 12.

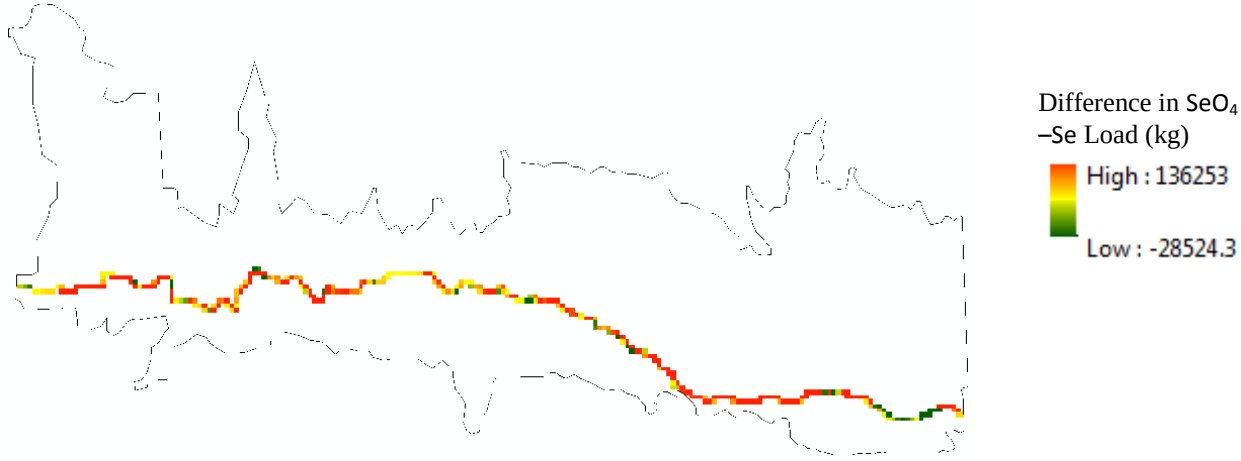

Figure 5.6g: Spatial Pattern of difference in total SeO_4 –Se mass loadings between baseline and scenario 14.

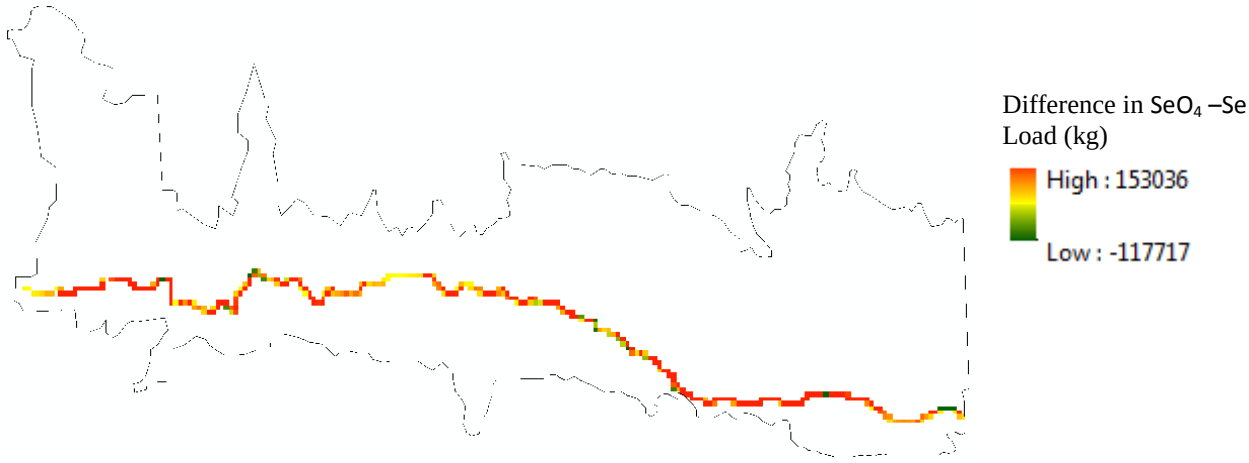

Figure 5.6h: Spatial Pattern of difference in total SeO_4 –Se mass loadings between baseline and scenario 16.

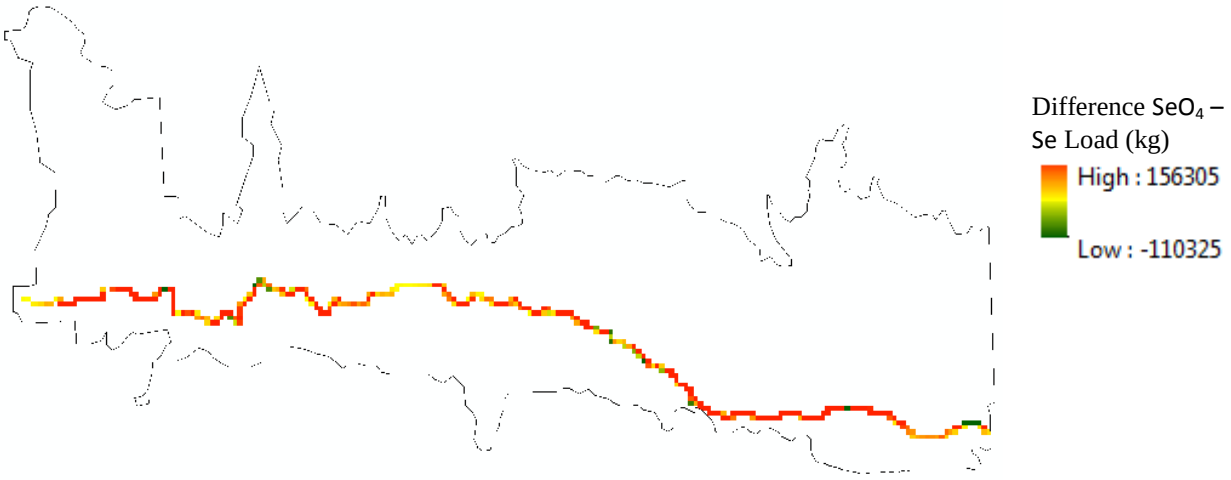

Figure 5.6i: Spatial Pattern of difference in total SeO_4 –Se mass loadings between baseline and scenario 18.

Figure 5.7 to 5.10, show the time series of daily mass loadings of NO_3 to the Arkansas River from the aquifer. Figure 5.7 shows independent scenarios 1 to 6; Figure 5.8 shows 2 BMPs applied concurrently - 8 and 10; Figure 5.9 shows 3 BMPs applied concurrently - 12 and 14; and Figure 5.10 shows 4 BMPs applied concurrently - 16 and 18. Overall 4 BMPs combination showed the greatest decrease of NO_3 mass loading to Arkansas River compared to the others which is clear from the Figure 5.11.

The total percentage of decrease of NO_3 loads for all 18 scenarios is compared with the baseline scenario whereas same for SeO_4 loadings, Scenario 18 has the highest percentage of reduction with 34.7%, followed by scenario 16 with 29.8%. Scenario 17 shows a 29% reduction; and scenario 14, 10 and 13 with 27.3%, 26.9% and 25.4% respectively. The scenarios 9, 15, 12, 11, and 8 show the medium degree of percentage reduction with 24.7%, 23.7%, 22%, 19.7% and 15.4% respectively. Out of the independent scenarios 1 to 6, scenario 6 and 4 show the maximum reduction with 14.9% and 14.5%. The least reduction was shown by scenario 1 and 2 with 0.6% and 1.1%; whereas scenarios 7, 5 and 3 with 12.7%, 12% and 8.3% respectively show

a moderate percent decrease in NO_3 loads to the river. The total NO_3 mass loadings along the Arkansas River cells is shown in Figure 5.12. Figures 5.12a to 5.12i show the spatial difference of SeO_4 mass loads between scenarios 2, 4, 6, 8, 10, 12, 14, 16, 18 and the baseline scenario of the 40 year simulation period along the Arkansas River. The maximum and minimum differences of NO_3 mass load is observed in scenario 14 and scenario 2 respectively.

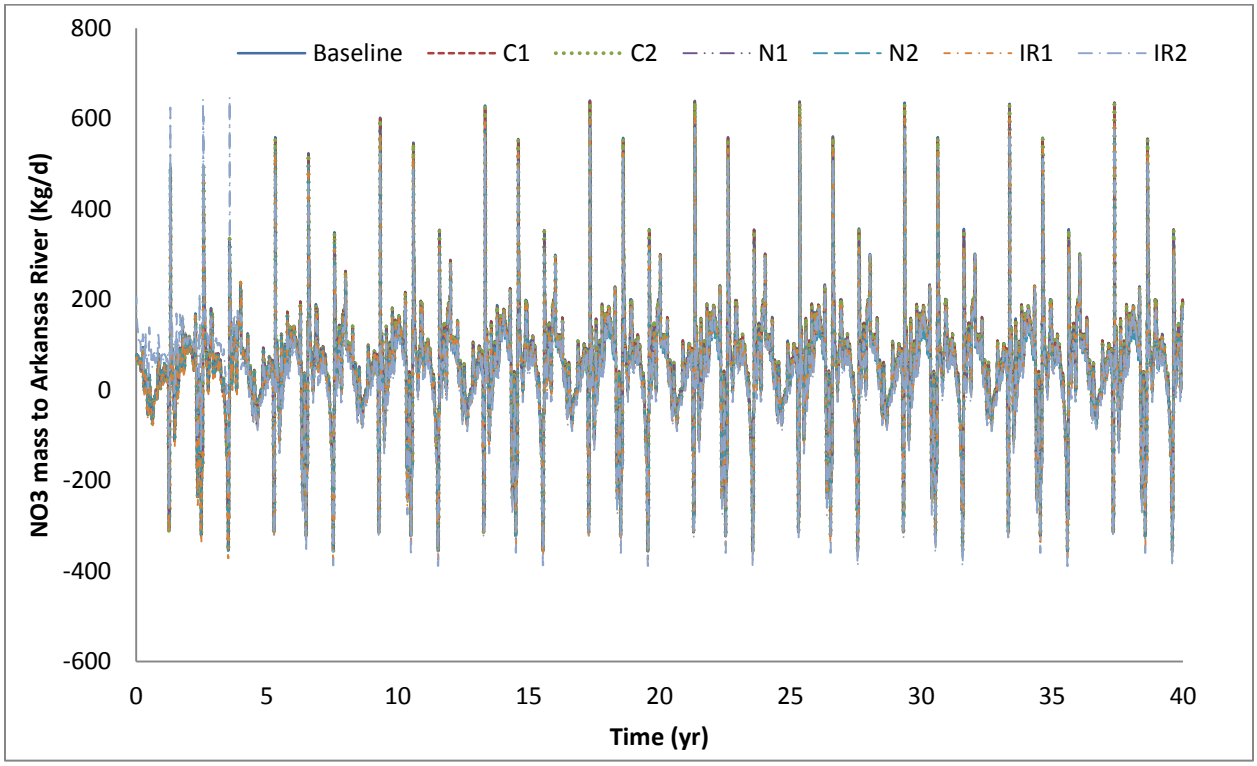

Figure 5.7: Mass Loadings of NO_3 – N for scenario's baseline, 1, 2, 3, 4, 5 and 6.

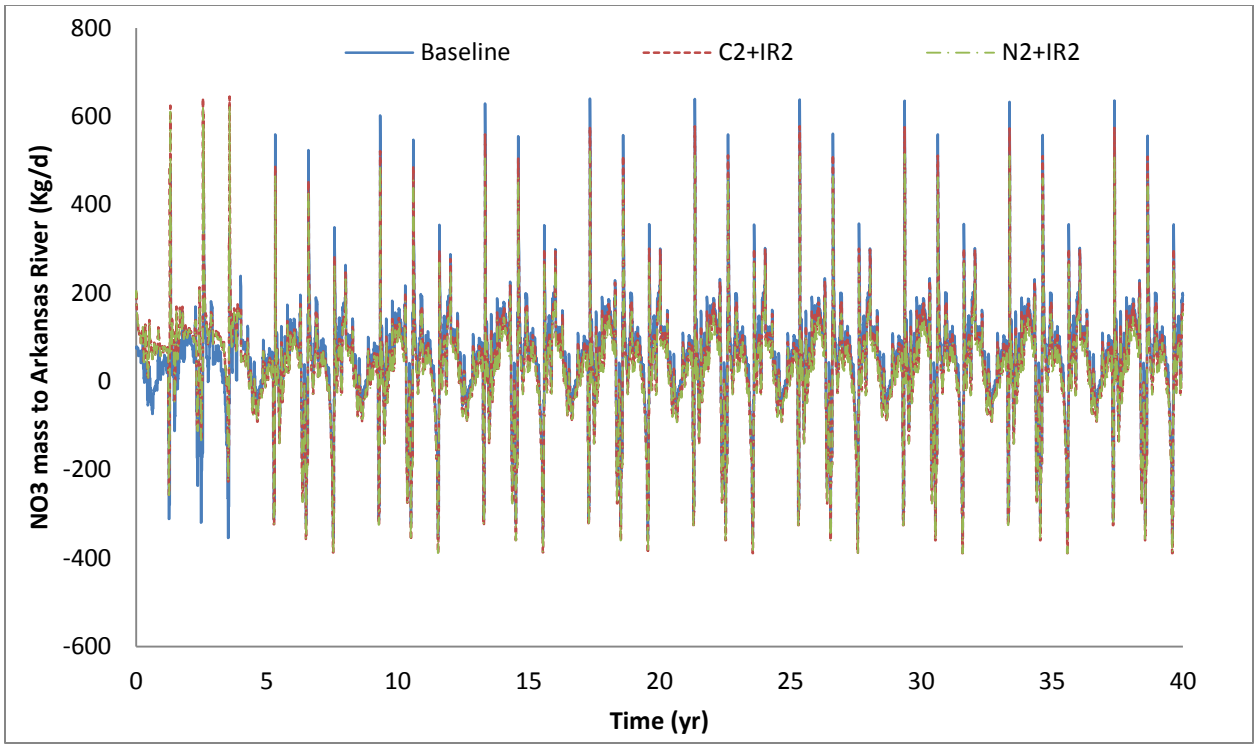

Figure 5.8: Mass Loadings of NO_3 – N for scenario's baseline, 8 and 10.

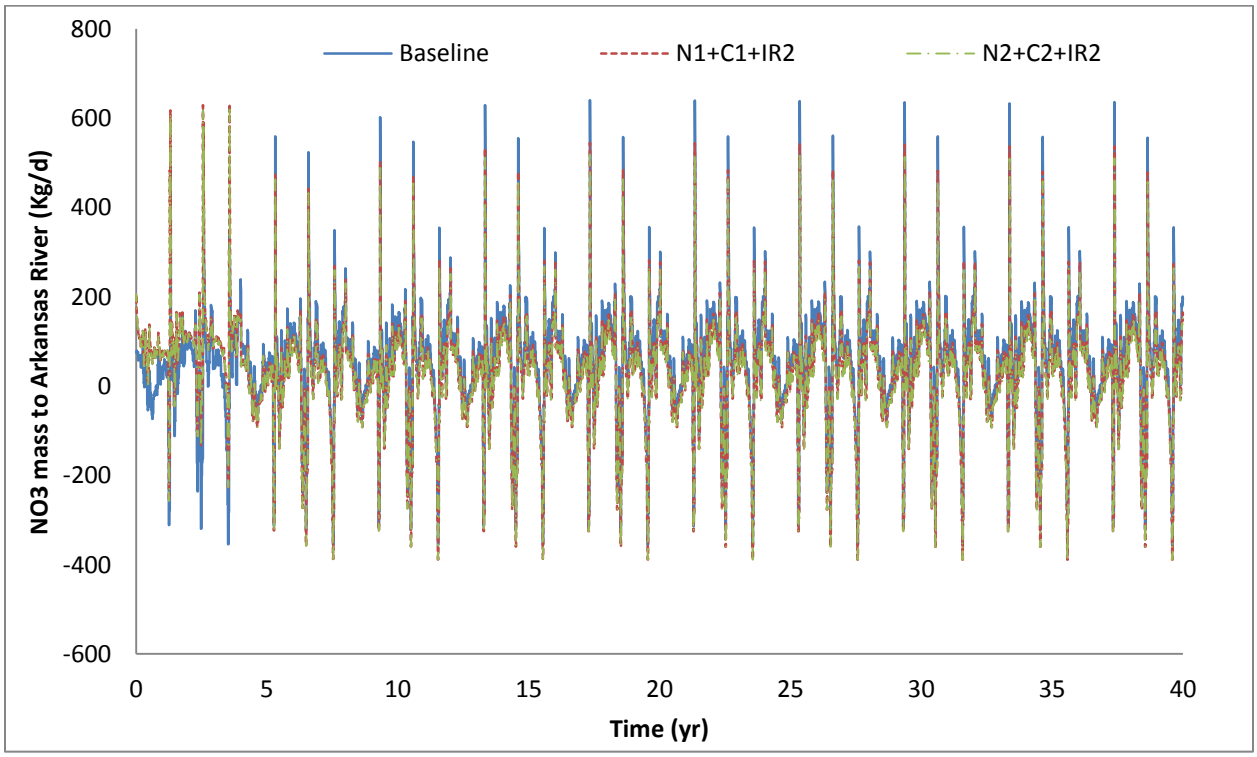

Figure 5.9: Mass Loadings of NO_3 – N for scenario's baseline, 12 and 14.

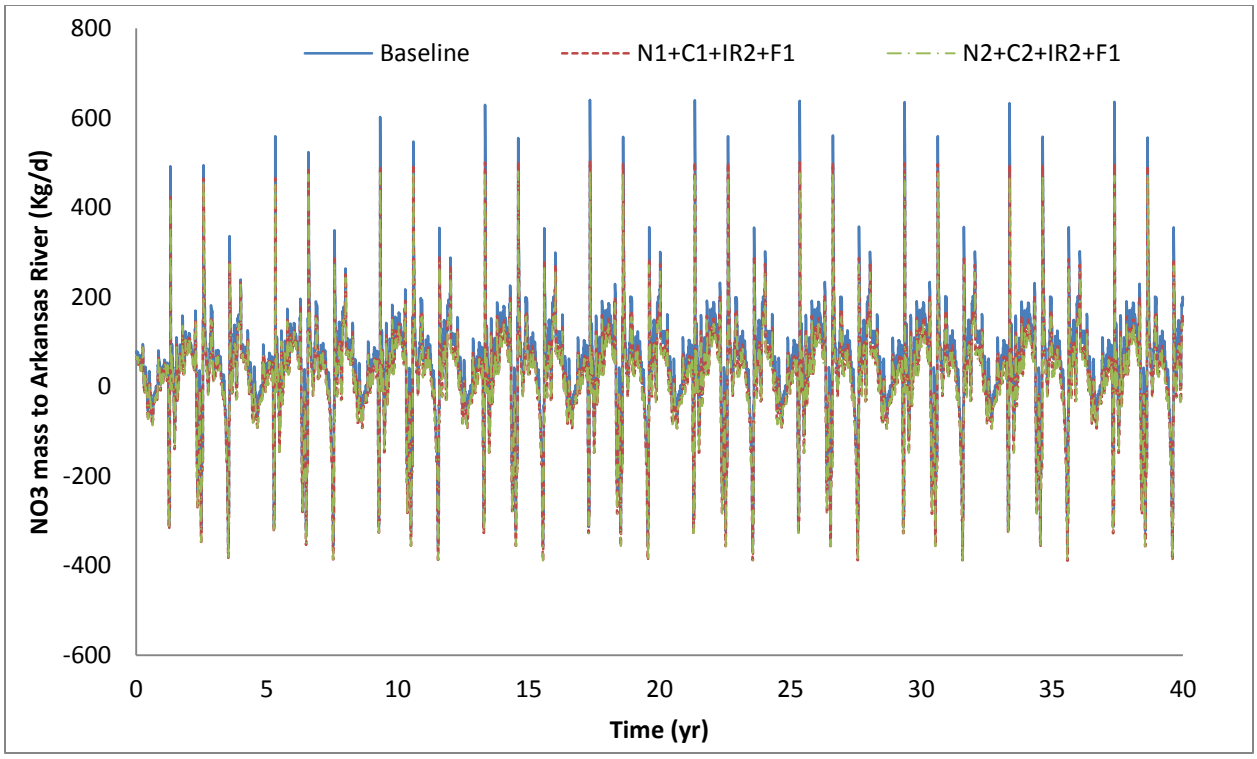

Figure 5.10: Mass Loadings of NO_3 – N for scenario's baseline, 16 and 18.

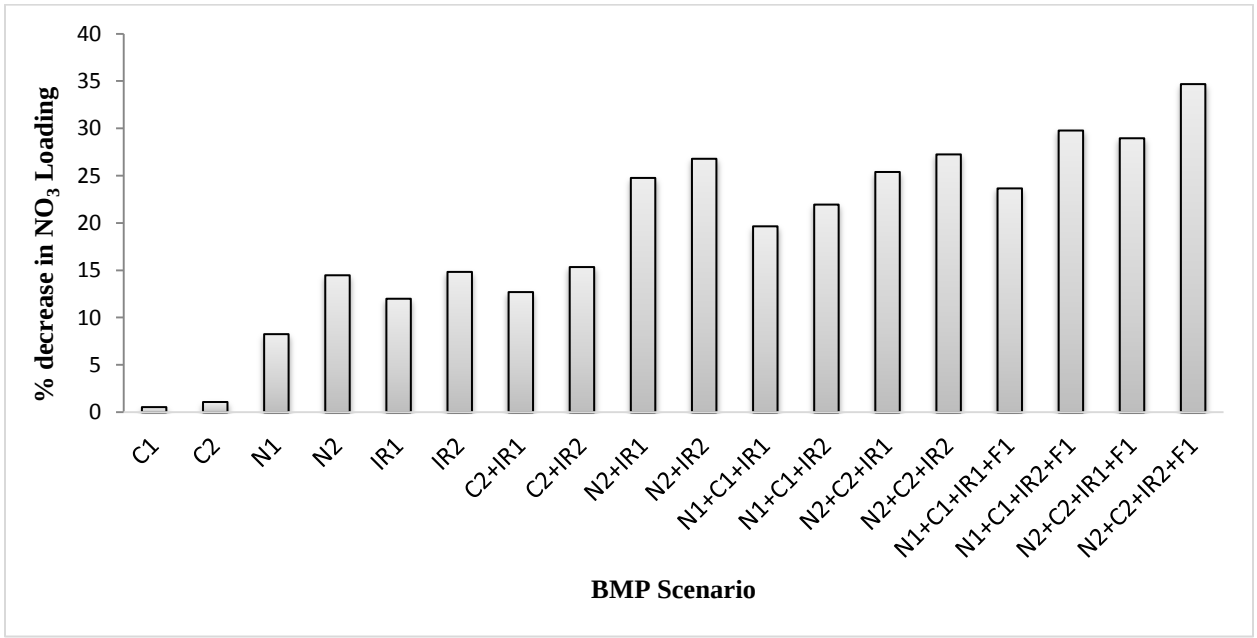

Figure 5.11: Percentage decrease of NO_3 – N mass loadings of all scenarios to the River Arkansas compared to baseline scenario.

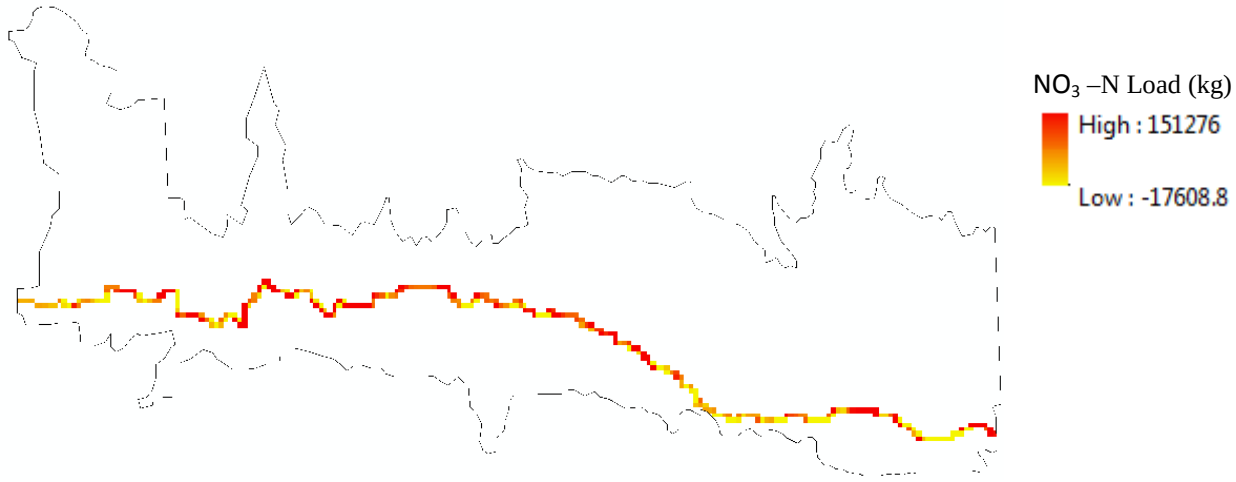

Figure 5.12: Spatial Pattern of baseline scenario total NO_3 – N mass loadings to Arkansas River from the aquifer for total 40 years simulation period.

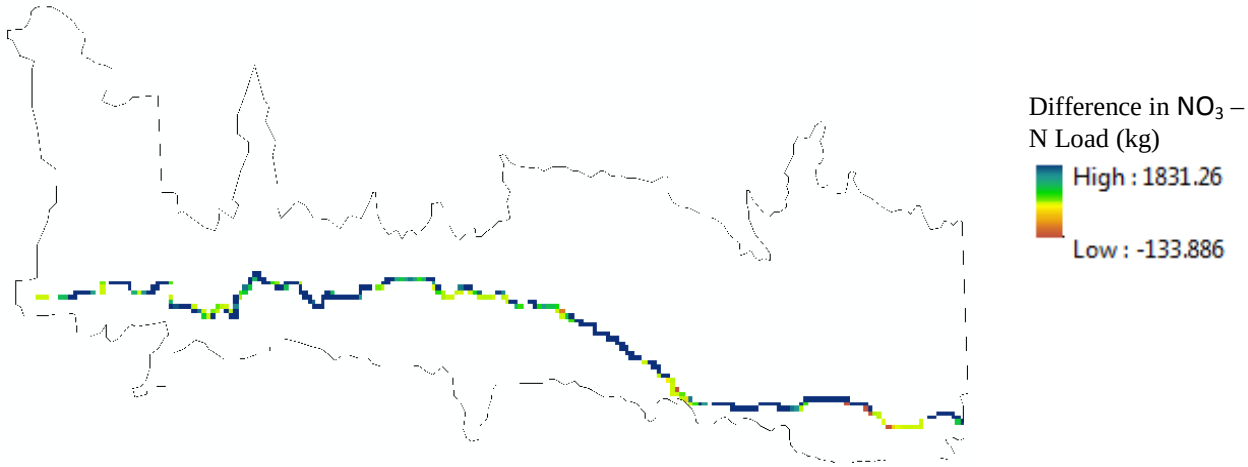

Figure 5.12a: Spatial Pattern of difference in total NO_3 – N mass loadings between baseline and scenario 2.

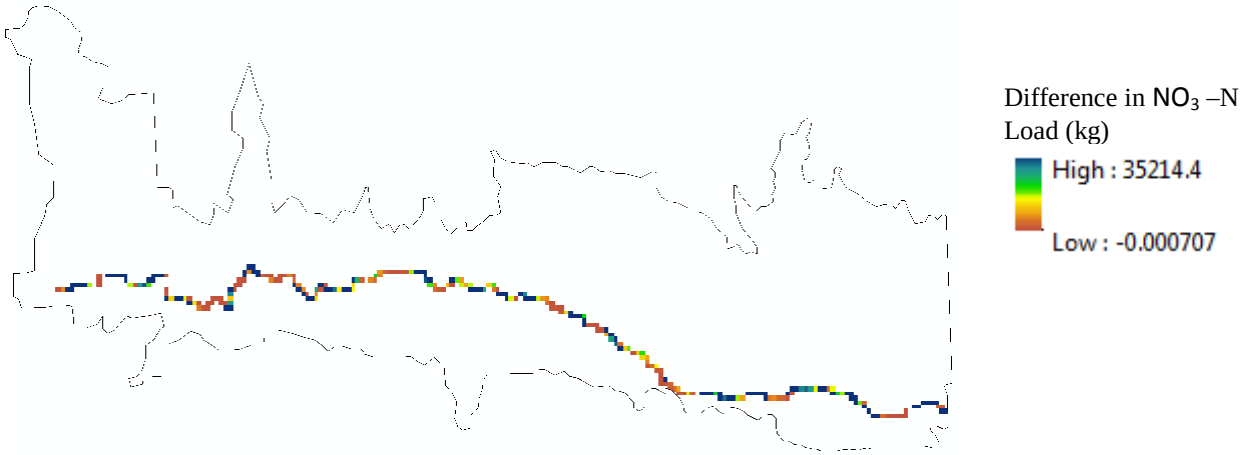

Figure 5.12b: Spatial Pattern of difference in total NO_3 – N mass loadings between baseline and scenario 4.

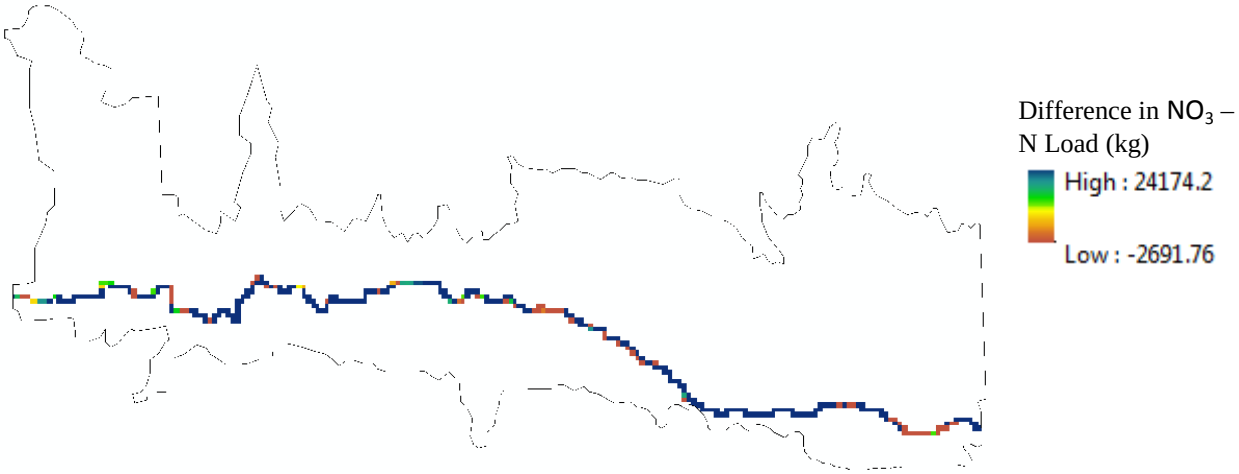

Figure 5.12c: Spatial Pattern of difference in total NO_3 – N mass loadings between baseline and scenario 6.

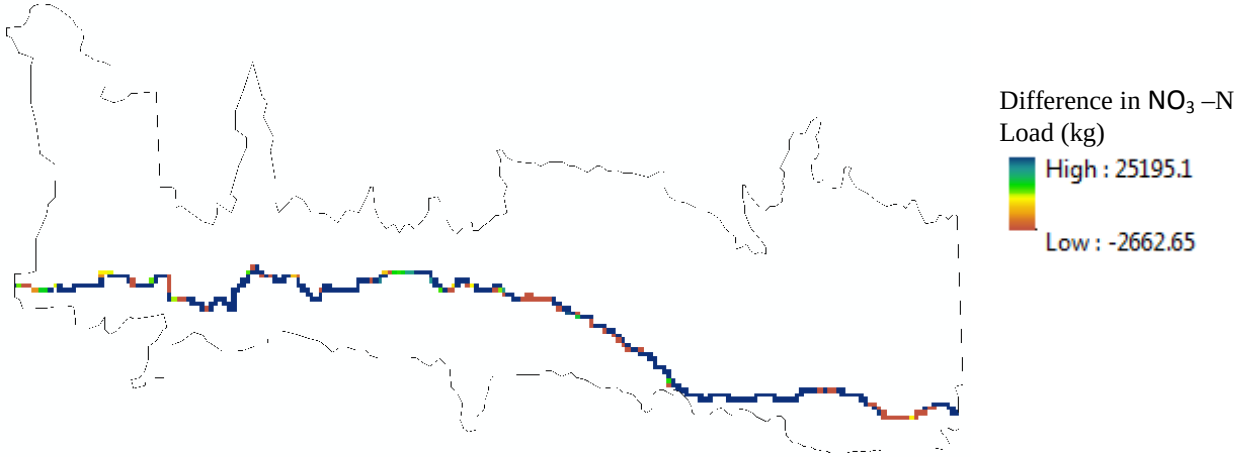

Figure 5.12d: Spatial Pattern of difference in total NO_3 – N mass loadings between baseline and scenario 8.

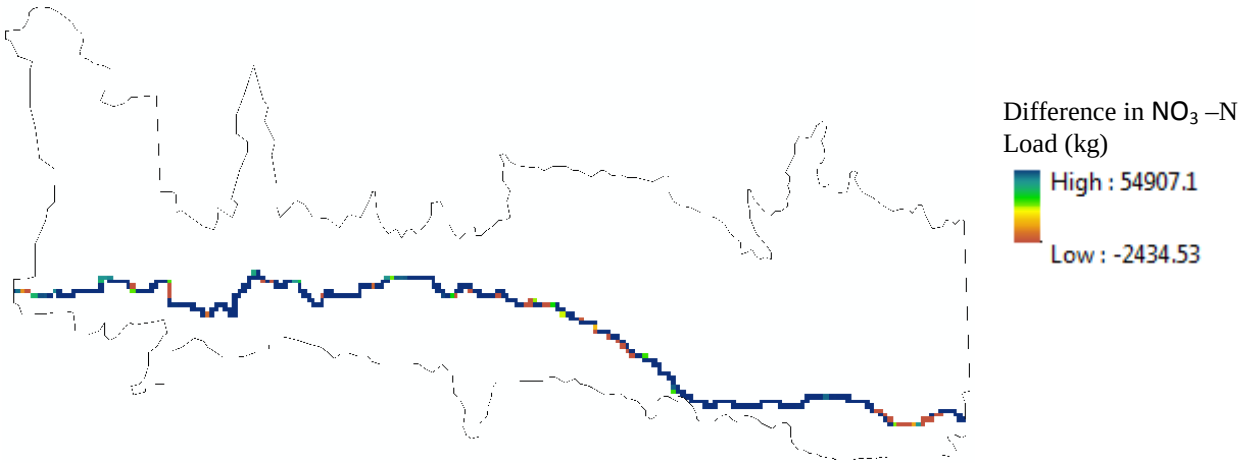

Figure 5.12e: Spatial Pattern of difference in total NO_3 – N mass loadings between baseline and scenario 10.

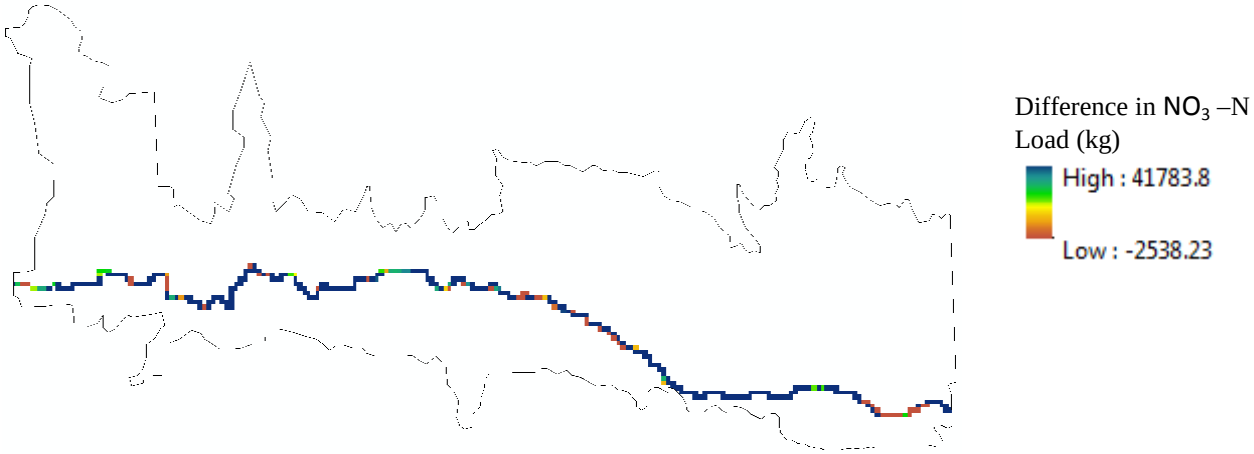

Figure 5.12f: Spatial Pattern of difference in total NO_3 – N mass loadings between baseline and scenario 12.

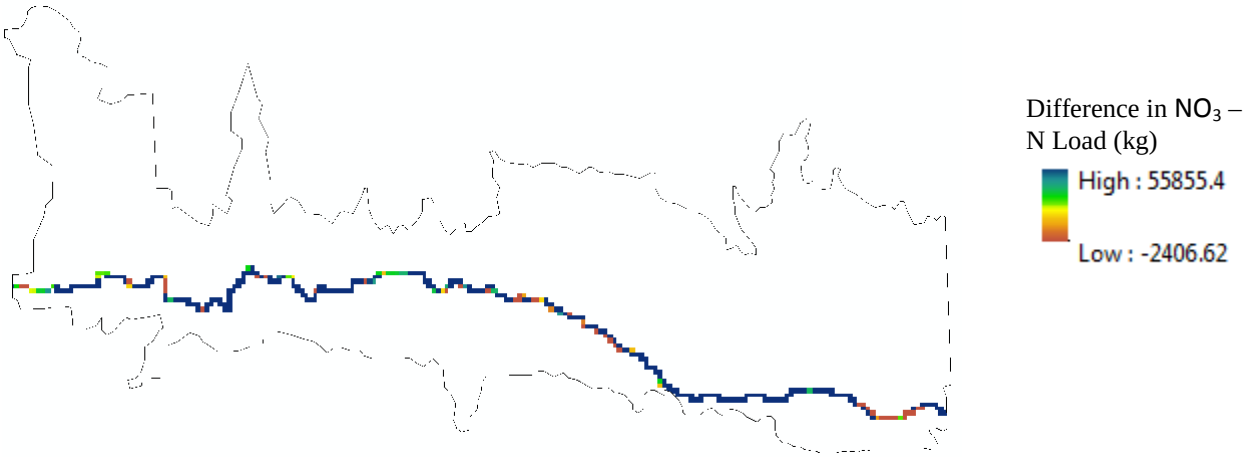

Figure 5.12g: Spatial Pattern of difference in total NO_3 – N mass loadings between baseline and scenario 14.

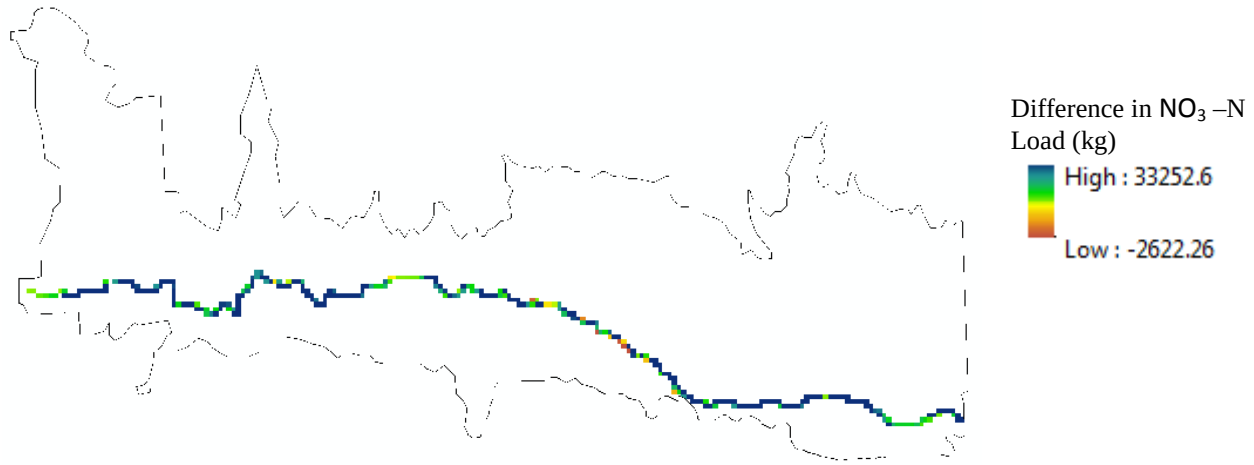

Figure 5.12h: Spatial Pattern of difference in total NO_3 – N mass loadings between baseline and scenario 16.

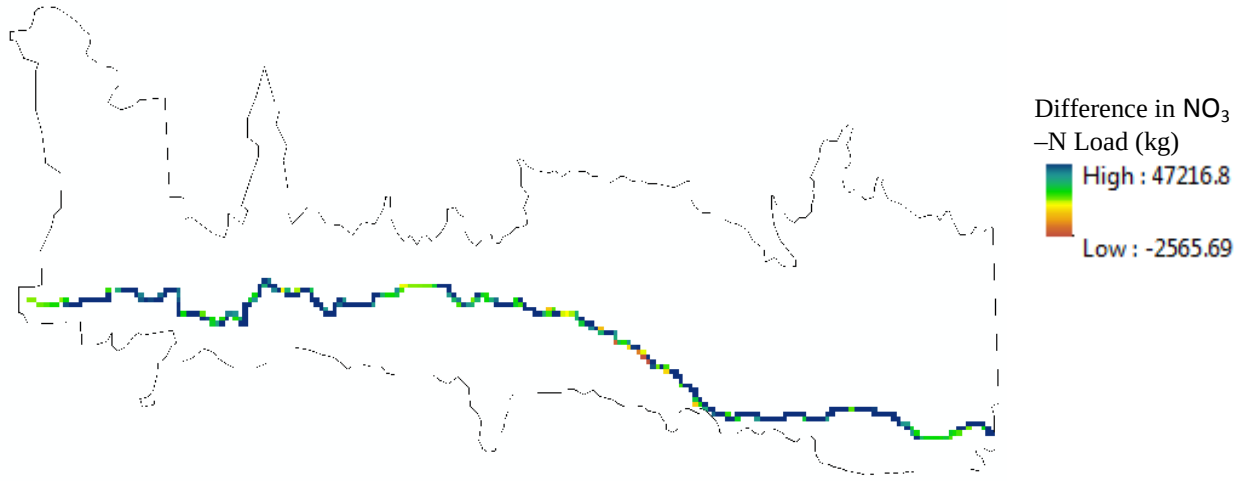

Figure 5.12i: Spatial Pattern of difference in total NO_3 – N mass loadings between baseline and scenario 18.

5.2.2 COMMAND AREA AVERAGE CONCENTRATIONS

The SeO_4 concentrations for each command area is calculated for the 40th year simulation for each scenario and compared to the baseline simulation and the percentage reduction concentration values are shown in Table 5.2. The multiple scenario BMPs has shown a strong impact in the Amity 2, Amity 3, Fort Bent, XY Graham 1, XY Graham 2 and Outside command areas with 27.8%, 16.8%, 35.4%, 11.4%, 40.4% and 32.3% respectively for SeO_4 reduction at the end of the 40-year simulation period. Independent scenario 2 (canal concentration) shown considerable impact in Buffalo1, Buffalo2, Lamar1, Lamar2 and Southside command areas with 6.7%, 13.3%, 15.3%, 13% and 4.9% respectively percent decrease. Similarly, the independent scenario 4 (fertilizer loading) shows considerable impact in Amity 1, Amity 2, Fort Lyon 2, and Lamar 3 command areas with 11.1%, 14.8%, 16.2% and 8.8% percent decrease respectively. The BMPs, except canal concentrations (1 and 2) and fertilizer loading (3 and 4), d~~oesn't~~ don't show any decrease in the command areas of Buffalo 1, Buffalo 2, Fort Lyon 1, Fort Lyon 2, Hyde Ditch, Lamar 1, Lamar 2, and Lamar 3.

Scenario 1 and 2 show maximum impact in Lamar 1 and Lamar 2 command areas with 7.7% and 15.3% respectively; scenarios 3 and 4 in Fort Lyon 2 with 12.1% and 16.2% respectively; scenarios 5, 7, 9, and 13 in outside command area with 10.1%, 11.4%,12.8%, and 13.8% respectively; scenarios 6, 8, 10,11,12, and 14 in Fort Bent command area with 23.5%, 23.8%, 23.7%, 17.8%, 23.8%, and 24% respectively. Scenarios 15, 16, 17, and 18 in XY Graham 2 with 38.5%, 36.1%, 40.4%, and 37.7% respectively. Overall, Fort Bent shows greater impact to most of the BMPs. The spatial SeO_4 concentrations for baseline scenario at the 40th year is shown in Figure 5.13. The spatial difference in the concentrations of SeO_4 between scenarios 2, 4, 6, 8, 10, 12, 14, 16, and 18 and the baseline scenario is shown from Figure 5.14a to 5.14i respectively of 40th year where the maximum and minimum decrease in the concentrations have been observed. Mainly in Fort Lyon command area, the SeO_4 concentration has increased compared to the baseline; this is because the water table depth has increased as shown in Figure 5.15.

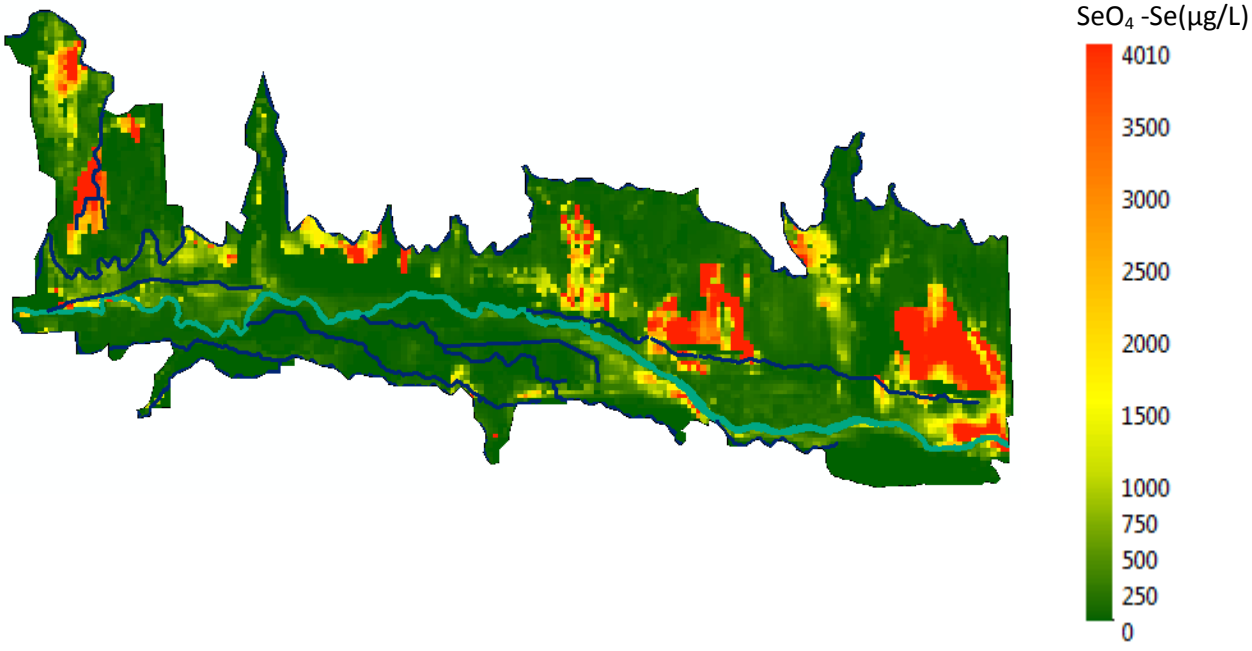

Figure 5.13: Spatial Pattern of baseline scenario SeO_4 –Se concentration at 40th year.

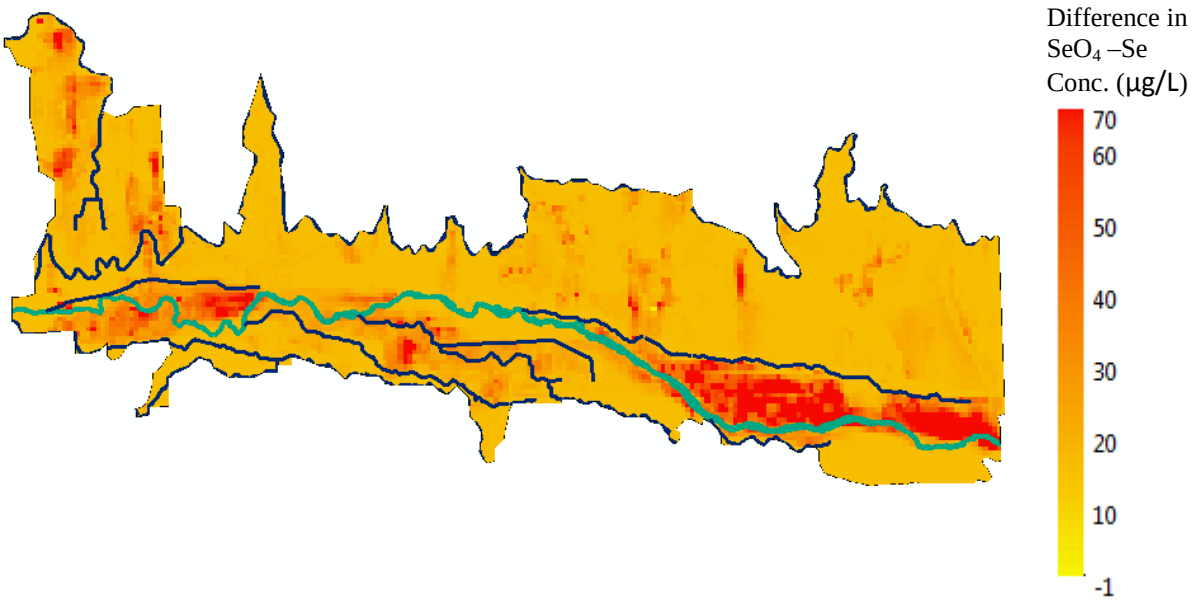

Figure 5.14a: Spatial Pattern of difference in SeO_4 –Se concentrations between baseline and scenario 2 of 40th year.

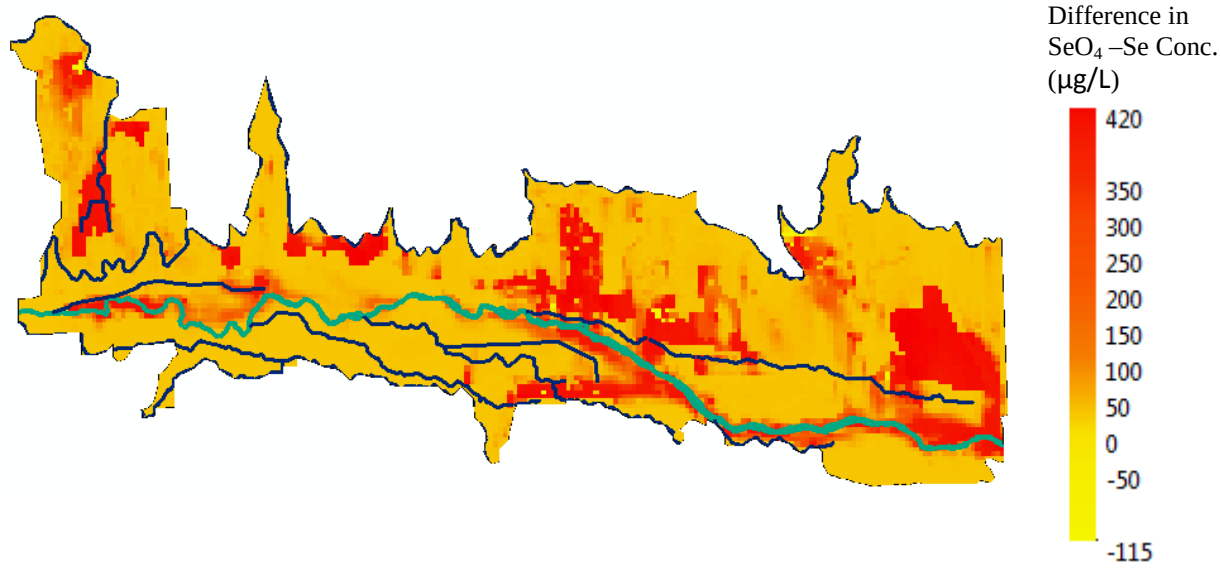

Figure 5.14b: Spatial Pattern of difference in SeO_4 –Se concentrations between baseline and scenario 4 of 40th year.

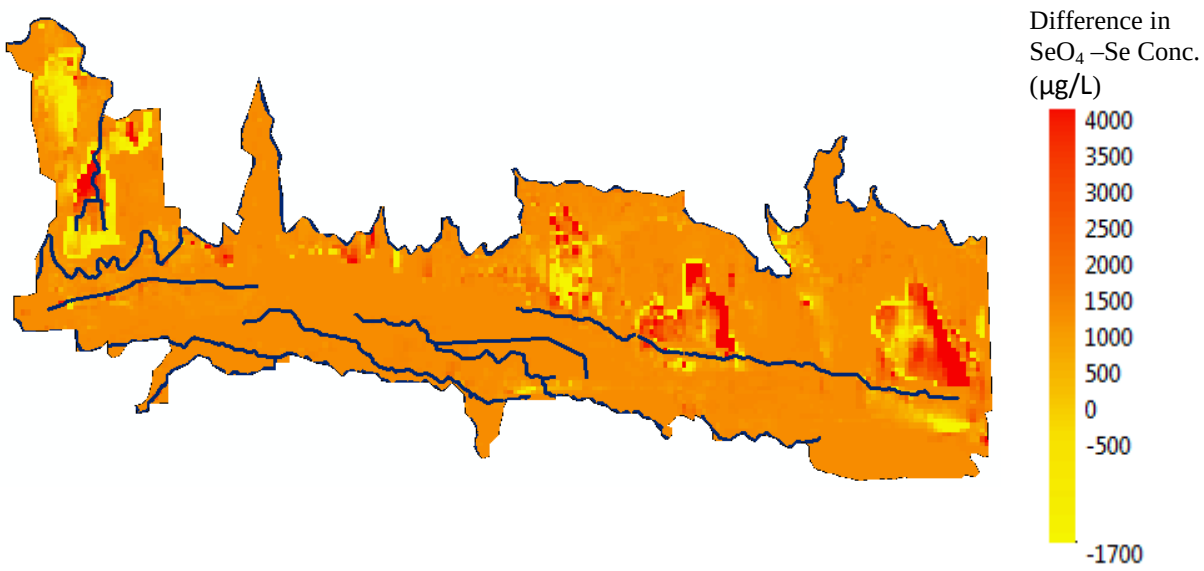

Figure 5.14c: Spatial Pattern of difference in SeO_4 –Se concentrations between baseline and scenario 6 of 40th year.

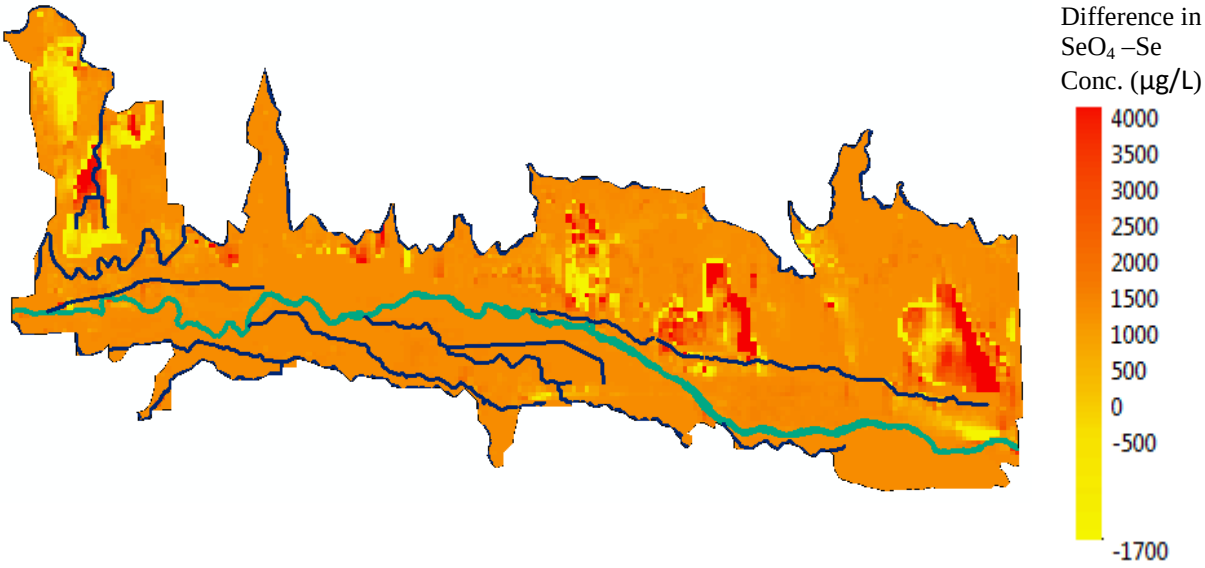

Figure 5.14d: Spatial Pattern of difference in SeO_4 –Se concentrations between baseline and scenario 8 of 40th year.

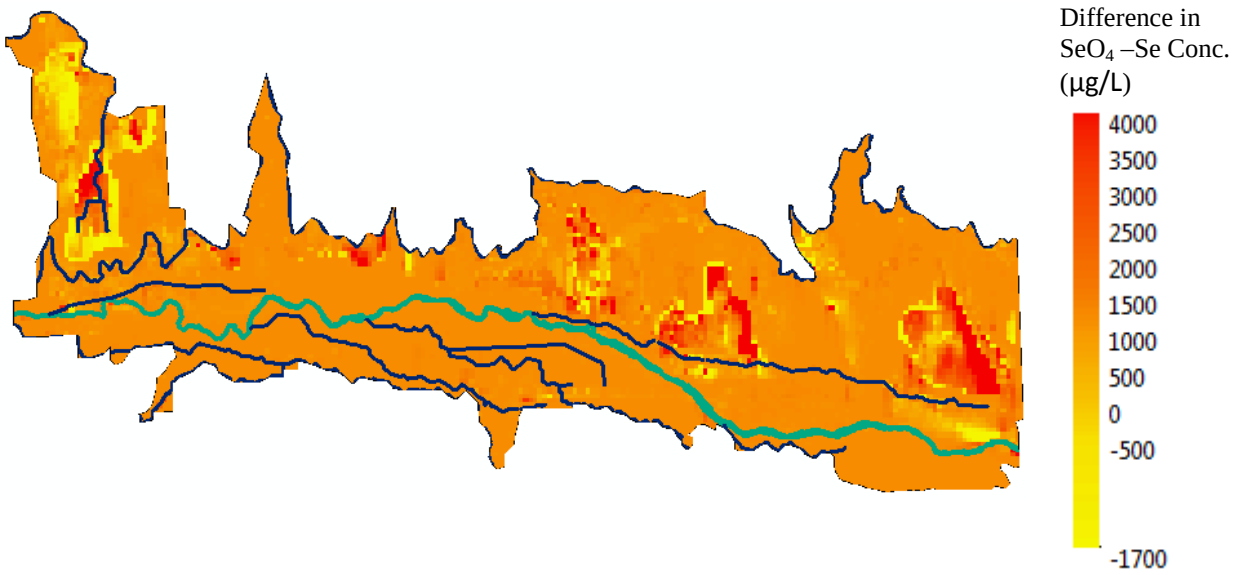

Figure 5.14e: Spatial Pattern of difference in SeO_4 –Se concentrations between baseline and scenario 10 of 40th year.

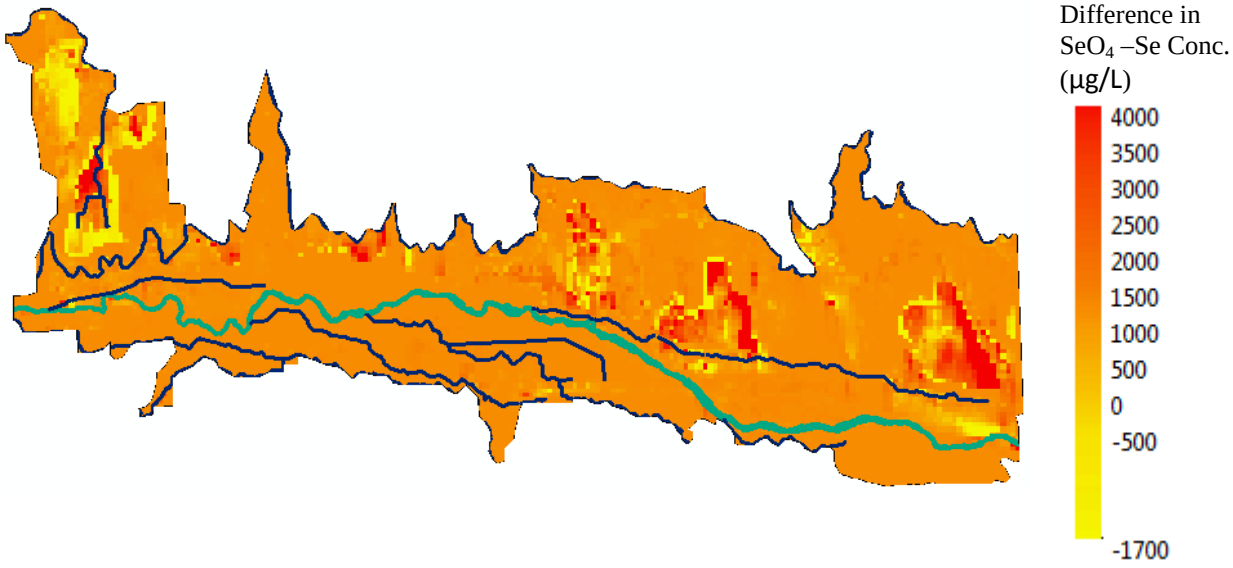

Figure 5.14f: Spatial Pattern of difference in SeO_4 –Se concentrations between baseline and scenario 12 of 40th year.

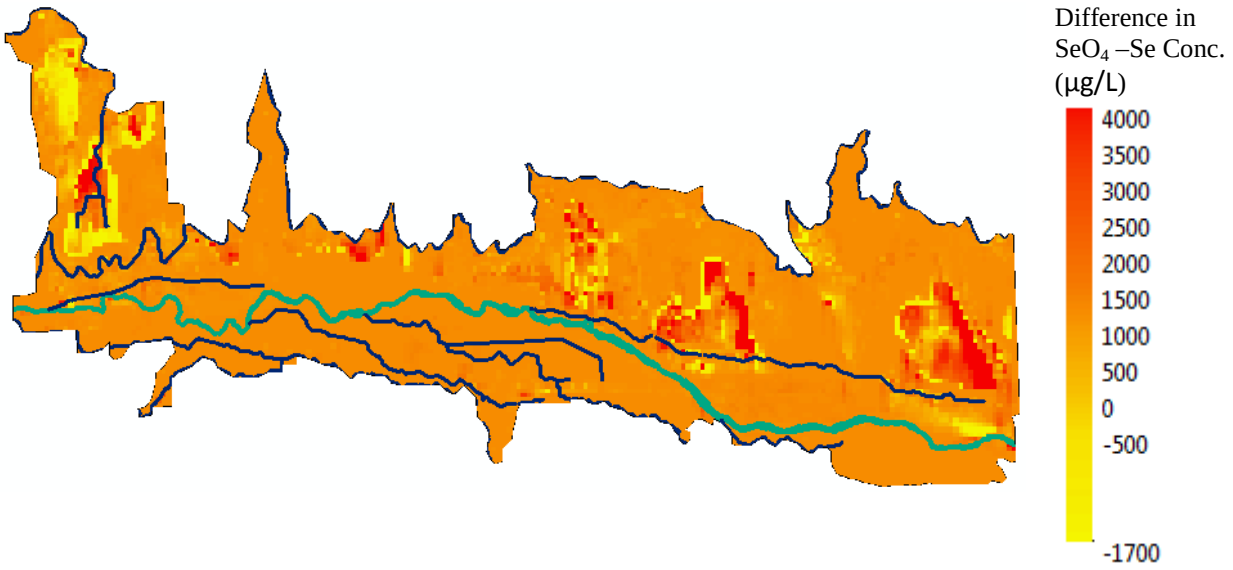

Figure 5.14g: Spatial Pattern of difference in SeO_4 –Se concentrations between baseline and scenario 14 of 40th year.

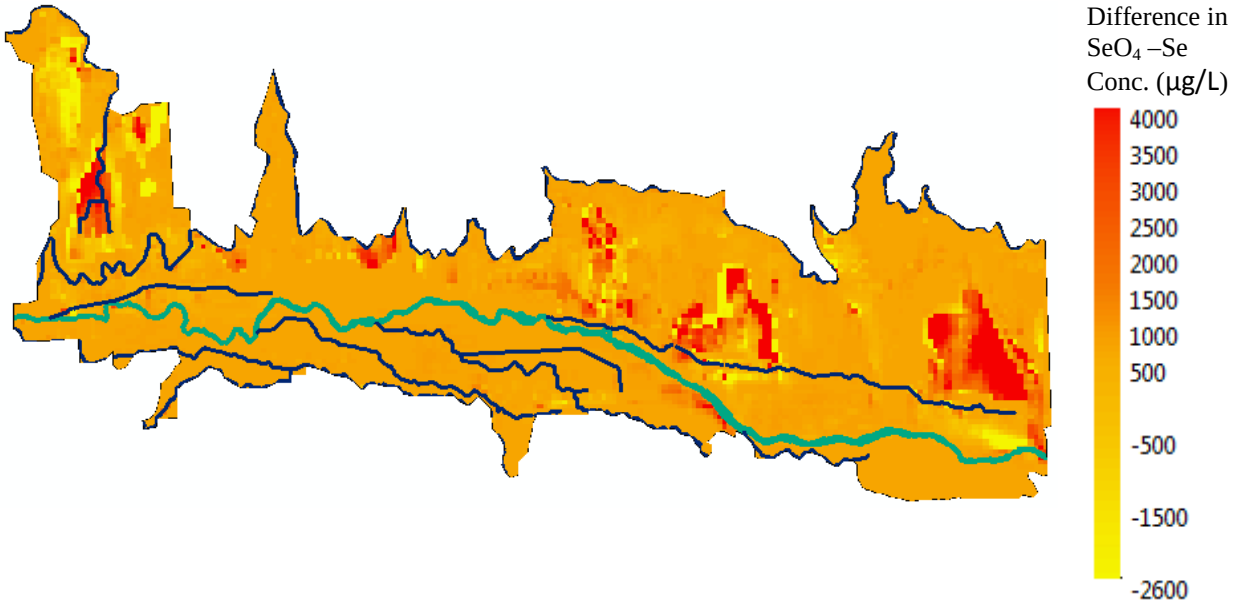

Figure 5.14h: Spatial Pattern of difference in SeO_4 –Se concentrations between baseline and scenario 16 of 40th year.

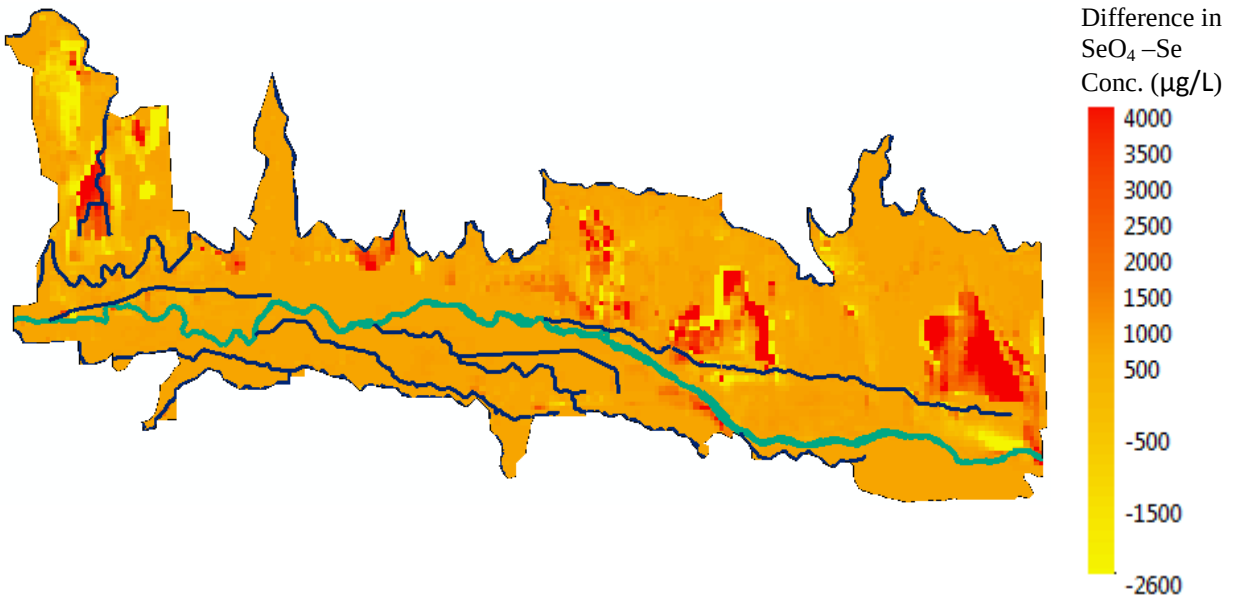

Figure 5.14i: Spatial Pattern of difference in SeO_4 –Se concentrations between baseline and scenario 18 of 40th year.

Table 5.2: Percent decrease of SeO_4 –Se of all scenarios compared with baseline scenario at the end of 40-yr simulation. Red highlight shows minimum and Blue highlight shows maximum decrease in each command area.

Scenario	Amity 1	Amity 2	Amity 3	Buffalo 1	Buffalo 2	Fort Bent	Fort Lyon1	Fort Lyon2	Hyde ditch	Lamar 1	Lamar 2	Lamar 3	South side	XY Graham1	XY Graham2	Outside
1	0.16	0.23	0.06	3.35	6.70	0.13	0.34	0.52	2.24	7.68	6.66	1.22	2.46	3.73	0.55	0.66
2	0.30	0.45	0.12	6.68	13.35	0.24	0.67	1.01	4.46	15.27	12.98	2.40	4.86	7.39	1.10	1.31
3	8.84	10.17	4.23	1.12	1.02	0.20	1.31	12.05	0.88	2.65	0.15	4.47	2.36	3.02	1.85	2.22
4	11.14	14.75	7.00	2.07	1.90	0.34	1.87	16.18	1.56	5.03	0.30	8.77	4.58	5.37	3.31	3.53
5	-2.21	-15.95	1.39	-7.26	-10.96	9.94	-41.11	-82.68	-3.63	-10.90	-3.70	-7.26	-2.96	1.50	-3.89	10.15
6	0.18	-9.50	2.59	-17.78	-25.06	23.55	-55.36	-137.03	-14.55	-22.75	-7.80	-17.01	-5.42	-0.60	-5.94	14.69
7	-1.99	-15.74	1.46	-1.69	1.54	10.19	-40.73	-82.16	0.02	1.27	5.83	-5.44	0.53	6.57	-3.16	11.35
8	0.36	-9.39	2.63	-13.11	-13.72	23.80	-55.09	-136.73	-11.42	-12.68	-0.13	-15.52	-2.97	3.51	-5.42	15.63
9	6.77	7.91	5.91	-5.52	-9.03	10.22	-39.20	-63.20	-2.04	-4.90	-3.38	4.73	1.19	6.32	0.33	12.72
10	5.22	14.37	5.72	-15.80	-22.92	23.73	-53.64	-121.82	-12.77	-15.58	-7.41	-3.43	-1.73	4.31	-1.92	16.99
11	4.17	-18.73	2.26	-12.97	-18.32	17.80	-50.95	-62.83	-11.93	-13.93	-3.64	-4.84	-2.33	4.22	-2.79	13.93
12	4.27	7.45	4.55	-14.38	-18.32	23.78	-53.95	-124.91	-11.93	-13.95	-3.63	-6.92	-2.33	4.22	-3.38	16.67
13	6.97	8.07	5.97	0.03	3.19	10.47	-38.83	-62.73	1.57	6.92	6.12	6.54	4.17	11.36	1.04	13.83
14	5.38	14.45	5.75	-11.15	-11.87	23.98	-53.38	-121.57	-9.69	-5.80	0.23	-1.93	0.32	8.39	-1.41	17.92
15	7.34	7.10	11.17	-18.90	-17.69	30.20	-66.06	-208.69	-23.12	-8.44	-0.47	-8.04	-2.82	6.86	38.49	27.46
16	8.30	24.79	16.22	-34.15	-37.51	35.22	-59.63	-206.59	-32.63	-25.86	-6.00	-12.50	-5.26	5.97	36.10	29.87
17	8.29	12.05	12.41	-15.34	-10.09	30.33	-65.82	-208.14	-21.25	-0.96	3.25	-0.61	0.42	11.14	40.40	30.08
18	8.77	27.77	16.78	-30.92	-30.49	35.35	-59.42	-206.26	-30.89	-18.87	-2.83	-6.13	-2.54	9.85	37.74	32.34

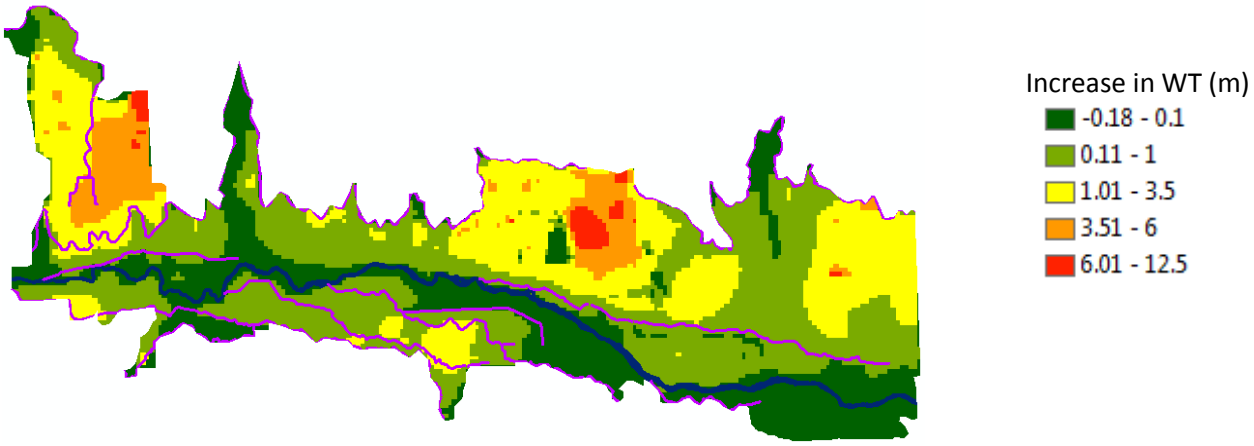

Figure 5.15: Spatial pattern of difference in Water Table depths (m) between scenario 18 and baseline.

The NO_3 concentrations for each command area is calculated for the 40th year simulation for each scenario and compared to the baseline simulation. These along with the percent decrease in concentration values are shown in Table 5.3. The multiple scenario BMPs have shown strong impact in the Amity 1, Amity 2, Amity 3, Fort Lyon 2, South side, XY Graham 1, XY Graham 2 and Outside command areas with 25.7%, 67.1%, 43.9%, 49.2%, 23.4%, 38.4%, 31.2%, and 28.7% respectively of NO_3 reduction at the end of the 40-year simulation period. The independent scenario 2 (canal concentration) shows considerable impact in Buffalo 1 and Buffalo 2 with 6.7% and 7.9% percent decrease respectively. Similarly, independent scenarios 3 and 4 (fertilizer loading) show moderate reduction in NO_3 in all command areas, but the maximum impact of scenario 3 was shown in Amity 2 (24.3%) and Fort Lyon 2 (24.8%); for scenario 4 in Fort Lyon 2 (35.9%) and XY Graham 2 (36.6%). Scenario 1 has shown very minimal impact in all command areas except in Buffalo 2 with a 4% decrease.

Scenarios 5 and 6 show maximum impact in Amity 2 with 18.2% and 39% respectively; scenarios 7, 8, 9,10, 12,13,14,15,16,17, and 18 show maximum impact in Amity 2 command area with 18.3%, 39%, 45.5%, 57.3%, 52.1%, 45.5%, 57.3%, 55.8%, 63.9%, 60.4%, and 67.1% decrease in NO_3 concentration respectively; whereas scenario 11 shows XY Graham 1 with 22.1% decrease in NO_3 concentration. Overall command areas, Amity 2 show maximum reduction for most the BMPs. The spatial NO_3 concentrations for the baseline scenario at the 40th year is shown in Figure 5.13. The spatial difference in the concentrations of NO_3 between the 2, 4, 6, 8, 10, 12, 14, 16, and 18 scenarios and the baseline scenario is shown from Figure 5.17a to 5.17i respectively of 40th year where the maximum and minimum decrease in the concentrations has been observed.

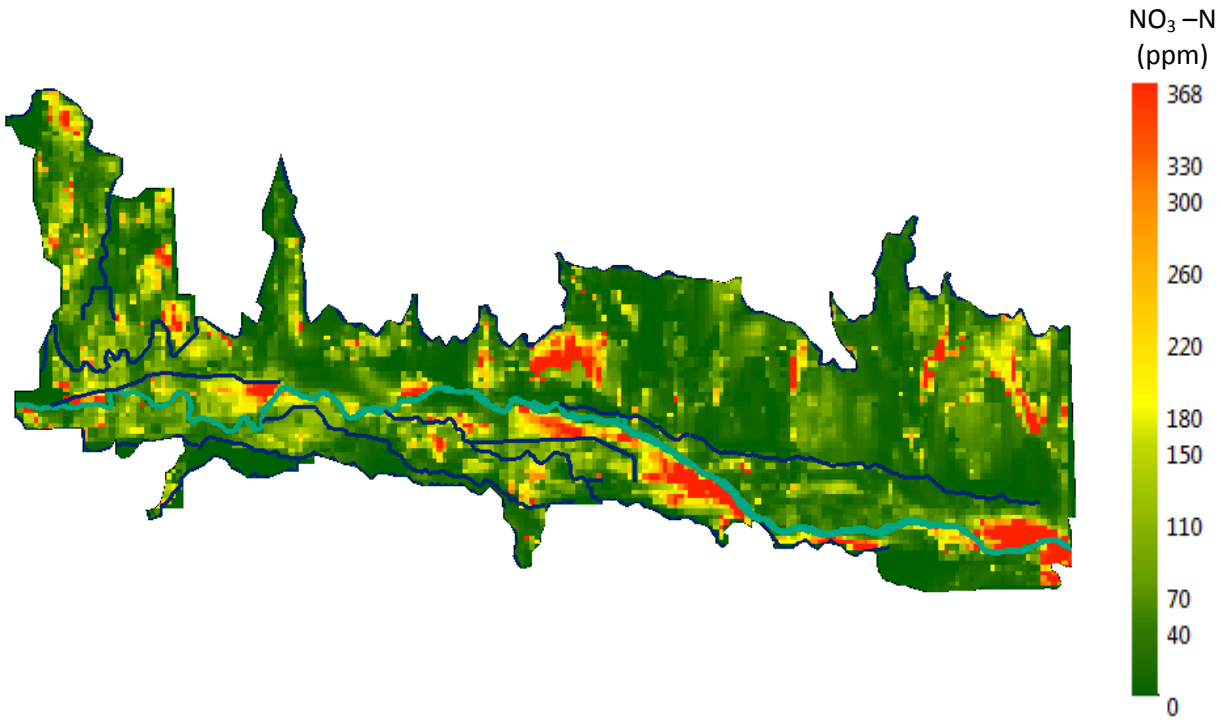

Figure 5.16: Spatial Pattern of Cell by Cell NO_3 –N concentration of Base Line scenario at 40th year simulation.

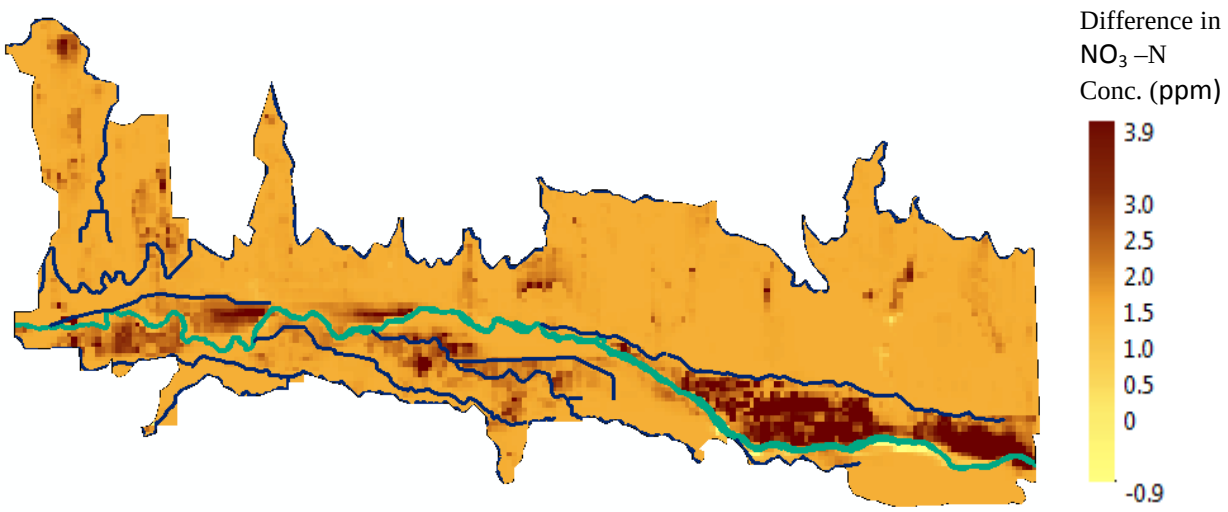

Figure 5.17a: Spatial Pattern of difference in NO_3 –N concentrations between baseline and scenario 2 of 40th year.

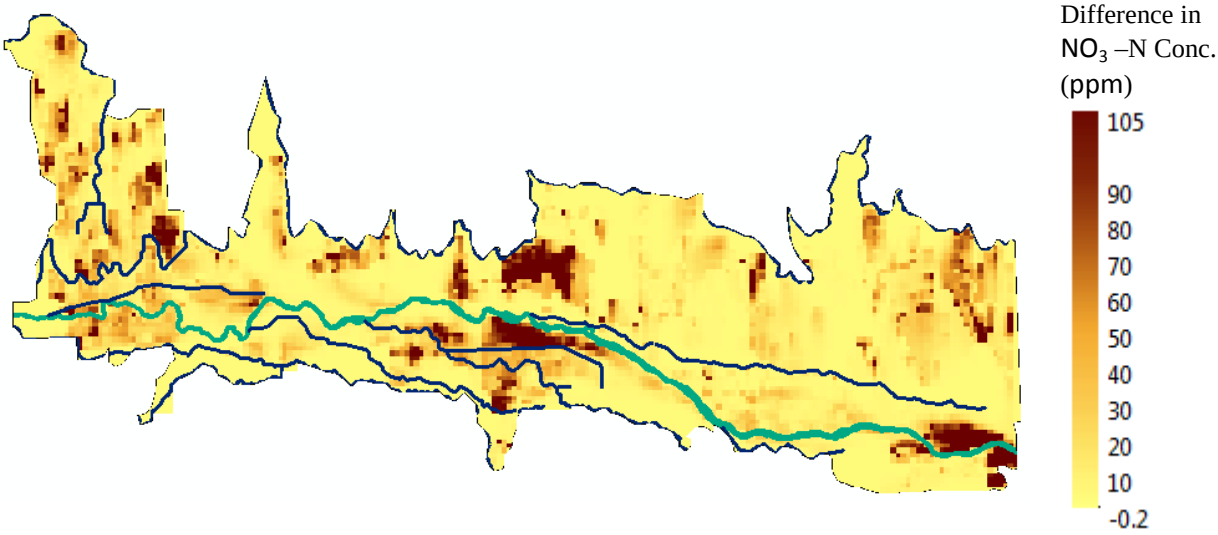

Figure 5.17b: Spatial Pattern of difference in NO_3 –N concentrations between baseline and scenario 4 of 40th year.

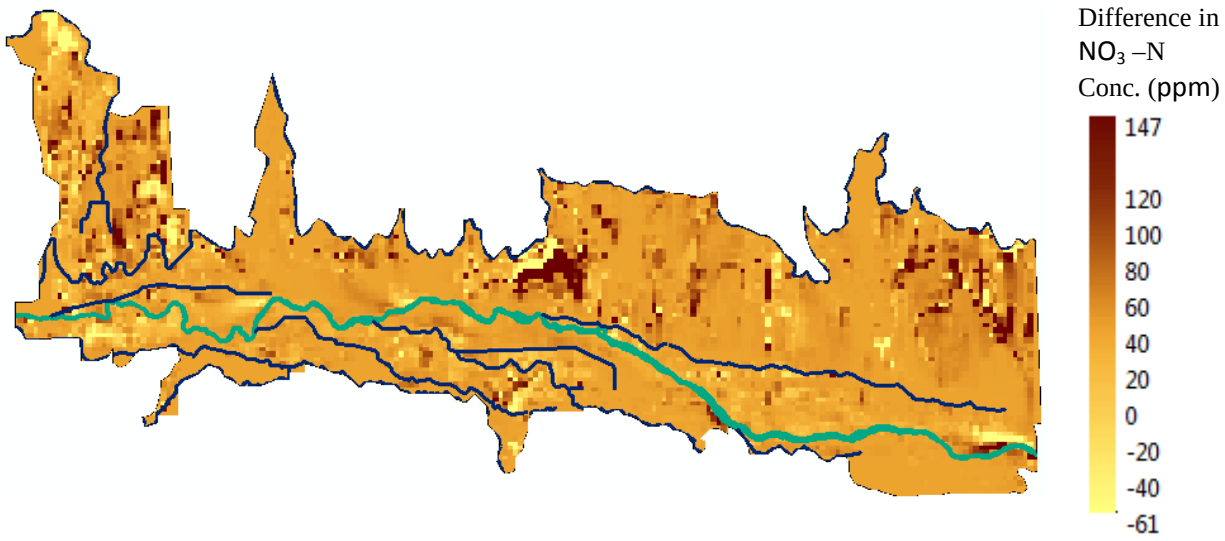

Figure 5.17c: Spatial Pattern of difference in NO_3 –N concentrations between baseline and scenario 6 of 40th year.

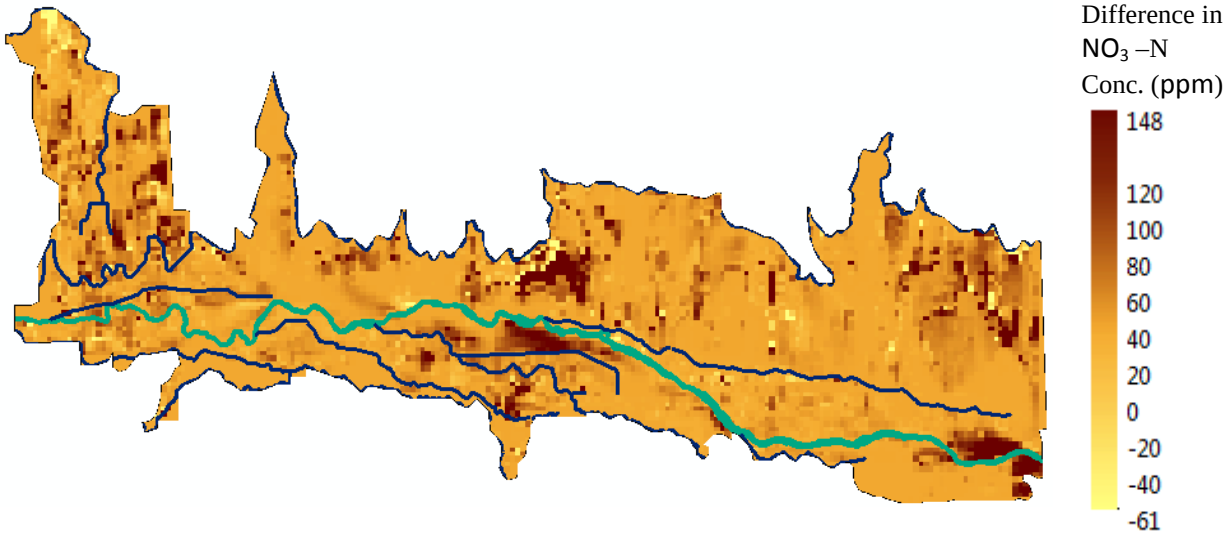

Figure 5.17d: Spatial Pattern of difference in NO_3 –N concentrations between baseline and scenario 8 of 40th year.

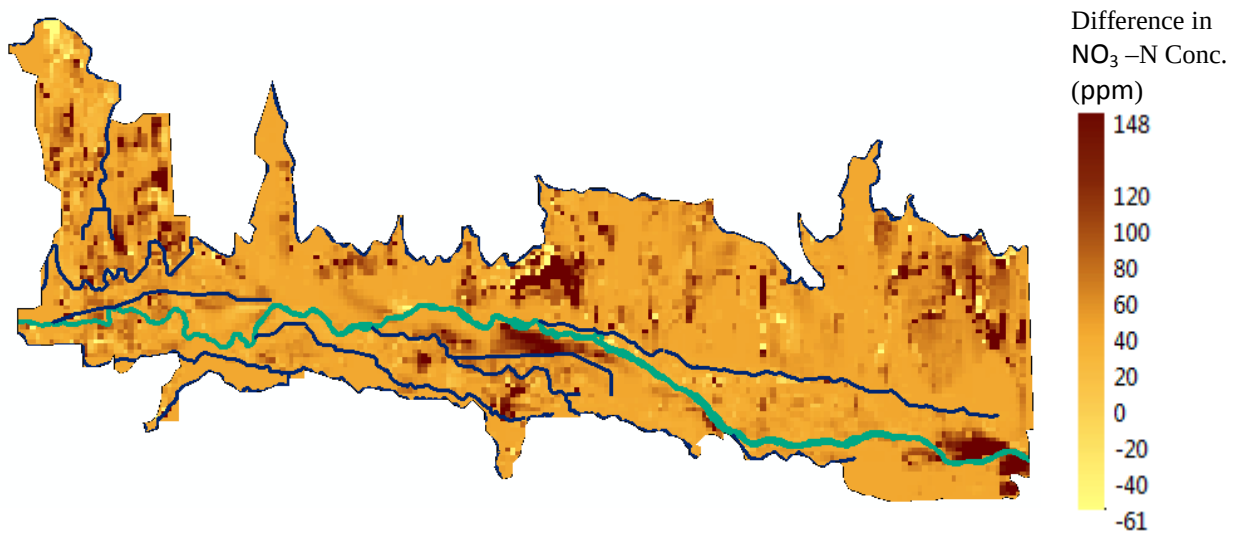

Figure 5.17e: Spatial Pattern of difference in NO_3 –N concentrations between baseline and scenario 10 of 40th year.

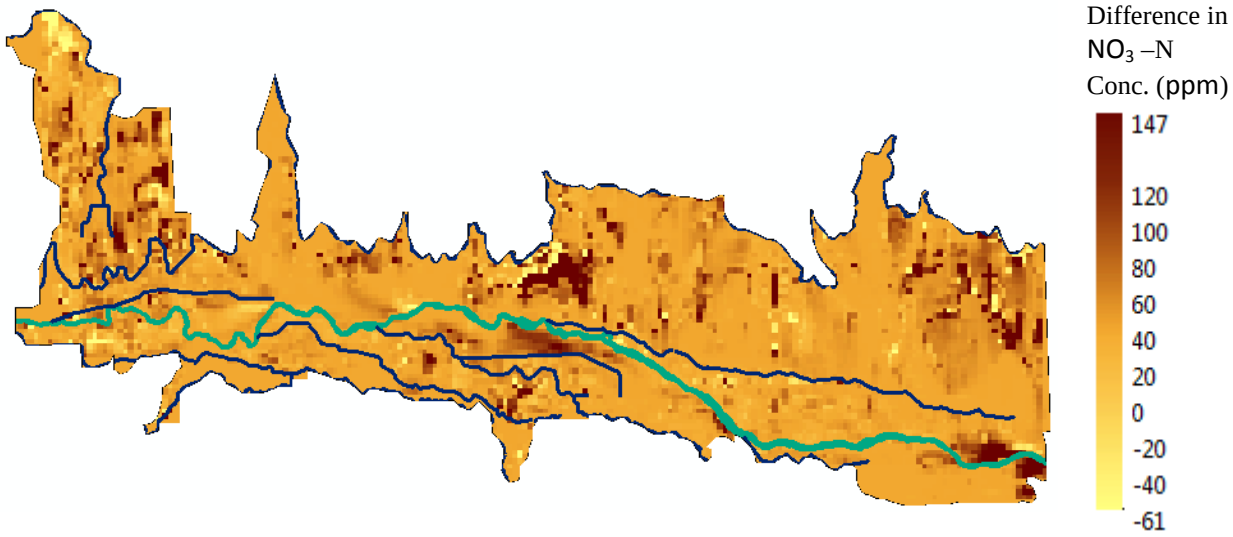

Figure 5.17f: Spatial Pattern of difference in NO_3 –N concentrations between baseline and scenario 12 of 40th year.

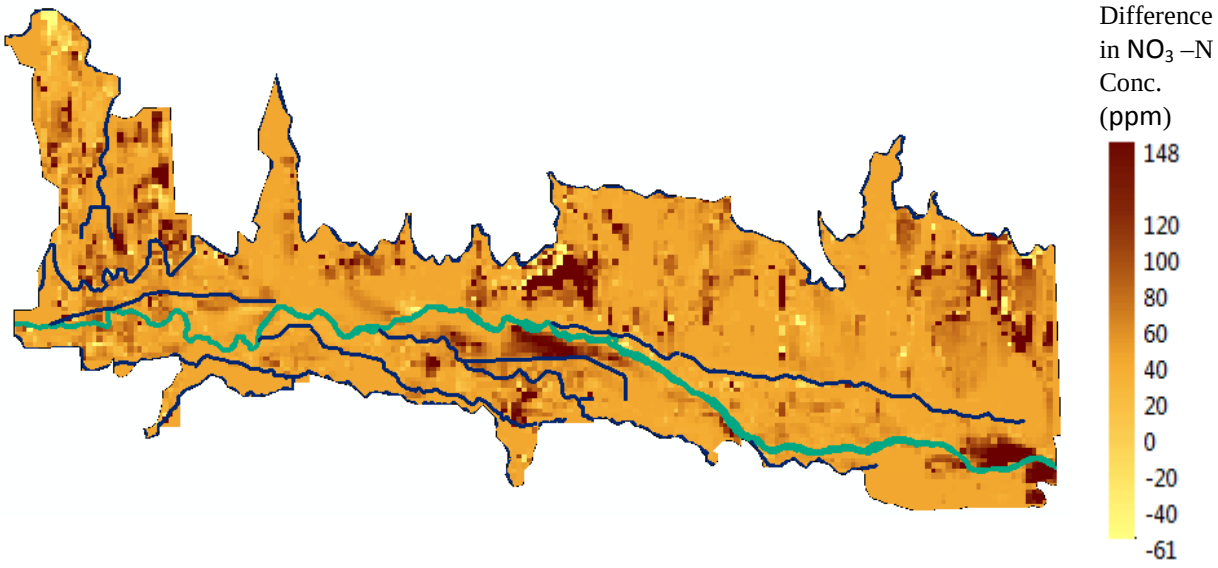

Figure 5.17g: Spatial Pattern of difference in NO_3 –N concentrations between baseline and scenario 14 of 40th year.

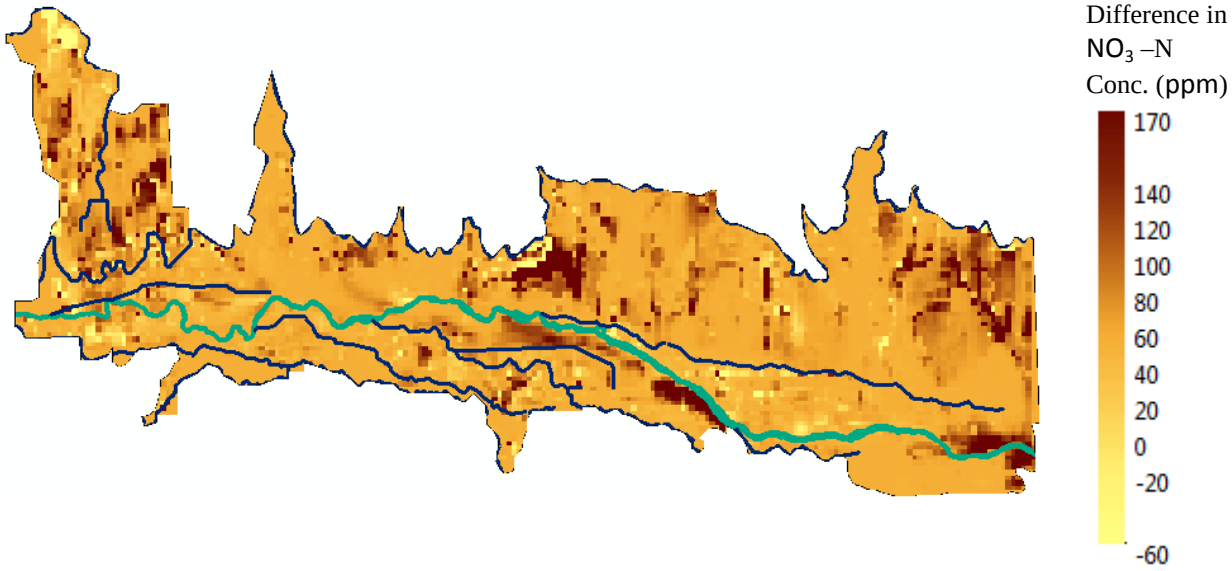

Figure 5.17h: Spatial Pattern of difference in NO_3 –N concentrations between baseline and scenario 16 of 40th year.

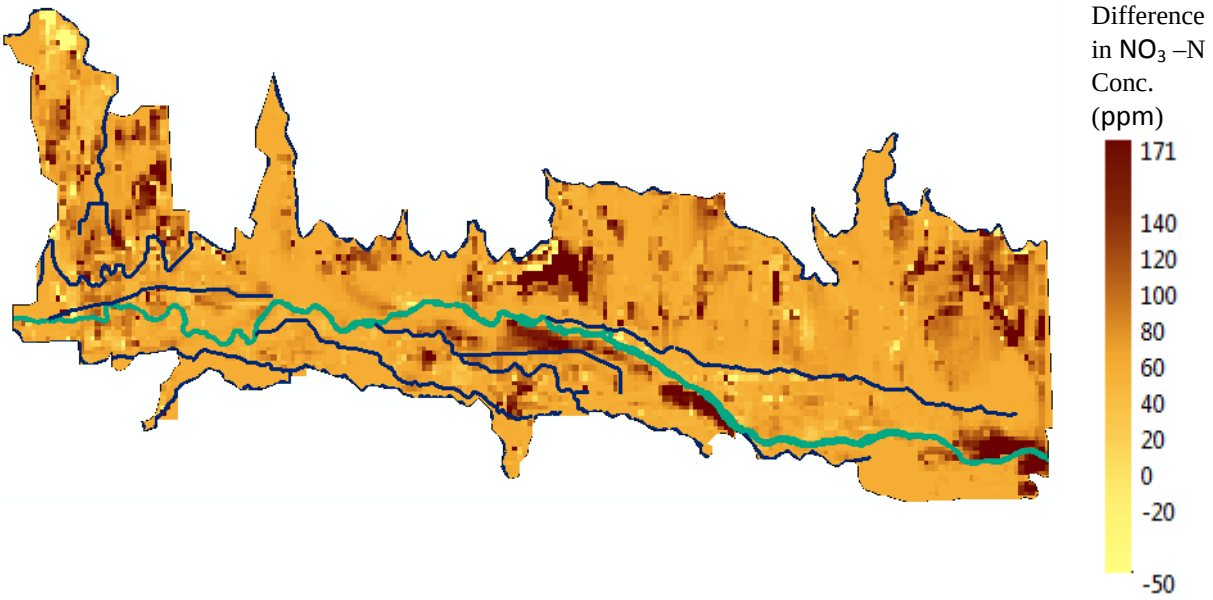

Figure 5.17i: Spatial Pattern of difference in NO_3 –N concentrations between baseline and scenario 18 of 40th year.

Table 5.3: Percent reduction of NO_3 –N of all scenarios compared with baseline scenario at the end of 40-yr simulation. Red highlight shows minimum and Blue highlight shows maximum decrease in each command area.

Scenario	Amity 1	Amity 2	Amity 3	Buffalo 1	Buffalo 2	Fort Bent	Fort Lyon1	Fort Lyon2	Hyde ditch	Lamar 1	Lamar 2	Lamar 3	South side	XY Graham1	XY Graham2	Outside
1	0.12	0.09	0.05	3.37	3.97	0.02	0.16	0.13	0.38	0.52	0.27	0.36	-0.13	0.18	0.02	0.45
2	0.23	0.18	0.10	6.68	7.87	0.03	0.32	0.27	0.75	1.04	0.54	0.72	-0.26	0.36	0.03	0.90
3	15.40	24.31	14.81	6.36	10.21	0.25	16.35	24.81	8.54	15.75	6.12	16.20	15.03	21.02	1.14	11.51
4	23.02	35.79	22.17	11.61	19.25	0.45	25.41	35.87	14.40	28.02	11.12	29.42	23.82	36.62	2.03	19.65
5	0.15	18.22	8.09	-4.58	-7.79	-4.95	-7.82	-4.65	-0.22	-16.49	-4.23	-10.79	-0.03	1.59	0.96	2.47
6	4.10	39.01	17.55	-14.95	-19.99	-2.79	-14.12	8.91	-4.85	-32.30	-6.62	-13.57	0.16	1.20	1.66	8.12
7	0.34	18.29	8.16	1.09	-0.98	-4.91	-7.61	-4.51	0.39	-15.65	-3.83	-10.21	-0.27	1.83	0.98	3.25
8	4.27	39.04	17.59	-10.39	-14.34	-2.76	-13.96	8.99	-4.36	-31.63	-6.28	-13.07	-0.07	1.40	1.68	8.68
9	21.51	45.46	26.65	7.75	14.71	-4.56	14.19	34.99	13.20	18.50	7.97	23.78	23.66	37.57	2.88	21.28
10	22.77	57.29	32.71	-0.92	6.90	-2.50	6.01	39.52	9.05	9.92	6.32	25.05	23.63	37.37	3.55	25.34
11	12.35	19.45	19.38	-4.84	-2.85	-5.41	-5.99	17.87	3.81	-7.35	0.44	1.41	14.82	22.07	2.73	15.49
12	16.50	52.09	28.53	-5.01	-2.85	-2.62	-0.43	31.49	3.81	-7.36	0.80	8.72	14.82	22.07	2.74	18.38
13	21.67	45.49	26.70	13.15	20.91	-4.52	14.33	35.05	13.77	19.16	8.34	24.26	23.41	37.78	2.89	22.00
14	22.91	57.31	32.74	3.34	11.96	-2.47	6.11	39.54	9.50	10.43	6.62	25.45	23.41	37.54	3.56	25.87
15	17.47	55.81	38.04	-7.50	-8.77	-3.31	3.66	41.03	7.08	0.62	1.89	4.62	14.68	23.15	30.74	19.73
16	20.22	63.92	41.96	-16.53	-19.45	-1.62	-2.40	44.02	3.43	-9.98	0.60	6.10	14.82	23.08	30.58	20.67
17	23.33	60.43	40.48	1.72	8.69	-3.22	7.60	47.23	12.18	16.44	7.74	21.02	23.40	38.39	31.33	27.92
18	25.65	67.09	43.80	-6.86	-0.49	-1.55	1.09	49.20	8.52	8.05	6.52	23.65	23.47	38.35	31.16	28.71

From Table 5.2 and 5.3, the NO_3 has shown better decrease in concentration compared to SeO_4 for all command areas. The maximum reduction of SeO_4 shows in XY Graham 2 with 40.4% for scenario 17, whereas the NO_3 shows 67.1% in the Amity 2 for scenario 18. These percentage decreases in concentrations are calculated using the command averages in each command area at the 40^{th} year.

5.3 COMPARISON OF DOWNSTREAM AND UPSTREAM STUDY REGION

A comparison was made with the similar study done in the Upstream Study Region (USR) for the reduction of SeO_4 and NO_3 .The chemical parameter rates and best management practices adopted in the study are tabulated in Table 5.4.

Table 5.4: Comparison table of Upstream and Downstream study region in LARV.

S.No	Comparison Item	Upstream	Downstream
1	Study Area	50,600 ha	55,200 ha
2	Irrigated Area	26,400ha	33,000 ha
3	Command Areas	6	16
4	Canals	6	8
5	Influential Parameters*	λnit $\lambda_{NO_3}^{auto}$ $\lambda_{O_2}^{auto}$	$\lambda_{O_2}^{auto}$
6	Model Simulation Period	2006 to 2009	2003 to 2007
7	BMP simulation Period	36 years	40 years
8	Mass Loadings reduction SeO_4 -Se NO_3 - N	 34.5% 52%	 22.7% 34.7%
9	Effective BMP	Fertilizer reduction (30%) + Canal conc. Reduction (30%) + Heterotrophic denitrification and reduction of SeO_4 (50%)	Fertilizer reduction (40%) + Canal conc. Reduction (40%) + Irrigation Volume reduction (35%) + Land Fallowing (25%)

* Chemical parameter rates are taken from Upstream where the parameter rates are taken from literature in similar studies and used PEST to estimate the parameter rates.

From the comparison, the DSR shows less reduction of SeO_4 and NO_3 mass loadings compared to the USR. This is because the effective remediation strategy is entirely different in

both cases. The main difference of highest reduction in USR is the implementation of a riparian buffer zone (heterotrophic denitrification and heterotrophic reduction of SeO_4). However, this BMP has very complex kinetics to apply in the model, so this was not considered as a management alternative in DSR. Thus, the maximum percentage reduction of applied BMP has been considered as 40%, while in USR it is only 30%.

CHAPTER NO: 6

6 CONCLUSIONS AND RECOMMENDATIONS

6.1 MAIN CONCLUSIONS

The research summarizes the study of best management practices to reduce the SeO_4 and NO_3 mass loadings to the Arkansas River and their concentrations in the groundwater in regional scale irrigated agricultural groundwater systems. The study includes applying the MODFLOW and RT3D models to the 55,200 ha region within the Lower Arkansas River Valley in southeastern Colorado. These models are chosen because the MODFLOW was the *defacto* model to simulate the groundwater flow and their predictions, whereas the RT3D model is the fate and transport model used in the similarly successful study of the Upstream Study Region in the Lower Arkansas River Valley in southeastern Colorado.

The calibrated RT3D model was used to investigate the best management practices in the Downstream Study Region (DSR) in the Lower Arkansas River Valley (LARV) in southeastern Colorado for both Se and NO_3. Practices investigated include reduction in canal concentration for both SeO_4 and NO_3 (20% and 40%); N fertilizer reduction (20% and 40%); reduction in volume of applied irrigation water (20% and 35%); and several combinations of these practices with fallowing of irrigated land (25%). These scenarios are compared with the baseline scenario where there is no land and water management alternative applied.

These practices were applied individually and concurrently as shown in Table 5.1. Calibration simulations were run for 2003-2007 and then an additional 40 years, with the 10-year hydrologic period repeated for four times. This duration was deemed necessary to allow the land-

management practices to adequately impact the mass loadings of N and Se to surface water due to the long travel time of groundwater.

Overall, the practices had considerable impact on the resulting C_{SeO_4} in groundwater for some command areas (0.06% to 40%), whereas in other areas the concentrations were increased due to lowered water table, which reduces the soil moisture content. However, the mass loadings of SeO_4 to the Arkansas River were significant when implementing the irrigation volume reduction (13.1% to 13.5%). Moreover, when combining this practice with ~~of~~ N fertilizer and canal concentration of SeO_4 and NO_3 reduction, irrigation volume reduction resulted in 14.8% to 19.3%. The other individual scenarios like N fertilizer reduction and canal concentration of SeO_4 and NO_3 reduction showed less reduction in mass loadings to the Arkansas River which is clearly shown in Figure 5.5.

Similarly, the practices had major impact on the resulting C_{NO3} in groundwater for all command areas (0.05% to 67%); where the N fertilizer reduction practices showed major reduction, almost all command areas compared to canal concentration of SeO_4 and NO_3 and irrigation volume reduction practices. For NO_3, the mass loadings showed a significant decrease from 8% to 15% through fertilizer reduction and irrigation volume reduction practices. On the other hand, canal concentration reduction showed a minor impact from 0.5% to 1%; this is clearly seen in Figure 5.10. Thus, in combination scenarios, fertilizer reduction and irrigation volume reduction along with canal concentration reduction in SeO_4 and NO_3 scenarios showed greater reduction results of a 13% to 27.3% decrease in NO_3 mass loadings to the Arkansas River.

Results indicate that combining the practices of decreasing fertilizer loading, decreasing canal concentration, and irrigation volume reduction combined with land fallowing decreased the mass

loading of SeO_4 and NO_3 to the Arkansas River by approximately 15-23% and 20-35%, respectively. Analysis of spatial variations in concentration and load reduction suggests further that local areas within the aquifer and along the Arkansas River can be targeted for changes in land-management practices such as reduction in groundwater concentration and mass loadings.

These results should be tempered by an understanding of the limitations of the model as stated in Sec 3.5 in Chapter 3. Even with these limitations, however, there is an obvious and desired overall decrease in groundwater concentrations and mass loadings when employing these land-management practices.

6.2 FUTURE RESEARCH

The areas where future research can possibly improve the current research, which was limited by lack of time and resources, are as follows: limitation of time and resources as follows:

Implementation of lining of the canals to reduce the seepage into the groundwater: This might behave well as a BMP to reduce the Se and NO_3 in groundwater system.

Linking the groundwater mass loadings of Se and NO_3 from this study to the surface water: OTIS software could be used to estimate the final concentration of Se in the Arkansas River and its tributaries (where the streams and rivers have a stringent CDPHE chronic standard of 4.6µg/L for Se concentration).

Incorporating phosphorus (P) and sulfur (S) cycling in order to calculate the influence of PO_4 and SO_4 on Se species. As P is generally a nutrient of focus in agricultural systems, and since SO_4 is the principal constituent of salt in the LARV, multiple benefits would be derived from including these cycles in RT3D.

7 REFERENCES

Abuereish, O.M., and J.N. Lahham. 1987. Selenium in soils and plants of the Jordan Valley. J. Arid Environ. 12:1-7.

Agency For Toxic Subsatnces And Disease Registry (ATSDR) , 2003 Public Health Statement – Selenium Cas #:7782-49-2, Departmnet of Health and Human Services.

Afzal, S., M. Younas, and K. Ali. 2000. Selenium speciation sutides from Soan-Sakesar Valley, Salt Range, Pakistan. Water International. 25:425-436.

Ahlrichs, J. S., and L. R. Hossner. 1987. Selenate and selenite mobility in overburden by saturated flow. J Environ Qual. 16:95-98.

Ajwa, H. A., G. S. Bañuelos, and H. F. Mayland (1998), Selenium uptake by plants from soils amended with inorganic and organic materials, J Environ Qual, 27, 10.

Alfthan, G., D. Wang, A. Aro, and J. Soveri. 1994. The geochemistry of selenium in groundwaters in Finland. Science of the Total Environment. 162:93-103.

Anderson, M.S., H.W. Lakin, K.C. Beeson, F.F. Smith, and E. Thacker. 1961 1%1. Selenium in agriculture. USDA Agric. Handb. 200. U.S. Gov. Print. Office, Washington, DC.

Bailey, R.T., T.K. Gates., Halvorson A.D., (2013a), Simulating variably-saturated reactive transport of selenium and nitrogen in agricultural groundwater systems, J. Cont. Hydrol., 149, 27 - 45.

Bailey, R.T., Morway, E.D., Niswonger, R.G., and T.K. Gates (2013b), Modeling variably-saturated multi-species reactive transport with MODFLOW-UZF and RT3D. GroundWater.

Beck, M.A., Levander, O.A., and J. Handy (2003), Selenium deficiency and viral infection. J. Nutr. 133 (5 Suppl 1): 1463S-7S.

Bisbjerg, B., and G. Gissel-Nielsen (1969), The Uptake of Applied Selenium by Agricultural Plants, Plant and Soil, 31(2), 12.

Bratter, P., Negretti de Bratter, W.G. Jaffe and H. Mendy Castellano. 1991. Selenium status of children livingin seleniferous areas of Venezuela. J. Trace Elem. Electrolytes in Health & Dis. 5(4).

Burkhalter, J. P., and Gates, T. K. (2005). "Agroecological impacts from salinization and waterlogging in an irrigated river valley". Journal of Irrigation and Drainage Engineering, ASCE, 131(2): 197 - 209.

Bye, R., and W. Lund .1982. Determination of selenium in pyrite by the atomic absorption-hydride generate technique. Fresenius Z Anal Chem. 313:211-212.

Cantrell, M.A., Brye, K.R., Miller, D.M., Mason, E. and Fairey, J. (2014) Extraction Characteristics of Selenium as Affected by Coal Fly Ash Type, Water Extractant, and Extraction Time. Journal of Environmental Protection, 5,1126-1144.

Clement, T.P., Sun, Y., Hooker, B.S., and J.N. Peterson (1998), Modeling multispecies reactive transport in groundwater. Groundwater Mon. & Rem., 18, 79-92.

Clement, T.P. (1997), RT3D – A modular computer code for simulating reactive multi-species transport in 3-dimensional groundwater aquifer. Draft report. PNNL-SA-28967. Richland, Washington: Pacific Northwest National Laboratory

David Y. Boon, 1989, Selenium in Agriculture and the Environment, Soil Science Society of America (SSSA) and America Society of Agronomy, Special Publication no.23.

Deason, J.P., 1986, U.S. Department of the Interior investigations of irrigation-induced contamination problems, in Summers, J.B., and Anderson, S.S., eds., Toxic substances in agricultural water supply and drainage—Defining the problems—Proceedings of regional meeting of the U.S. Committee on Irrigation and Drainage, September 1986, Boulder, Colo.: Washington, D.C., U.S. Government Printing Office, p. 201–210.

Dhillon, K.S. and S.K. Dhillon. 1997. Distribution of seleniferous soils in North-west India and associatedtoxicity problems in the soil-plant-animal-human continuum. Land Contam. & Reclamation 5:313-322.

Dhillon, K.S. and S.K. Dhillon. 1991. Selenium toxicity in soils, plants and animals in some parts of Punjab,India. Int. J. Environ. Studies 37:15-24.

Engberg, R.A., and M.A. Sylvester. 1993. Concentrations, distribution and sources of selenium from irrigated lands in western United States. J. Irrig. Drain. Eng. 119:522–536.

Eric D.Morway, Timothy K. Gates, and Richard G.Niswonger, 2013, Appraising options to reduce shallow groundwater tables and enhance flow conditions over regional scales in an irrigated alluvial aquifer system. Journal of Hydrology 495: 216 -237.

Fernández-Martínez, A., and L. Charlet. 2009. Selenium environmental cycling and bioavailability: a structural chemist point of view. Reviews in Environmental Science and Bio/Technology. 8:81-110.

Gates, T. K., B. M. Cody, J. P. Donnelly, A. W. Herting, R. T. Bailey, and J. Mueller Price. 2009. Assessing selenium contamination in the irrigated stream-aquifer system of the Arkansas River, Colorado. J Environ Qual. 38:2344-2356.

Gates, T.K., Garcia, L.A., Hemphill, R.A., Morway, E.D., and A. Elhaddad (2012), Irrigation practices, water consumption, and return flows in Colorado's Lower Arkansas River Valley: Field and model investigations. Colorado Water Institute Completion Report No. 221, Colorado State University, Fort Collins, CO.

H.F. Mayland, L.F. James, K.E. Panter, and J.L. Sonderegger (1989) Selenium in Seleniferous Environments, Selenium in Agriculture and the Environment, Soil Science Society of America and American Society of Agronomy, Special Publication no.23.

James M. Mc Neal, Laurie S. Balistrieri, 1989, Geo Chemistry and Occurrence of Selenium: An overview, Selenium in Agriculture and the Environment, Soil Science Society of America and American Society of Agronomy, Special Publication no.23.

James E. Oldfield, 2002, Selenium (Se) World Atlas Updated Edition, Selenium-Tellurium Development Association (STDA).

Kipp, K.L., Jr., Hsieh, P.A., and Charlton, S.R., 2008, Guide to the revised groundwater flow and heat transport simulator: HYDROTHERM — Version 3: U.S. Geological Survey Techniques and Methods 6−A25, 160 p.

Knott, S.G. and C.W.R. McCray. 1959. Two naturally occurring outbreaks of selenosis in Queensland. Aust.Vet. J. 35:161-165.

Lakin, H.W. 1948. Selenium occurrence in certain soils of the United States, with a discussion of related topics: Seventh report. USDA Tech. Bull. 953. U.S. Gov. Print. Office, Washington, DC.

Lakin, H.W., and D.F. Davidson. 1973. Selenium. U.S. Geo!. Surv. Prof. Pap. 820:573-576.

Levander, O. A., and R. F. Burk. 2006. Update of human dietary standards for selenium. p. 399-410. In D. L. Hatfield, M. J. Berry and V. N. Gladyshev (ed.). Selenium its molecular biology and role in human helath. Springer, New York.

McDonald, M.G., and Harbaugh, A.W., 1988, A modular three-dimensional finite-difference groundwater flow model: Techniques of Water-Resources Investigations of the United States Geological Survey, Book 6, Chapter A1, 586 p.

Mizutani, T., K. Kanaya and T. Osaka. 2001. Map of selenium content in soil of Japan. J. Health Sci. 47:407-413.

Moxon, A.L. 1937. Alkali disease or selenium poisoning. South Dakota Agric. Exp. Stn. Bull. 311.

Moxon, A.L., O.E. Olson, and W.V. Searight. 1939. Selenium in rocks, soils, and plants. South Dakota Agric. Exp. Stn. Tech. Bull. 2:1-94.

Muth, O.H., J.E. Oldfield, L.F. Remmert and J.R. Schubert. 1958. Effects of selenium and vitamin E on whitemuscle disease. Science 128:1090.

National Academy of Science-National Research Council, 1983. Selenium in nutrition. Rev, ed. Board on Agric. NAS-NRC, Washington, DC.

Niswonger, R.G., Panday, Sorab, and Ibaraki, Motomu, 2011, MODFLOW-NWT, A Newton formulation for MODFLOW-2005: U.S. Geological Survey Techniques and Methods 6-A37, 44 p.

Niswonger, R.G., Prudic, D.E., and Regan, R.S., 2006, Documentation of the Unsaturated-Zone Flow (UZF1) Package for modeling unsaturated flow between the land surface and the water table with MODFLOW-2005: U.S. Geological Techniques and Methods Book 6, Chapter A19, 62 p.

Ohlendorf, H.M., Hoffman, D.J., Saiki, M.K., and Aldrich, T.W., 1986, Embryonic mortality and abnormalities of aquatic birds—Apparent impact of selenium from irrigation drainwater: Science of the Total Environment, v. 52, p. 49–63.

Ohlendorf, H.M., Kilness, A.W., Simmons, J.L., Stroud, R.K., Hoffman, D.J., and Moore, J.F., 1988, Selenium toxicosis in wild aquatic birds: Journal of Toxicology and Environmental Health, v. 24, p. 67–92.

Oldfield, l.E. 1972. Selenium deficiency in soils and its effect on animal health. p. 57-63. In H.L. Cannon and H.C. Hopps (ed.) Geochemical environment in relation to health and disease. Spec. Pap. 140. Geo!. Soc. of Am., Boulder, CO.

Peterson, P.J. and G.W. Butler. 1962. The uptake and assimilation of selenite by higher plants. Aust. J. Biol.Sci. 15:126-146.

Reuter, D.l. 1975. Selenium in soils and plant: A review in relation to selenium deficiency in South Australia. Agricultural Record 2:44-50.

R.C. Severson, Scott E. Fisher, Jr., and L.P.Gough, 1990. Proceedings of the 1990 Billings land Reclamation Symposium on Selenium in ARID AND Semiarid Environments, Western United States, U.S. Geological Survey Circular 1064.

Rosenfeld, I., and O.A. Beath. 1964. Selenium. Geobotany, biochemistry, toxicity and nutrition. Academic Press, New York.

Riley, C. 1996. Selenium in Food and Health. Chapman and Hall, London, 338 pp.

Ruksan, B.E., O. Gaggino, S. Neder, E.W. Rodriguez and M. Zanelli. 1993. Effects of solanum malacoxylonand selenium on neutrophils in sheep. Proc. 8th Int. Symp. on Trace Elements in Man and Animals. May 16-22. Dresden, Germany.

Ruksan, B.R. and M.L. Zanelli. 1992. La glutation peroxidasa en la deteccion de la deficiencia de selenio enbovinos de la Argentina. XIII Congress, Panam. de Ciencias Vet. Santiago, Chile, 5-9 Oct (in Spanish), 3 pp.

Ryan T. Bailey , Erica C. Romero, Timothy K. Gates. 2014 Assessing best management practices for remediation of selenium loading in groundwater to streams in an irrigated region, Journal of Hydrology 521 (2015) 341–359

Sager, M. (2006), Selelnium in agriculture, food, and nutrition, Pure Applied Chemistry, 78(1), 23.

Seiler, R. L. 1997. Methods to identify areas susceptible to irrigation-induced selenium contamination in the Western United States, edited by US Dept. of the Interior, USGS, Washington, D.C., p. 4. Fact Sheet FS-038-97.

Shibata, Y., M. Morita and K. Fueva. 1992. Selenium and arsenic in biology: their chemical forms and biologicalfunctions. Adv. Biophys. 28:31-80.

Sors, T. G., D. R. Ellis, and D. E. Salt (2005), Selenium uptake, translocation, assimilation and metabolic fate in plants, Photosynth Res, 86(3), 373-389.

Stolz, J. F., P. Basu, and R. S. Oremland. 2002. Microbial transformation of elements: the case of arsenic and selenium. Int. Microbiol. 5:201-207.

Swaine, D.l. 1955. The trace-element content of soils. Tech. Commun. 48. Commonw. Bur. of Soil Sci., Harpenden, England.

Timothy K. Gates, Luis A.Garcia, Ryan A.Hemphill, Eric D. Morway, Aymn Elhaddad, 2012, Irrigation Practices, Water Consumption, & return dflows in Colorado's Lower Arkansas River Valley, field and Model Investigations, Technical Completion Report No:221, Colorado Water Institute, Technical Report No: TR12-10, Colorado Agricultural Experiment Station.

Yang, G., J. Chen, Z. Wen, K. Ge, L. Zhu, X. Chen and K. Chen. 1984. The role of selenium in Keshandisease. In: Draper, H.H., Ed. Advances in Nutritional Research, Plenum Press, NY. pp. 203-231.

Wang, G., R. Zhou and S. Sun. 1979. Difference between blood Se concentrations of residents of Keshandisease-affected and non-affected areas - correlation between the selenium content of blood and hair. ChineseJ. Prev. Med. 13:204-211.

Winkel, L.H.E., Johnson, C.A., Lenz, M., Grundl, T., Leupin, O.X., Amini, M., and L. Charlet (2012), Environmental Selenium Research: From Microscopic Processes to Global Understanding. Env. Sci. Tech. 46, 571-579.

Zhang, H. H., Z. F. Wu, C. L. Yang, B. Xia, D. R. Xu, and H. X. Yuan. 2008. Spatial distributions and potential risk analysis of total soil selenium in Guangdong Province, China. J Environ Qual. 37:780-787.

APPENDIX A

This Appendix describes the UZF-MODFLOW model input files and output files to simulate the groundwater flow in the study region.

As explained in Sec 3.1 in Chapter 3, the MODFLOW is the *defacto* for the groundwater flow simulations and predictions in any size area of study. This MODFLOW uses the Newton formulation which solves the asymmetric matrices, which in turn are numerically solved by the GMRES and CGSTAB. Also, this model includes the simulation of flow in Unsaturated Zone Flow (UZF) (Niswonger et al, 2006) using the one-dimensional Richard's Equation, which neglects the diffusive term. This UZF-MODFLOW model uses the UPW package rather than the Layer Property Flow (LPF) or the Block Centered Flow (BCF) packages, which are usually used by all other MODFLOW models.

The input files and output files involved in the UZF-MODFLOW are as follows:

Input Files

- .dis file includes the discretization data of the model domain which includes the number of layers, rows, columns, time steps, top and bottom elevation of each cell, and stress period information.
- .ba6 file is the basic file having data about the model grid with active and inactive cells layer-wise and initial head levels for each cell of the entire grid for each layer.
- .upw file includes information about aquifer properties like hydraulic conductivity and specific yield.

- .uzf file includes information about unsaturated zone details including hydraulic conductivity, saturated water content, applied infiltration rate, evapotranspiration rate, evapotranspiration extinction depth, and Brooks-Corey exponent, etc.
- .riv file includes surface water such as canal or river details. The data includes the layer, row, column, stage, conductance, and bottom elevation.
- .wel file includes the number of wells used during each stress period, layer, row, column, and pumping rate.
- .nwt file includes the numerical solver Newton method details.
- .oc file includes the output control which specifies saving hydraulic heads and flux budget to print.

Output Files

- .out file prints about the reading all input files and calculates the hydraulic heads and volumetric budget.
- .hed file prints the hydraulic heads for each cell for each layer in the model domain.
- .hff file provides input for the UZF-RT3D model with information related to flux and water content details for each cell in the entire model domain.

Figure B.1 shows the flow chart of the UZF-MODFLOW model, how it reads input file data, and how it calculates the volumetric stress for each stress period, hydraulic heads as explained in Sec 3.1 in Chapter 3. Figure B.2 and B.3 show the typical volumetric budget and hydraulic heads calculated by UZF –MODFLOW respectively.

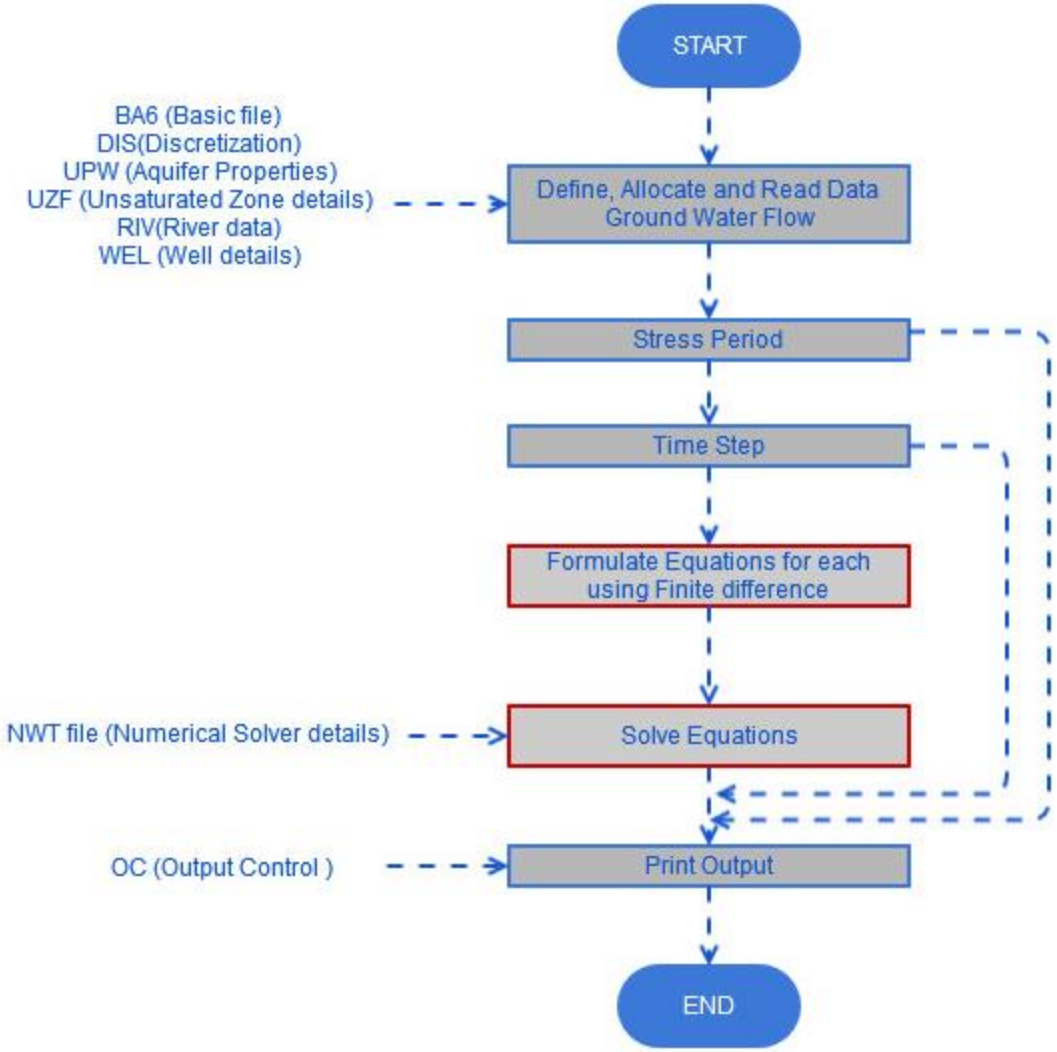

Figure B.1: Flow of data in UZF-MODFLOW. Data is input through the .ba6, .dis, .upw, .uzf, .nwt, .riv, .wel files.

```
UNSATURATED ZONE PACKAGE VOLUMETRIC BUDGET FOR  TIME STEP    1 STRESS PERIOD  292
 ---------------------------------------------------------------------------


    CUMULATIVE VOLUMES      L**3       RATES FOR THIS TIME STEP      L**3/T
    ------------------                 ------------------------

          IN:                                IN:
          ---                                ---
       INFILTRATION =  1888558070.4253       INFILTRATION =     4608202.7687

          OUT:                               OUT:
          ----                               ----
           UZF ET =  1095791630.1320             UZF ET =     1645591.6032
       UZF RECHARGE =   872890986.7543       UZF RECHARGE =     3698250.3723

          IN - OUT =   -80124546.4610           IN - OUT =     -735639.2068

          STORAGE:                           STORAGE:
          --------                           --------
     STORAGE CHANGE =   -69136976.2045     STORAGE CHANGE =     -711007.5051

 PERCENT DISCREPANCY IS DIFFERENCE BETWEEN IN-OUT MINUS CHANGE IN STORAGE
 DIVIDED BY THE AVERAGE OF IN AND OUT TIMES 100

 PERCENT DISCREPANCY =          -0.14     PERCENT DISCREPANCY =          -0.46
```

Figure B.2: Volumetric Budget for Unsaturated zone for stress period 292 by UZF-MODFLOW

```
1155.952  1158.218  1159.843  1161.003  1161.577  1161.830  1161.531
1155.107  1157.360  1158.966  1160.049  1160.641  1160.731  1160.467
1153.808  1156.031  1157.637  1158.747  1159.616  1159.860  1159.772
1152.545  1154.648  1156.322  1157.541  1158.505  1158.894  1158.879
1150.872  1153.254  1155.099  1156.479  1157.379  1157.816  1157.803
1149.195  1151.966  1154.009  1155.422  1156.246  1156.630  1156.580
1147.974  1150.842  1152.995  1154.329  1155.044  1155.336  1155.269
1146.132  1149.223  1151.401  1152.883  1153.765  1154.010  1153.957
1144.593  1147.595  1149.882  1151.481  1152.445  1152.733  1152.576
1144.092  1146.355  1148.448  1150.031  1150.987  1151.237  1151.023
1143.490  1145.145  1146.910  1148.581  1149.424  1149.693  1149.599
1142.317  1143.851  1145.487  1147.121  1147.987  1148.149  1148.163
1140.564  1142.396  1144.076  1145.606  1146.445  1146.634  1146.604
1138.760  1141.093  1142.779  1144.053  1144.780  1144.959  1144.855
1137.756  1140.117  1141.480  1142.359  1142.886  1143.108  1142.992
```

Figure B.3: Typical cell wise Hydraulic Heads for stress period 292 by UZF-MODFLOW

APPENDIX B

This Appendix describes the RT3D model input files and output files and how the model ~~will run~~ predicts the Se and NO_3 concentrations.

As explained in Sec 3.3 in Chapter 3, the UZF- RT3D model was developed from the multi-species transport model RT3D (Clement, 1997), and by linking the Variably-Saturated Transport (VST) package, which links the output of UZF-MODFLOW to the RT3D model, the Unsaturated Zone Flow (UZF) package (Niswonger et al, 2006) which simulates the one-dimensional vertical flow of water in the unsaturated zone using the one dimensional Richard Equation. So this linked UZF-RT3D model was used for the fate and transport of the C, Se and N species.

The input files and output files for the UZF- RT3D model are described as follows:

Input files

- .btn file includes all the data related to the initial concentrations of the all the species included in the fate and transport of the C, Se and N, as well as layer thickness, porosity, and geological data for each cell in the model surface grid.
- .agr file accounts for the reading and processing of data required for the cycling of C, Se and N species. The data deals with agricultural details such as crop cultivation and management, crop type, crop parameter values, root growth, nitrogen and selenium plant parameters, fertilizer loadings, and species concentrations in the infiltrating irrigation water for all the cells in the model surface grid.
- .irg file accounts for reading and processing of data related to irrigation. The data includes the amount of irrigation, type of irrigation, and species mass entering the system

through canal water, groundwater (pumped from wells) for each cell in the model surface grid.

- .rct file deals with the chemical reaction rates which change the species concentrations.
- .ssm file deals with the source-sink mixing and river cell solute concentration for each week, which is called ~~as~~ a stress period.
- .hff file deals with the outputs from UZF MODFLOW including infiltration fluxes and water content for each cell in the model grid.
- .adv file deals with the advection.
- .dsp file deals with the dispersion.

Output files

- Mass Balance file shows a reading of all the input files and shows the mass budget for each stress period.
- Concentration file shows the concentration of each time-step for each cell of all species
- Mass Loading file shows the mass loadings of the species to the river cells for each day.

Figure C.1 shows the flow chart of the UZF-RT3D model, how it reads input file data, and for each time step it calculates the concentration initially with advection, dispersion, and source and it sinks and then with chemical reaction rates as explained in Sec 3.3 in Chapter 3. Figure C.2 and C.3 show the typical mass balance output of the UZF-RT3D for SeO_4 and NO_3 respectively.

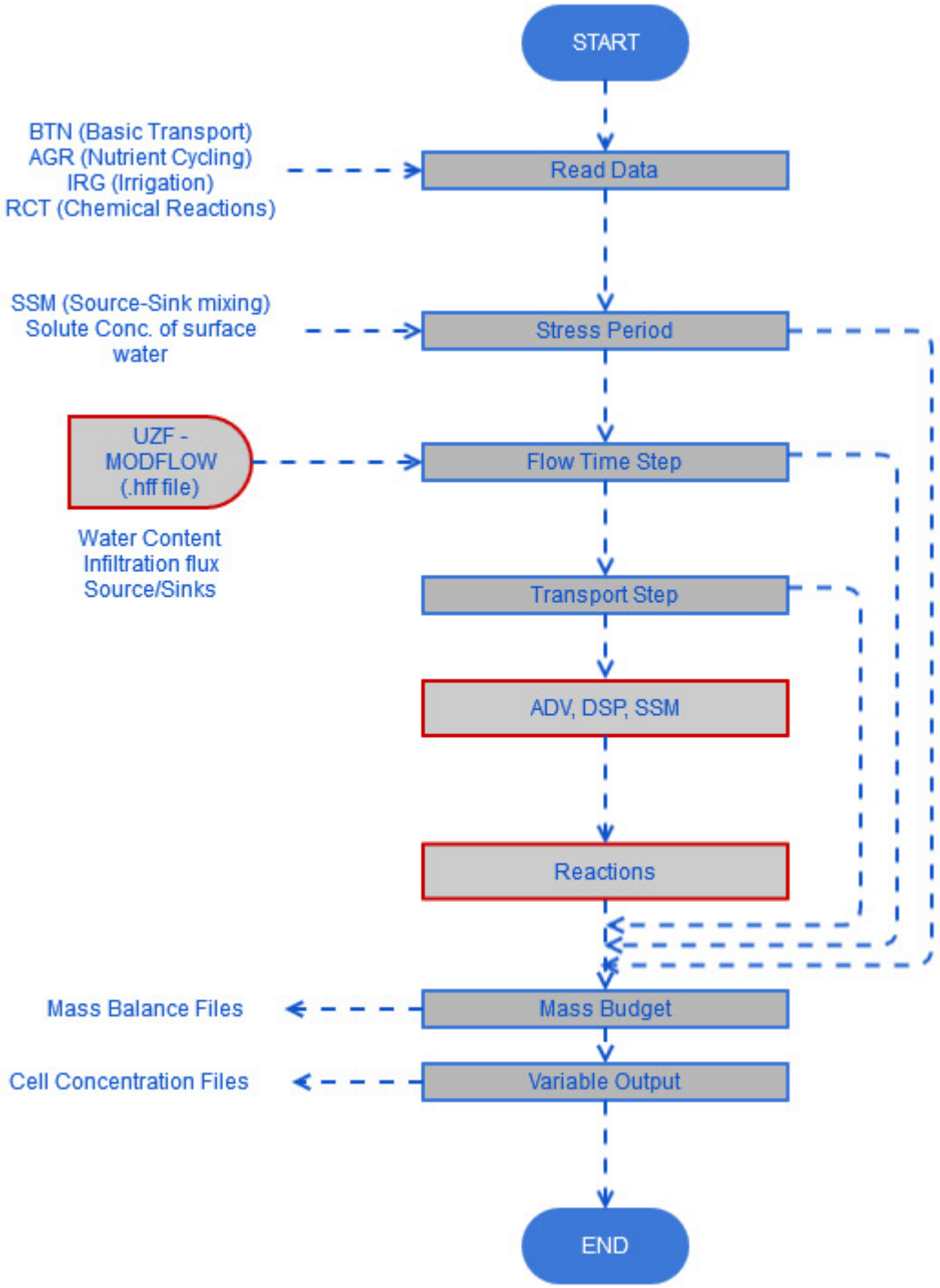

Figure C.1: Flow of data in RT3D. Data is input through the .btn, .agr, .irg, .ssm, .rct files, and .hff files, model output and mass-balance information is either for each transport time step or upon request.

```
FOR SPECIES NO.:   12  SEO4

              TOTAL CHANGE IN MASS USING CONCENTRATION (DMASS1)
                              TOTAL MASS =   DISSOLVED   +   SORBED   +   SOLID
                              INITIAL =   0.77046997E+11+ 0.50483550E+13+  0.0000000    = 0.51254017E+13
                              CURRENT =   0.10058713E+12+ 0.50483550E+13+  0.0000000    = 0.51489423E+13
                               DMASS1 =   0.23540531E+11

              TOTAL CHANGE IN MASS USING SOURCES/SINKS (DMASS2)
                                                          MASS IN            MASS OUT
                                   CONSTANT CONCENTRATION:    0.000000           0.000000
                                       CHEMICAL REACTIONS:   0.3204168E+11      -0.1148830E+11
                                            CONSTANT HEAD:    0.000000           0.000000
                                                    WELLS:    0.000000          0.1570868E+11
                                                  RIVERS:   0.2871180E+10      -0.2737526E+10
                                         CANAL IRRIGATION:   0.4282017E+10        0.000000
                                       AQUIFER IRRIGATION:   0.2315521E+09        0.000000
                                              FERTILIZER:    0.000000           0.000000
                                             CROP UPTAKE:    0.000000          -0.1505507E+10
                                                                              ---------------
                                                    TOTAL:   0.3942643E+11      -0.2265242E+08
                              DMASS2 =   0.3940378E+11

              % DISCREPANCY (DMASS2 TO DMASS1) =  -0.3076
```

Figure C.2: Mass balance summary for SeO_4 as output by UZF-RT3D.

```
FOR SPECIES NO.:    6  NO3

              TOTAL CHANGE IN MASS USING CONCENTRATION (DMASS1)
                              TOTAL MASS =   DISSOLVED   +   SORBED   +   SOLID
                              INITIAL =   0.57437542E+10+ 0.47856402E+12+  0.0000000    = 0.48430776E+12
                              CURRENT =   0.65389036E+10+ 0.47856402E+12+  0.0000000    = 0.48510291E+12
                               DMASS1 =   0.79514829E+09

              TOTAL CHANGE IN MASS USING SOURCES/SINKS (DMASS2)
                                                          MASS IN            MASS OUT
                                   CONSTANT CONCENTRATION:    0.000000           0.000000
                                       CHEMICAL REACTIONS:   0.1298533E+11      -0.7452780E+09
                                            CONSTANT HEAD:    0.000000           0.000000
                                                    WELLS:    0.000000          0.1585881E+11
                                                  RIVERS:   0.2945168E+09      -0.3481307E+09
                                         CANAL IRRIGATION:   0.4945795E+09        0.000000
                                       AQUIFER IRRIGATION:   0.8139218E+08        0.000000
                                              FERTILIZER:    0.000000           0.000000
                                             CROP UPTAKE:    0.000000          -0.1189031E+11
                                                                              ---------------
                                                    TOTAL:   0.1385582E+11       0.2875092E+10
                              DMASS2 =   0.1098073E+11

              % DISCREPANCY (DMASS2 TO DMASS1) =  -2.0657
```

Figure C.3: Mass balance summary for NO_3 as output by UZF-

APPENDIX C

Observed field data tables for Selenium, Nitrate and Dissolved Oxygen.

Selenium

Date	Days	S.No	Amity 1	Amity 2	Amity 3	Buffalo 1	Buffalo 2	Fort Bent	Fort Lyon1	Fort Lyon2	Hyde ditch	Lamar 1	Lamar 2	Lamar 3	South side	XY Graham1	XY Graham2	Outside
4/25/2003	115	1	0	0	0	0	0	0	0	0	0	0	0	0	0	0	0	0
5/29/2003	149	2	0	0	0	0	0	0	0	0	0	0	0	0	0	0	0	0
6/30/2003	181	3	0.00	0.00	0.00	0.00	0.00	0.00	0.00	0.00	0.00	0.00	11.90	10.40	0.00	17.10	0.00	26.40
7/27/2003	208	4	16.29	37.10	50.41	18.80	77.90	0.78	16.65	1594.20	1.92	6.04	6.22	0.00	9.02	0.00	20.75	12.26
10/25/2003	298	5	20.15	29.27	45.98	72.85	32.13	0.00	8.28	1508.35	0.75	0.00	12.79	11.01	9.47	40.08	16.08	18.78
1/12/2004	377	6	17.47	12.14	82.32	0.00	55.00	0.50	24.95	1737.20	2.82	5.77	7.68	0.00	0.00	14.80	15.03	14.37
3/15/2004	440	7	13.91	18.06	74.88	46.50	40.40	0.66	69.19	1743.33	3.66	7.31	10.56	8.84	10.80	18.45	19.15	18.51
4/30/2004	486	8	10.50	18.29	73.58	40.50	41.90	0.77	57.51	1202.03	3.74	8.87	9.55	11.20	9.36	22.40	0.00	17.36
6/1/2004	518	9	17.23	18.37	77.43	49.70	38.70	2.25	55.43	1281.47	3.71	3.59	9.04	6.66	9.36	23.45	20.03	20.42
6/28/2004	545	10	14.22	55.30	90.97	31.20	62.60	3.96	70.80	1278.17	4.19	1.57	8.33	6.39	9.52	27.80	18.40	18.14
8/2/2004	580	11	15.87	32.35	60.65	51.20	36.45	0.90	58.70	1330.40	2.48	1.63	6.95	0.00	110.00	0.00	9.82	16.71
11/4/2004	674	12	12.76	29.87	52.93	43.15	47.10	2.60	153.68	624.63	2.22	2.04	8.10	5.66	6.76	16.33	21.27	16.90
1/10/2005	741	13	19.73	26.74	58.44	26.00	35.65	2.72	55.83	25.20	1.71	3.98	7.19	5.02	8.08	0.00	18.40	20.35
3/15/2005	805	14	15.72	18.41	85.36	27.00	22.87	1.27	60.30	32.10	0.55	2.94	9.15	9.46	10.40	17.85	15.07	20.30
6/27/2005	909	15	18.15	21.20	66.79	16.95	17.91	0.00	58.80	29.70	0.70	2.55	0.00	0.00	9.83	0.00	15.57	19.69
7/19/2005	931	16	18.57	26.98	51.81	17.60	23.54	3.99	67.20	70.40	1.39	1.63	8.50	21.10	11.70	20.75	14.63	19.36
8/16/2005	959	17	20.80	21.56	55.89	13.76	19.32	3.38	57.78	42.80	1.51	3.66	9.49	22.00	9.27	21.37	18.89	24.43
11/19/2005	1054	18	22.37	13.46	61.46	0.00	33.00	0.80	68.58	23.96	0.71	0.91	7.62	0.00	11.40	0.00	0.00	25.49
1/10/2006	1106	19	27.75	21.87	90.44	18.87	23.64	0.67	50.53	21.81	2.29	1.70	9.44	26.20	11.00	16.07	17.77	22.74
3/11/2006	1166	20	25.37	39.71	60.37	0.00	22.78	0.00	39.48	21.79	7.10	3.47	0.00	0.00	12.90	0.00	0.00	33.80
5/13/2006	1229	21	26.50	27.06	64.38	31.10	26.17	0.67	49.15	10.26	2.73	2.45	9.84	0.00	8.25	28.74	19.69	16.31
6/13/2006	1260	22	18.00	24.32	60.95	170.00	59.50	0.00	72.10	11.66	0.40	0.00	0.00	0.00	8.53	0.00	0.00	29.84
7/11/2006	1288	23	21.09	0.40	45.99	74.15	24.73	0.54	39.70	17.42	0.54	2.95	10.17	0.00	24.20	0.00	18.50	24.49
8/8/2006	1316	24	19.21	26.96	91.30	0.00	71.60	0.83	49.33	21.15	1.16	1.83	11.58	0.00	11.60	38.10	0.00	38.16
11/18/2006	1418	25	18.15	0.40	0.00	109.90	3.54	1.01	94.85	18.40	0.00	2.07	11.12	0.00	0.00	31.93	13.88	21.75
3/10/2007	1530	26	19.40	19.25	83.24	46.90	45.05	0.00	53.96	13.92	7.69	4.63	13.45	0.00	14.80	42.20	17.90	59.90
5/15/2007	1596	27	17.50	0.00	22.65	63.50	63.65	7.10	62.89	52.20	0.00	0.00	0.00	0.00	170.00	0.00	0.00	30.20
6/19/2007	1631	28	16.55	31.15	88.72	35.30	59.25	0.00	52.30	60.90	0.55	11.83	15.15	0.00	54.00	18.85	18.15	41.10
7/22/2007	1664	29	7.26	30.77	130.08	26.05	50.10	4.19	154.43	43.75	0.40	6.27	17.43	0.00	6.42	22.15	18.10	37.06
8/14/2007	1687	30	8.88	12.20	116.29	0.00	82.30	0.00	70.19	38.00	0.40	3.80	18.88	12.50	0.00	25.44	17.95	28.70
Average - Calibration			**15.80**	**26.90**	**68.45**	**40.69**	**44.61**	**1.64**	**57.39**	**1123.37**	**2.52**	**4.37**	**8.96**	**8.29**	**19.28**	**22.03**	**17.40**	**18.37**
Average - Testing			**19.10**	**21.15**	**72.69**	**52.01**	**39.13**	**2.32**	**65.08**	**31.13**	**1.97**	**3.55**	**11.89**	**20.45**	**25.99**	**26.56**	**17.37**	**29.56**

Nitrate

Date	Days	S.No	Amity 1	Amity 2	Amity 3	Buffalo 1	Buffalo 2	Fort Bent	Fort Lyon1	Fort Lyon2	Hyde ditch	Lamar 1	Lamar 2	Lamar 3	South side	XY Graham1	XY Graham2	Outside
4/25/2003	115	1	0	0	0	0	0	0	0	0	0	0	0	0	0	0	0	0
5/29/2003	149	2	0	0	0	0	0	0	0	0	0	0	0	0	0	0	0	0
6/30/2003	181	3	0.00	0.00	0.00	0.00	0.00	0.00	0.00	0.00	0.00	0.00	0.00	0.00	0.00	0.00	0.00	0.00
7/27/2003	208	4	2.50	0.00	0.00	0.00	0.00	0.40	19.87	0.00	0.00	5.15	1.03	0.00	0.00	0.00	0.00	0.00
10/25/2003	298	5	1.85	2.83	4.33	3.25	2.65	0.00	0.00	233.35	0.10	0.00	1.55	9.30	2.00	5.10	3.60	2.58
1/12/2004	377	6	0.00	0.00	0.00	0.00	0.00	0.10	0.00	0.00	0.00	28.10	1.70	0.00	0.00	0.00	5.70	0.00
3/15/2004	440	7	1.53	2.28	3.02	3.55	2.85	0.00	15.00	343.43	0.10	0.10	1.40	5.70	2.80	3.50	0.00	4.14
4/30/2004	486	8	0.00	0.00	0.00	0.00	0.00	0.10	0.00	0.00	0.00	4.75	1.36	0.00	0.00	2.90	0.00	9.50
6/1/2004	518	9	1.33	2.40	3.10	2.75	2.80	0.00	11.28	205.53	0.10	0.00	0.00	0.00	2.60	0.00	5.70	1.50
6/28/2004	545	10	0.00	0.00	0.00	0.00	0.00	0.60	0.00	0.00	0.00	2.90	1.44	5.90	0.00	3.05	5.85	11.20
8/2/2004	580	11	1.63	2.48	3.15	2.85	3.05	0.00	10.13	170.10	2.30	0.00	0.00	0.00	43.20	0.00	2.40	2.82
11/4/2004	674	12	0.00	0.00	0.00	0.00	0.00	0.60	0.00	0.00	0.00	1.55	1.36	0.00	0.00	1.55	0.00	8.50
1/10/2005	741	13	2.53	2.66	2.27	1.90	2.10	0.00	10.93	1.65	0.10	0.00	0.00	11.00	2.00	0.00	5.57	2.30
3/15/2005	805	14	0.00	0.00	0.00	0.00	0.00	0.40	0.00	0.00	0.00	4.90	1.82	5.10	0.00	2.20	0.00	0.70
6/27/2005	909	15	2.93	2.30	2.26	1.20	1.45	0.00	9.78	1.85	0.10	0.00	0.00	0.00	2.60	0.00	5.00	2.00
7/19/2005	931	16	0.00	0.00	0.00	0.00	0.00	1.90	0.00	0.00	0.00	5.45	1.55	0.00	0.00	0.00	0.00	0.00
8/16/2005	959	17	4.43	2.23	4.21	1.45	2.65	0.00	7.80	1.35	0.10	0.00	0.00	7.80	2.70	3.45	5.57	3.12
11/19/2005	1054	18	0.00	0.00	0.00	0.00	0.00	0.30	0.00	0.00	0.00	0.10	2.20	0.00	0.00	0.00	0.00	0.00
1/10/2006	1106	19	3.35	2.45	2.68	2.45	2.40	0.00	6.53	1.35	0.10	0.00	1.75	7.60	3.20	2.05	5.03	2.65
3/11/2006	1166	20	0.00	0.00	0.00	0.00	0.00	0.00	0.00	0.00	0.00	0.90	0.00	0.00	0.00	0.00	0.00	0.00
5/13/2006	1229	21	2.30	3.00	2.04	1.10	2.60	0.30	5.92	0.95	0.10	0.00	1.80	0.00	2.80	2.95	6.10	2.55
6/13/2006	1260	22	0.00	3.60	1.79	0.00	5.90	0.00	0.00	0.00	0.00	0.00	0.00	0.00	2.70	0.00	0.00	3.87
7/11/2006	1288	23	3.13	0.10	5.10	2.40	1.50	0.30	3.03	2.90	0.10	1.00	2.03	0.00	0.00	0.00	4.35	17.33
8/8/2006	1316	24	1.80	3.23	2.93	0.00	4.20	0.00	3.50	0.00	0.00	1.85	0.00	0.00	3.10	0.00	0.00	6.05
11/18/2006	1418	25	3.35	0.10	0.00	8.45	0.50	0.70	4.10	0.95	0.00	0.00	2.13	0.00	0.00	8.60	4.25	5.37
3/10/2007	1530	26	1.40	2.85	4.90	0.00	0.00	0.00	0.00	0.00	0.10	1.40	2.65	0.00	0.00	14.30	4.90	7.35
5/15/2007	1596	27	0.00	0.00	2.25	10.10	5.00	0.00	3.08	2.60	0.00	0.00	0.00	0.00	59.90	0.00	0.00	0.70
6/19/2007	1631	28	1.90	0.00	0.00	0.00	0.00	0.00	5.10	0.00	0.00	6.15	0.00	0.00	0.00	0.00	0.00	0.00
7/22/2007	1664	29	0.10	2.52	4.38	3.80	4.60	0.40	3.13	2.35	0.10	0.00	2.88	0.00	1.60	7.00	5.05	7.92
8/14/2007	1687	30	0.20	0.78	8.10	0.00	0.00	0.00	1.93	2.85	1.00	0.55	2.68	0.00	0.00	7.60	3.90	6.05
Average - Calibration			**1.90**	**2.53**	**3.17**	**2.86**	**2.69**	**0.37**	**13.44**	**190.81**	**0.54**	**6.78**	**1.46**	**7.40**	**10.52**	**3.05**	**4.80**	**4.80**
Average - Testing			**2.26**	**2.10**	**3.69**	**3.87**	**3.08**	**0.65**	**4.90**	**1.91**	**0.21**	**2.18**	**2.18**	**7.70**	**9.83**	**6.56**	**4.91**	**5.41**

DISSOLVED OXYGEN

Date	Days	S.No	Amity 1	Amity 2	Amity 3	Buffalo 1	Buffalo 2	Fort Bent	Fort Lyon1	Fort Lyon2	Hyde ditch	Lamar 1	Lamar 2	Lamar 3	South side	XY Graham1	XY Graham2	Outside
4/25/2003	115	1	0	0	0	0	0	0	0	0	0	0	0	0	0	0	0	0
5/29/2003	149	2	0	0	0	0	0	0	0	0	0	0	0	0	0	0	0	0
6/30/2003	181	3	0.00	0.00	0.00	0.00	0.00	0.00	0.00	0.00	0.00	0.00	3.92	1.84	0.00	2.99	0.00	3.66
7/27/2003	208	4	1.89	3.15	1.81	2.77	2.36	2.96	2.28	2.88	0.43	0.31	2.50	0.00	0.20	0.00	4.27	0.71
10/25/2003	298	5	2.68	1.66	1.58	2.66	1.51	0.00	0.98	2.85	0.41	0.00	4.67	1.44	0.52	3.03	2.73	1.63
1/12/2004	377	6	3.91	1.86	2.94	0.00	2.65	2.11	2.40	3.79	0.47	1.07	2.56	0.00	0.00	3.61	5.25	0.72
3/15/2004	440	7	3.82	3.57	3.52	2.66	1.68	4.28	1.99	3.11	0.88	1.56	4.42	1.64	0.63	3.09	4.82	2.07
4/30/2004	486	8	3.07	4.08	3.95	3.22	1.54	3.06	2.40	3.46	0.58	1.76	4.31	2.34	0.60	3.42	0.00	2.12
6/1/2004	518	9	2.11	4.47	4.24	5.42	4.80	2.58	3.59	4.90	0.76	0.44	4.43	2.85	0.51	4.14	4.89	2.22
6/28/2004	545	10	2.91	3.28	4.19	4.61	2.64	2.97	3.48	4.63	0.62	0.56	4.31	2.06	0.44	3.92	5.21	2.88
8/2/2004	580	11	4.54	3.62	4.00	5.03	2.77	1.79	3.79	6.59	2.61	0.57	4.09	0.00	0.49	0.00	2.67	2.48
11/4/2004	674	12	3.02	4.19	3.53	3.52	3.98	1.93	3.28	3.59	2.69	1.11	3.64	1.52	1.19	2.94	4.29	3.03
1/10/2005	741	13	2.93	4.18	2.76	2.38	0.85	2.55	2.52	4.19	1.59	0.65	3.29	1.00	0.55	0.00	3.30	3.05
3/15/2005	805	14	4.79	3.71	3.14	1.47	0.94	3.66	1.92	2.96	1.62	1.15	3.85	1.80	0.60	2.68	5.14	2.47
6/27/2005	909	15	3.77	5.45	3.53	2.03	1.42	0.00	2.53	3.66	0.79	0.33	0.00	0.00	1.87	0.00	4.34	3.20
7/19/2005	931	16	3.07	2.82	3.24	3.39	1.86	2.72	1.96	2.45	0.20	0.42	3.21	3.08	0.67	1.79	2.69	1.52
8/16/2005	959	17	1.54	5.28	3.60	2.62	1.41	4.54	2.51	2.57	0.59	0.28	3.54	2.37	0.45	2.12	2.75	2.87
11/19/2005	1054	18	3.54	2.37	3.64	0.00	2.86	3.12	2.12	1.79	0.22	1.10	0.87	0.00	0.46	0.00	0.00	1.98
1/10/2006	1106	19	2.71	4.37	3.24	1.76	0.87	3.32	2.18	1.59	0.56	0.58	5.46	3.92	1.63	3.47	3.70	3.02
3/11/2006	1166	20	2.41	4.92	4.88	0.00	2.80	0.00	2.59	1.38	0.80	0.89	0.00	0.00	9.09	0.00	0.00	6.29
5/13/2006	1229	21	2.42	4.75	3.95	4.93	1.44	5.33	4.59	3.15	1.94	0.29	3.72	0.00	1.68	2.47	4.86	2.92
6/13/2006	1260	22	3.63	4.58	4.56	0.00	3.82	0.00	2.41	3.37	1.42	0.00	0.00	0.00	0.53	0.00	0.00	2.72
7/11/2006	1288	23	1.73	0.42	3.66	4.22	1.81	5.60	3.81	2.34	0.64	0.55	3.18	0.00	1.89	0.00	4.68	2.97
8/8/2006	1316	24	2.81	3.83	2.66	0.00	2.51	5.28	3.03	1.54	1.02	3.03	3.47	0.00	0.28	0.00	0.00	1.93
11/18/2006	1418	25	7.85	1.77	0.00	2.60	0.38	2.97	1.76	1.98	0.00	2.58	4.14	0.00	0.00	3.01	2.08	2.74
3/10/2007	1530	26	1.11	4.21	4.41	1.46	4.78	0.00	2.10	2.62	2.85	0.00	4.83	0.00	0.69	2.81	2.20	3.27
5/15/2007	1596	27	1.76	0.00	3.35	4.32	8.38	2.12	3.06	0.90	0.00	0.00	0.00	0.00	8.47	0.00	0.00	5.09
6/19/2007	1631	28	1.16	5.14	6.04	4.71	4.62	0.00	4.74	2.48	0.51	0.83	4.59	0.00	0.89	5.10	4.12	3.39
7/22/2007	1664	29	0.33	1.67	3.66	3.47	1.42	0.15	2.32	1.02	0.62	1.22	0.79	0.00	0.17	1.20	1.39	0.79
8/14/2007	1687	30	1.08	3.08	3.45	0.00	1.72	0.00	3.44	1.78	1.45	3.69	4.85	1.82	1.31	4.46	3.06	2.16
Average - Calibration			**3.24**	**3.43**	**3.24**	**3.37**	**2.34**	**2.79**	**2.60**	**3.90**	**1.15**	**0.92**	**3.83**	**1.83**	**0.57**	**3.31**	**4.26**	**2.25**
Average - Testing			**2.56**	**3.64**	**3.86**	**3.23**	**2.63**	**3.52**	**2.82**	**2.16**	**0.97**	**1.21**	**3.55**	**2.80**	**2.01**	**2.93**	**3.26**	**2.93**

LIST OF ABBREVIATIONS

The following are the abbreviations of the General Crop, Root Growth, Nitrogen Plant and Selenium Plant parameters shown in the Sec 3.4.1 in Chapter 3.

PLDY	Planting day (day index of the year)
HVTP	Type of harvest cycle, either annual or perennial. If perennial, then HVTP refers to the number of years in the perennial cycle.
FYR	For perennial crops, FYR refers to the number of years at the beginning of the perennial cycle that the crop receives fertilizer.
HVDY	Harvest day (day index of the year). For perennial crops, HVDY refers to the harvest day in the last year of the perennial cycle.
PGDY	Plow day (day index of the year). For perennial crops, refers to the plowing day in the last year of the perennial cycle.
PGDP	The depth of plowing (m)
RTHV	The root mass at harvest time per unit land area (kg ha^{-1})
CBRT	Carbon mass fraction of the root mass (0 to 1)
STPG	The mass of after-harvest stover mass per unit land area (kg ha^{-1})
CBST	Carbon mass fraction of the stover mass (0 to 1)
FLR	Fraction of roots that is alive at harvest time (0 to 1). This specifies the fraction of root mass that is incorporated into the soil at harvest time (1-FLR) as opposed to the fraction of root mass that is incorporated into the soil at plowing time (FLR).
MNMS	Seasonal mass of manure applied, per unit land area (kg ha^{-1})
MNC	Carbon mass fraction of manure (0 to 1)
RTDP	Maximum seasonal rooting depth (m)

RTB	B shape parameter for defining seasonal root growth curve (-)
RTC	C shape parameter for defining seasonal root growth curve (-)
RBETA	Depth distribution parameter for root mass, defining the variation of root mass with depth. (-)
CNRT	Carbon-Nitrogen ratio for crop root mass (-)
CNST	Carbon-Nitrogen ratio for stover mass (-)
FNO3	Seasonal amount of applied NO_3 fertilizer (kg h^{-1})
FNH4	Seasonal amount of applied NH_4 fertilizer (kg h^{-1})
FUREA	Seasonal amount of applied urea (kg h^{-1})
NUP	Seasonal crop uptake of nitrogen (kg ha^{-1})
NB	B shape parameter for curve defining daily uptake of nitrogen (-)
NC	C shape parameter for curve defining daily uptake of nitrogen (-)
NBETA	Depth distribution parameter for nitrogen uptake (-)
MNCN	Carbon-nitrogen ratio for manure (-)
SEST	Selenium mass fraction of stover mass (0 to 1)
SERT	Selenium mass fraction of root mass (0 to 1)
FSE	Seasonal amount of applied Se fertilizer (g ha^{-1})
SEUP	Seasonal crop uptake of selenium (g ha^{-1})
MNSE	Selenium mass fraction of manure (0 to 1)